Learning Segmentation and Economic Development*

Santiago Franco
Boston University

Jose M. Quintero
University of Chicago

September, 2026

Abstract

How does peer learning shape economic development? We answer this question with a heterogeneous-agent model of multiple labor markets and modern and traditional sectors, capturing key features of dual economies in developing countries. Workers sort across sectors and labor markets and accumulate human capital by learning from peers. Learning opportunities are sector-specific and depend on peer composition within the labor market. The model predicts that more skilled workers sort into the modern sector and, as a consequence, workers in this sector experience faster wage growth because they are exposed to higher-skilled peers. We test this prediction using longitudinal worker data from Chile and find empirical support for it. Finally, we estimate the model and use it to quantify the aggregate consequences of improving learning opportunities for traditional-sector workers. We find that improving learning opportunities generates meaningful welfare gains, but raises income per capita substantially only when accompanied by higher returns to human capital, which encourage workers to enter the modern sector.

*Franco: safranco@bu.edu. Quintero: jmquintero925@uchicago.edu. We thank Alvaro Contreras and Mohammad Jarrahi for outstanding research assistance. We are grateful to Santiago Caicedo, Levi Crews, Masao Fukui, Chang-Tai Hsieh, Greg Kaplan, David Lagakos, Aleksei Oskolkov, Pascual Restrepo, Esteban Rossi-Hansberg, Rob Shimer, Fernando Alvarez, Rodrigo Adão, and Roman David Zarate for insightful discussions. We thank the Subsecretaría de Previsión Social of Chile for access to the data.

1 Introduction

Human interactions are a crucial source of learning. People learn from others in the workplace, in the places they live, or from individuals in similar occupations who perform related tasks. Developing countries tend to be characterized by dual economies, in which workers are employed across modern and traditional sectors that coexist despite large differences in scale. This idea, central to the study of economic development, goes back to Lewis (1954) and is often reflected in agricultural versus non-agricultural productivity gaps, rural versus urban income differences, and the coexistence of many small firms alongside relatively few large firms within the same industries.[1] In turn, such dual economies likely shape who interacts with whom, segmenting the learning opportunities available to workers. In this paper, we study how these segmented learning markets influence workers' human capital and, through this channel, economic development. How do segmented learning markets affect workers' learning? How does workers' human capital influence their labor market choices? What are the aggregate implications for income and welfare?

We answer these questions using a quantitative model of learning from peers in a dual economy, combined with panel data from Chile. The model features multiple labor markets and includes modern and traditional sectors. Workers differ in skill, choose where to work, and accumulate human capital by learning from peers in their labor market. Within labor markets, learning is segmented by sector, so workers' human capital accumulation depends on the skill composition of peers in their own sector. The model predicts that higher-skill workers select into the modern sector and, when learning is sufficiently segmented, this sorting generates a dynamic modern-sector wage premium through faster wage growth. We then test these predictions using the Chilean panel, which allows us to track workers across labor markets and between the modern and traditional sectors. Consistent with the model, modern-sector workers earn higher wages and experience faster wage growth. We provide suggestive evidence that part of this dynamic premium is driven by learning from peers: exposure to higher-paid peers predicts higher future wage growth, and modern-sector workers are more exposed to such peers. Finally, we estimate the model and use it to quantify the aggregate income and welfare effects of segmented learning. In doing so, we highlight the interaction between learning opportunities and workers' incentives to enter the modern sector.

We build a heterogeneous-agent model that captures key features of dual economies in developing countries. Labor markets differ in productivity and include a modern and a traditional sector. Modern-sector firms operate a scalable constant-returns-to-scale technology but are subject to labor regulations in the form of payroll taxes. Traditional-sector firms avoid these regulations but operate a decreasing-returns-to-scale technology, capturing small-scale production or subsistence self-employment. Workers differ in skill, choose where to work, and accumulate human capital over time. In this sense, our framework relates to recent quantitative dual-economy models with human capital accumulation, such as Ma et al. (2024) and Amaral and Rivera-Padilla (2024). Our main departure is the introduction of a local learning externality: workers learn from peers in their sector but do not internalize how their sectoral choice affects the learning opportunities of others. This mechanism generates different patterns of skill accumulation across sectors and connects our

[1] Gollin (2014) offers a recent review of the Lewis model and the dual economy concept.

framework to classic work on knowledge spillovers and social learning (Lucas, 2004; Lucas and Moll, 2014), as well as to empirical and quantitative studies of learning from coworkers and urban interactions (Jarosch et al., 2021; Herkenhoff et al., 2024; Crews, 2024; Lhuillier, 2024).

We characterize the steady-state equilibrium of our framework and highlight two key predictions. Within each labor market, higher-skill workers select into the modern sector, where the constant-returns-to-scale technology makes high productivity particularly valuable despite regulatory costs. In contrast, lower-skill workers find it optimal to operate in the traditional sector, where decreasing returns are less binding at small scale and regulations are avoided. This sorting pattern also shapes workers' learning opportunities. When learning is sufficiently segmented toward workers' own sector, modern-sector workers are therefore relatively more exposed to higher-skill peers. As a result, they accumulate human capital faster and experience steeper wage growth than traditional-sector workers, generating a dynamic modern-sector wage premium.

We then examine the model's predictions using worker panel data from Chile. This country provides a natural setting for our analysis because its labor market features large formal and informal sectors, which map closely to the modern and traditional sectors in the model. We use the Encuesta de Protección Social (EPS), a nationally representative longitudinal survey that tracks about 17,000 workers over 2002–2016. We classify workers into modern and traditional sectors based on their formality status. Informal workers lack formal labor contracts and do not make payroll contributions, consistent with our modeling of the traditional sector. In the EPS, pension contributions provide a direct measure of participation in the formal payroll system. In addition, informal workers face costs that rise with output, such as expected fines or avoidance expenses, generating decreasing returns to scale in the traditional sector (Perry et al., 2007; Ulyssea, 2020b). Accordingly, we classify traditional-sector workers as those either not holding a labor contract or not contributing to a pension fund. The EPS also provides complete formal and informal employment histories dating back to 1980, allowing us to follow workers across sectors over their careers. With these data in hand, we test the model's predictions and provide evidence on the learning mechanism that generates them.

First, we show that higher-skilled workers sort into the modern sector. We start by documenting that modern-sector workers tend to have higher educational attainment. Then, to capture skill differences across sectors beyond observable characteristics, we estimate a wage regression with worker fixed effects, modern-sector status, and a large vector of controls. We interpret the worker fixed effects as capturing persistent differences in worker skill. We find that the distribution of worker fixed effects among modern-sector workers first-order stochastically dominates that among traditional-sector workers. These results are thus consistent with the model's sorting prediction.

Second, we provide evidence for the model's dynamic modern-sector wage premium. We analyze individual wage trajectories and examine how future wage growth relates to current modern-sector participation, controlling for worker fixed effects, demographics, and job characteristics. We find that modern-sector workers experience faster wage growth than traditional-sector workers, with the estimated premium rising over time and peaking at approximately 4% after four years. Because our specification includes worker fixed effects, identification comes from workers who change sectors. These results therefore suggest that transitioning into the modern sector is associated with cumulative wage gains over the following years.

Third, we provide evidence that learning from better-paid peers contributes to the dynamic modern-sector wage premium. Guided by our framework, we use information on workers' region, industry, occupation, and firm size to define labor markets that proxy for the peers workers may interact with. Then, in the spirit of Jarosch et al. (2021) and Herkenhoff et al. (2024), we examine whether exposure to higher-paid peers is associated with future wage growth. We find that workers exposed to higher-paid peers experience significantly faster future wage growth. A one-standard-deviation increase in peer wages is associated with a 4% wage increase five years later. Moreover, consistent with our sorting results, modern-sector workers are systematically exposed to higher-paid peers. Overall, these findings suggest that peer learning, together with the sorting of higher-skilled workers, contributes to the dynamic modern-sector wage premium.

After examining the model's predictions, we turn to its structural estimation using empirical moments from the Chilean data. We recover the parameters governing worker exit, labor-market mobility, and the initial skill distribution using minimum-distance estimators. To do so, we use the empirical age distribution, the fraction of workers who switch labor markets, and the tail of the entry-wage distribution. We estimate the remaining parameters by simulated method of moments, including those governing the traditional-sector technology, peer learning in both sectors, the degree of segmentation across sectors, and skill volatility. We target the modern-sector employment share, the variance of modern-sector wages, one-year sector transition probabilities, and five-year within-sector wage-quintile transition probabilities. The estimated model uncovers strong decreasing returns in the traditional sector and substantial learning segmentation. Traditional workers are 2.6 times more likely to learn from a traditional-sector peer than from an equally represented modern-sector peer. The model also reproduces key untargeted moments, including the wage-experience profiles of modern and traditional workers and the dynamic modern-sector wage premium.

In the final section, we use the estimated model to conduct counterfactual exercises quantifying the role of learning segmentation in shaping workers' income and welfare. We first consider an exercise that reduces the cost of operating in the modern sector by lowering payroll taxes. Effectively, lower payroll taxes allow traditional workers who move into the modern sector to access the same learning opportunities as other modern-sector workers. We then contrast this exercise with a counterfactual in which we directly provide traditional-sector workers with the same learning environment as modern-sector workers by changing their learning technology.

Our first counterfactual exercise reduces the cost of operating in the modern sector by eliminating payroll taxes. This tax cut increases the share of modern-sector workers by 12 percentage points and raises income per capita by 1.6% in the long run. The increase in income is fundamentally dynamic. Lower payroll taxes raise the return to human capital and strengthen workers' incentives to transition into the modern sector, where learning opportunities are better and human capital accumulates faster. The welfare gains from better learning opportunities reach 0.4% in consumption-equivalent terms. These aggregate gains mask substantial heterogeneity. Workers who move into the modern sector gain the most, with average learning-related welfare gains of about 1.2%. In contrast, workers who remain in either sector benefit to a much smaller extent.

Our second counterfactual exercise directly equalizes learning opportunities across sectors by changing traditional-sector workers' learning technology. This change generates welfare gains for workers who remain in the traditional sector, averaging 0.5% in consumption-equivalent terms. Aggregate welfare gains from learning reach around 0.2%, about half of those generated by eliminating payroll taxes. Interestingly, despite directly improving learning opportunities for a larger group of workers, long-run aggregate income increases by only 0.02% in this exercise.

The contrast between these two experiments highlights an important interaction between learning opportunities and technology adoption. Lowering payroll taxes improves learning opportunities only for workers who transition into the modern sector, but it also raises the value of human capital and encourages workers to make that transition. In contrast, directly improving learning opportunities in the traditional sector reduces workers' incentives to transition into the modern sector, as the value of accumulating human capital increases much less. As a result, more workers remain in the traditional sector, where they operate a smaller-scale technology, despite having access to better learning opportunities. These results provide quantitative evidence of a complementarity between access to better learning opportunities and the incentives to adopt modern technologies.

Related Literature. Our work contributes to four strands of the literature. First, we are closely related to the literature on learning from peers. We generalize the ideas in Lucas (2004) by allowing endogenous learning environments in both the modern and traditional sectors, with interactions within and across them. We also provide empirical evidence for this peer-learning mechanism. We are also related to the subsequent endogenous growth frameworks of Lucas and Moll (2014), Perla and Tonetti (2014), and Akcigit et al. (2018), but we depart from them by emphasizing how worker sorting across sectors shapes aggregate income in developing economies. We also highlight the idea that workers learn from better peers, as in Jarosch et al. (2021) and Herkenhoff et al. (2024), with the distinction that learning in our framework is not limited to the firm. In this sense, we are closer to Crews (2024) and Lhuillier (2024), who study worker sorting across cities with local learning externalities. Closest to our empirical exercise, Lhuillier (2024) estimates learning technologies by projecting future wage growth on the wages of nearby individuals in French cities. We implement a similar design across labor markets and sectors in a developing economy. Finally, labor regulations in the modern sector generate an endogenous productivity cutoff that separates workers across sectors, akin to the exporting-related sorting mechanism in Perla et al. (2021).

Second, we relate to papers that study how human capital accumulation shapes wage dynamics in developing economies. Building on Lagakos et al. (2018), Ma et al. (2024) show that firm-provided training in developing countries accelerates workers' skill formation, helping explain differences in age-wage profiles between developed and developing economies. We differ from their framework by emphasizing learning from peers as the fundamental driver of differences in human capital accumulation between the modern and traditional sectors. This mechanism can also rationalize the differences in age-wage profiles for developed and developing countries. Along these lines, Engbom (2022) finds that countries with higher rates of job-to-job transitions exhibit steeper wage profiles. In contrast, Donovan et al. (2023) document that workers in developing economies transition more frequently between jobs without moving into better-paying ones. Abstracting from labor market frictions, we offer a reconciling explanation for these findings by showing how segmented labor markets in developing countries hinder human capital accumulation, generating flatter wage profiles over the life cycle.

Third, our work connects to the literature on how technological differences across sectors shape aggregate productivity in economic development.[2] Lagakos (2016) shows how retail firms in low-income countries optimally adopt traditional technologies with lower measured productivity when ownership of durable goods is low. Duarte and Restuccia (2019) and Schwartzman (2025) study structural transformation from traditional to modern services and show that the reallocation of demand and workers across these segments is quantitatively important for income differences. We complement these results by showing that worker reallocation across traditional and modern sectors can raise aggregate income by improving the learning opportunities of lower-skill workers.

A related strand of this literature studies complementarities between human capital and technology. Herrendorf and Schoellman (2018) and Amaral and Rivera-Padilla (2024) show how complementarities between workers' human capital investments and firms' technology amplify cross-country income differences. Engbom et al. (2025) shows how low education levels in developing countries give rise to an endogenous dual economy with a prevalent traditional-sector organization of production. We differ from these studies by allowing human capital to accumulate continuously over the life cycle, rather than through a one-time investment. We also emphasize how peer composition within modern and traditional sectors shapes learning and wage dynamics.

Finally, by linking the modern and traditional sectors to formality status, we contribute to the literature on informal labor markets and their aggregate implications. Ulyssea (2020b) provides a comprehensive review of recent work on firms and workers in informal markets. Ulyssea (2018) develops a firm dynamics model with intensive and extensive margins of informality, while Dix-Carneiro et al. (2021) evaluate trade gains in economies with a large informal sector. Both papers use static frameworks that abstract from workers' human capital dynamics. Meghir et al. (2015), in contrast, consider a dynamic wage-posting setting, but workers' skills are homogeneous and fixed over time. We depart from these studies by emphasizing worker heterogeneity and wage dynamics arising from peer learning. More closely related to our approach are Lopez Garcia (2015) and Bobba et al. (2022), who link informality to schooling investments, and Akcigit et al. (2024) and Lopez-Martin (2019), who study the implications of informality for growth. We instead abstract from growth and one-time schooling decisions and emphasize continuous skill accumulation and sectoral mobility over the life cycle. Endogenous skill accumulation then shapes workers' choices between the modern-formal and traditional-informal sectors.[3]

The rest of the paper is organized as follows. Section 2 outlines our framework and its predictions. Section 3 describes the data and tests the model's predictions. Section 4 details our quantification strategy. Section 5 presents our counterfactual exercises, and Section 6 concludes.

[2] Herrendorf et al. (2014) provide an overview of this literature in the broader context of structural transformation, and Gollin and Rogerson (2025) highlight the recent use of heterogeneous-agent models in this literature.

[3] Ulyssea (2020a) notes that workers' forward-looking formality decisions remain poorly understood.

2 A Model of Peer Learning in a Dual Economy

In this section, we present a continuous-time heterogeneous-worker model in which workers differ in human capital, sort across sectors and labor markets, and accumulate human capital through peer learning. We then characterize the stationary equilibrium and derive predictions for worker sorting and wage growth across the two sectors. We test these predictions using Chilean panel data in Section 3.

2.1 Environment

Time is continuous and indexed by $t \geq 0$. The economy is populated by a unit mass of workers who work in one of N labor markets, indexed by $n \in \{1, \ldots, N\}$. Labor markets differ in a productivity term, A_n, which determines the efficiency with which a homogeneous good is produced. Each labor market hosts two sectors, a *modern* sector (M) and a *traditional* sector (T), which differ in the technologies they operate and the regulations they face.

Workers are heterogeneous in their human capital, $z \in \mathbb{R}_+$, which determines the efficiency units of labor they supply. At any instant, a worker is described by the triple (n, S, z), consisting of her labor market n, her sector $S \in \{M, T\}$, and her human capital z. Workers are infinitely lived but exit the economy when a Poisson death shock arrives with intensity $\delta > 0$. Each worker who exits is replaced by a newborn, who draws initial human capital z from an exogenous distribution $\psi(z)$ and is free to choose the labor market in which to begin her career. Workers discount the future at rate $\rho > 0$, derive flow utility $u(c)$ from consumption, and cannot save. Therefore, consumption equals current labor income, inclusive of a proportional government subsidy defined below.

We denote by $N_n^S(z, t)$ the mass of workers in labor market n and sector S with human capital z at time t. The mass of workers with human capital z in market n is $N_n(z, t) = N_n^M(z, t) + N_n^T(z, t)$, and the total population of the market is $L_n(t) = \int_0^\infty N_n(z, t)\, \mathrm{d}z$, with sectoral counterparts $L_n^S(t) = \int_0^\infty N_n^S(z, t)\, \mathrm{d}z$. These cross-sectional distributions are endogenously determined by workers' labor-market and sectoral choices.

2.1.1 Production and Wages

There are two perfectly competitive representative firms in each labor market, one in the modern sector and one in the traditional sector. Both firms produce a homogeneous good that is freely traded across markets and serves as the *numeraire*. The two firms differ in the technologies they operate. A modern-sector firm in market n combines workers in proportion to their human capital, whereas a traditional-sector firm combines workers' human capital through a concave schedule $\phi(\cdot)$:

$$Y_n^M(t) = A_n \int_0^\infty z\, \ell_n^M(z, t)\, \mathrm{d}z, \qquad Y_n^T(t) = A_n \int_0^\infty \phi(z)\, \ell_n^T(z, t)\, \mathrm{d}z,$$

where $A_n > 0$ is the productivity of labor market n, and $\ell_n^S(z, t)$ is the mass of workers with human capital z employed in sector S at time t. Both technologies are linear in labor, so conditional on human capital z, the two sectors differ only in how effectively they translate skill into output. The modern sector is linear in each worker's skill, whereas the traditional sector exhibits diminishing returns to worker skill, capturing small-scale production and subsistence self-employment. Formally, we assume that $\phi(0) = 0$, $\phi(z) \geq 0$, $\phi'(z) > 0$, and $\phi''(z) < 0$ for all z, and that ϕ satisfies the Inada conditions $\lim_{z \to 0} \phi'(z) = \infty$ and $\lim_{z \to \infty} \phi'(z) = 0$.

Labor regulations differ across sectors. The modern-sector firm faces a payroll tax $\tau \geq 0$, while the traditional-sector firm avoids it. Since labor markets are perfectly competitive, firms pay each worker her marginal product of labor, net of regulatory costs, leading to the wage schedules

$$w_n^M(z) = \frac{A_n}{1+\tau} z, \qquad \text{and} \qquad w_n^T(z) = A_n \phi(z), \tag{1}$$

where $w_n^M(z)$ and $w_n^T(z)$ denote the wages of workers with skill z in labor market n in the modern and traditional sectors, respectively. We assume that payroll tax revenues are rebated by a central authority to all workers, regardless of their sector, through a proportional wage subsidy at rate $b(t)$: a worker earning wage w consumes $(1 + b(t))\, w$. Since production is linear in labor and (A_n, τ, ϕ) are time invariant, the wage schedules in (1) do not depend on aggregate employment or time. Hence, a worker's labor income changes over time only when her state (n, S, z) changes, while her disposable income can also change through the subsidy $b(t)$.

There are two properties of the wage schedules in (1) worth highlighting. First, within a labor market, modern- and traditional-sector wages satisfy a single-crossing property. At low skill levels, traditional-sector wages are higher than modern-sector wages because of both technological differences in production, captured by $\phi(\cdot)$, and the presence of labor regulations in the modern sector. At high skill levels, wages in the modern sector are higher than in the traditional sector because the former increase linearly with worker skill, while the latter increase at a decreasing rate due to the concavity of $\phi(\cdot)$. Hence, absent any dynamics, the wage schedules in (1) imply that, within labor markets, high-skill workers sort into the modern sector and low-skill workers into the traditional sector. Of course, workers care not only about static returns. In Section 2.5, we show how this sorting pattern extends once we account for human capital accumulation.

Second, we assume that firms are perfectly competitive in the sense that they take wages as given. Since production in each sector exhibits constant returns to scale in the number of workers of a given skill level, firms pay each worker her marginal product, leading to the wage schedules in (1). This notion of perfect competition contrasts with Jarosch et al. (2021), who assume that firms can price the learning opportunities they provide to workers. In their framework, wages reflect not only workers' marginal products but also the value of learning at the firm. In contrast, as we explain in Section 2.1.3, learning in our framework occurs at the labor-market level. Hence, we assume that firms cannot price workers' learning opportunities. This assumption implies that wages reflect only technological differences across sectors and labor markets, rather than differences in the learning environments they provide.

2.1.2 Labor Market Mobility

Workers move across labor markets subject to mobility frictions and costs. First, they cannot move instantly across markets. Instead, they remain in their current labor market until they receive a moving opportunity, which arrives according to a Poisson process with intensity λ. Second, when an opportunity arrives, a worker observes a vector of idiosyncratic location tastes $\{\varepsilon_m\}_{m=1}^N$, which we assume are independently and identically distributed across workers and markets according to a Type-I extreme value distribution with scale $1/\nu$. The parameter ν governs the dispersion of tastes: as $\nu \to \infty$, tastes vanish and all workers locate in the market offering the highest continuation value, while a smaller ν spreads workers more evenly across markets. After observing the collection of location tastes, a worker in market n may move to any market $m \in \{1, \ldots, N\}$ by paying a bilateral mobility cost ξ_{nm}, with $\xi_{nn} = 0$.

We assume that workers can freely switch sectors within a labor market. Accordingly, we denote by $V_n(z,t)$ the value of a worker with skill z in market n at time t. We later formally define $V_n(z,t)$ in equation (7) as the upper envelope of the sector-specific values.

Conditional on receiving a relocation opportunity, a worker chooses the market that maximizes her continuation value net of mobility costs and idiosyncratic tastes. The continuation value of labor market mobility is

$$\mathcal{M}_n[V](z,t) = \lambda \left(\mathbb{E}_\varepsilon \left[\max_m \{V_m(z,t) - \xi_{nm} + \varepsilon_m\} \right] - V_n(z,t) \right),$$

where the expectation is taken over the idiosyncratic location tastes, ε_m. Under the extreme value assumption, this continuation value takes the closed form

$$\mathcal{M}_n[V](z,t) = \lambda \left[\frac{1}{\nu} \log \left(\sum_{m=1}^N e^{\nu(V_m(z,t) - \xi_{nm})} \right) - V_n(z,t) \right], \tag{2}$$

and the probability that a worker with skill z who receives an opportunity in market n relocates to market m is given by

$$m_{nm}(z,t) = \frac{e^{\nu(V_m(z,t) - \xi_{nm})}}{\sum_{k=1}^N e^{\nu(V_k(z,t) - \xi_{nk})}}.$$

These shares, together with the death-and-birth process, govern the reallocation of workers across markets in the distributional dynamics below.

2.1.3 Human Capital Accumulation

Workers accumulate skill by learning from other workers in their labor market. However, learning is segmented across sectors and depends on the skill distribution of workers in each sector. Formally, human capital for a worker in market n and sector S follows a geometric Brownian motion:

$$\mathrm{d}\log z_n^S(t) = \gamma Z_n^S(t)\mathrm{d}t + \sigma_S \mathrm{d}W(t), \tag{3}$$

where $\gamma > 0$ governs the importance of learning from peers, $Z_n^S(t)$ is a measure of the stock of human capital in sector S and market n, which we call *vibrancy* and define below, $W(t)$ is a standard Wiener process, and $\sigma_S > 0$ is a sector-specific volatility. The skill evolution equation (3) has an endogenous drift component, which depends on $Z_n^S(t)$, and an exogenous volatility component, disciplined by σ_S, which captures sector-specific shocks to skills.[4]

The *vibrancy* of market n and sector S is defined as

$$Z_n^S(t) = \left[\int_0^\infty z^\theta g_n^S(z,t)\mathrm{d}z\right]^{\frac{1}{\theta}}, \tag{4}$$

where $\theta \geq 1$ and $g_n^S(z,t)$ is the effective peer-skill distribution faced by workers in market n and sector S, which we specify below.[5] The parameter θ governs how different parts of the skill distribution combine in fostering human capital accumulation. In general, vibrancy is higher in environments populated by more skilled peers. When $\theta = 1$, vibrancy is the mean of peer human capital, so skills are perfect substitutes in learning. As $\theta \to \infty$, vibrancy is determined by the human capital of the most skilled worker.

The effective peer-skill distribution $g_n^S(z,t)$ is a mixture distribution that places weight π^S on workers in sector S and weight $1 - \pi^S$ on workers in the other sector, which we denote by $-S$. Hence, the effective peer-skill distribution takes the form

$$g_n^S(z,t) = \frac{\pi^S N_n^S(z,t) + (1-\pi^S)N_n^{-S}(z,t)}{\pi^S L_n^S(t) + (1-\pi^S)L_n^{-S}(t)}. \tag{5}$$

This expression is a well-defined density over workers' skill in market n and sector S: $g_n^S(z,t) \geq 0$ for all z, and $\int_0^\infty g_n^S(z,t)\,\mathrm{d}z = 1$.

The intuition behind (5) is as follows. Workers in market n can potentially be exposed to any worker with skill level z in the same labor market. However, exposure is not uniform across sectors. The parameter π^S captures the degree of *learning segmentation* by measuring how biased the interactions of workers in sector S are toward their own sector. When $\pi^S = 1$, workers in sector S learn only from workers in their own sector, so learning is fully segmented. When $\pi^S = 0$, workers in sector S learn only from workers in the other sector. Finally, when $\pi^S = 1/2$, workers are equally exposed to both sectors and learning is fully integrated.

[4]For example, sector-specific working conditions may generate different loadings σ_S on idiosyncratic skill shocks.

[5]Our general theory also admits $0 < \theta < 1$. However, restricting attention to $\theta \geq 1$ simplifies the sufficient conditions for a sorting equilibrium below.

2.2 Worker Values and Labor Supply

We now characterize workers' dynamic labor supply decisions. A worker in market n and sector S receives flow utility $u\big((1+b(t))\,w_n^S(z)\big)$ from consuming her subsidized wage. Over time, she accumulates human capital according to (3), can reallocate across labor markets when a moving opportunity arrives, and exits the economy when a death shock arrives.

To write the worker's problem, it is useful to express the law of motion for human capital in levels. By Itô's lemma, z evolves as

$$\mathrm{d}z_n^S(t) = \mu_n^S(t)\, z\, \mathrm{d}t + \sigma_S\, z\, \mathrm{d}W(t), \qquad \mu_n^S(t) \equiv \gamma\, Z_n^S(t) + \frac{1}{2}\sigma_S^2. \tag{6}$$

With this notation, the value of a worker with skill z in market n satisfies the Hamilton-Jacobi-Bellman (HJB) equation

$$\begin{aligned}(\rho+\delta)\, V_n(z,t) = \max_{S\in\{M,T\}} \Big\{ u\big((1+b(t))\, w_n^S(z)\big) + \mu_n^S(t)\, z\, \partial_z V_n(z,t) + \frac{\sigma_S^2}{2}\, z^2\, \partial_{zz} V_n(z,t) \Big\} \\ + \mathcal{M}_n[V](z,t) + \partial_t V_n(z,t).\end{aligned} \tag{7}$$

Equation (7) reveals four forces that shape workers' sectoral and labor-market decisions. The left-hand side captures the effective discounting of the worker's value, adjusted for the death rate. On the right-hand side, the first term is the flow value of consumption. The second term captures the continuation value from the expected growth of human capital, which is endogenously determined by peer composition in each sector. The third term captures the effect of skill volatility on the worker's value, which differs across sectors because skill shocks are sector specific. Finally, the last terms capture the option value of mobility across labor markets and changes in the value function over time. The mobility term does not depend on workers' sectoral choices because they can freely switch sectors within a labor market.

How do workers choose which sector to work in? Since there are no within-market reallocation costs, sector choice is embedded directly in the worker's dynamic problem and the labor supply decision $S_n^*(z,t)$ attains the maximum in (7). The optimal sectoral choice, together with the choice of destination market embedded in the mobility shares $m_{nm}(z,t)$, fully summarizes workers' policies. We characterize this labor supply decision in Section 2.5.

2.3 Skill Distribution Dynamics

We now derive the law of motion for the distribution of workers' human capital across markets and sectors. First, the flux of mass through skill level z in market n and sector S is

$$J_n^S(z,t) = \big(\mu_n^S(t) - \sigma_S^2\big)\, z\, N_n^S(z,t) - \frac{\sigma_S^2}{2} z^2\, \partial_z N_n^S(z,t). \tag{8}$$

Let $\mathbb{1}_n^S(z,t)$ be an indicator equal to one if sector S is optimal for a worker with skill z in market n, as implied by (7), and zero otherwise. Then, the mass of workers with skill level z in labor market n and sector S evolves according to the Kolmogorov forward equation (KFE):

$$\begin{aligned}\partial_t N_n^S(z,t) = -\partial_z J_n^S(z,t) + \lambda \left(\sum_{k=1}^{N} m_{kn}(z,t) N_k(z,t) \mathbb{1}_n^S(z,t) - N_n^S(z,t) \right) \\ + \delta \left[\psi(z) \Pi_n(z,t) \mathbb{1}_n^S(z,t) - N_n^S(z,t) \right],\end{aligned} \tag{9}$$

where $\Pi_n(z,t)$ is the probability that a newborn with skill z chooses market n:

$$\Pi_n(z,t) = \frac{e^{\nu V_n(z,t)}}{\sum_{k=1}^{N} e^{\nu V_k(z,t)}}. \tag{10}$$

The KFE in (9) combines three forces that shape the distribution of workers across sectors and labor markets. Anticipating the sorting equilibrium structure characterized in Proposition 1, sectoral decisions take the form of a threshold, $\bar{z}_n(t)$, such that workers with skill above the threshold choose the modern sector, while workers with skill below it choose the traditional sector. With this structure in mind, we now interpret each of the three terms in (9).

The first term, $-\partial_z J_n^S(z,t)$, captures changes in the distribution induced by human capital dynamics. By (6), workers' skill grows in expectation at rate $\mu_n^S(t)$, reflecting learning from peers, and fluctuates with idiosyncratic shocks scaled by σ_S. Away from the threshold $\bar{z}_n(t)$, both forces reshape the skill distribution within a sector. Near the threshold, they can also induce workers to switch sectors. Traditional workers who accumulate enough human capital find it optimal to move into the modern sector. Similarly, positive skill shocks can push traditional workers above the threshold, while negative shocks can move modern workers back into the traditional sector.

The second term captures the net reallocation of workers across labor markets. Workers who receive a moving opportunity choose among labor markets according to the choice probabilities $m_{kn}(z,t)$. Once in the destination market, they enter the sector that delivers the highest value, as indicated by $\mathbb{1}_n^S(z,t)$. Because the modern-sector threshold varies across labor markets, moving across markets can also induce workers to switch sectors.

Finally, the third term captures death turnover. Workers exit the economy at rate δ, while newborns enter with human capital drawn from $\psi(z)$ and choose market n with probability $\Pi_n(z,t)$. After choosing a market, newborns enter the sector that delivers the highest value. Equation (10) reflects that newborns, like incumbent workers who relocate, draw idiosyncratic location tastes and sort into the market that offers them the highest value. This channel changes the skill distribution because newborns draw new initial skill levels. It also reallocates mass across labor markets and sectors, since newborns may choose a different market or sector from the workers they replace.

The system is closed by a boundary condition stating that mass vanishes in the upper tail:

$$\lim_{z\to\infty} N_n^S(z,t) = 0, \qquad S \in \{M, T\}.$$

2.4 Equilibrium Definition

We are interested in a stationary equilibrium of this economy in which the cross-sectional distributions are time invariant, $\partial_t N_n^S(z,t) = 0$, and so are the value functions, $\partial_t V_n(z,t) = 0$. We therefore drop the time index from all equilibrium objects. Although individual workers relocate across markets, switch sectors, and accumulate skill over their lives, aggregate objects and the joint distribution of workers across markets, sectors, and human capital remain unchanged.

A stationary equilibrium consists of wages $w_n^M(z)$ and $w_n^T(z)$, value $V_n(z)$, labor supply decisions $S_n^*(z)$, sectoral masses $N_n^M(z)$ and $N_n^T(z)$, effective peer-skill distributions $g_n^M(z)$ and $g_n^T(z)$, vibrancies Z_n^M and Z_n^T, and subsidy rate b, such that:

(i) Optimal labor demand. Firms maximize profits, so wages satisfy (1).

(ii) Workers' dynamic problem. The value $V_n(z)$ and labor supply $S_n^*(z)$ are given by (7).

(iii) Stationary distribution. The sectoral masses solve the Kolmogorov forward equation (9) with its right-hand side equal to zero, together with the condition that mass vanishes in the upper tail.

(iv) Learning consistency. The effective peer-skill distributions $g_n^S(z)$ are given by (5), and the vibrancies Z_n^S coincide with those implied by the stationary distribution through (4).

(v) Government balanced budget. The government runs a balanced budget period by period,

$$b \sum_{n=1}^{N} \sum_{S \in \{M,T\}} \int_0^\infty w_n^S(z)\, N_n^S(z)\, \mathrm{d}z = \sum_{n=1}^{N} \int_0^\infty \tau\, w_n^M(z)\, N_n^M(z)\, \mathrm{d}z.$$

(vi) Labor market clearing. Labor demand equals labor supply in every market and sector, $\ell_n^S(z) = N_n^S(z)$, and the population adds up to the unit mass of workers,

$$\sum_{n=1}^{N} L_n = 1.$$

The definition of equilibrium highlights the local learning externality. Individual workers take vibrancies as given when making their labor supply decisions. Nevertheless, these vibrancies are endogenously determined by the resulting mass of workers across markets and sectors. In turn, workers' optimal sectoral choices affect the human capital evolution of others.

We solve for the stationary equilibrium numerically using a finite-difference scheme, following Achdou et al. (2022). Appendix C provides a detailed description of the algorithm.

2.5 Equilibrium Characterization

We now characterize the stationary equilibrium in three steps. First, conditional on the existence of values and an invariant distribution, we provide conditions under which workers sort across sectors, with more productive workers selecting into the modern sector. Second, we show that, under additional conditions, such a *sorting equilibrium* exists. Third, we discuss uniqueness. All proofs, together with auxiliary lemmas, are relegated to Appendix A.

From (7), it is useful to define the *flow advantage* of the modern sector,

$$\Delta_n(z) \equiv \underbrace{u\big((1+b)w_n^M(z)\big) - u\big((1+b)w_n^T(z)\big)}_{\text{static gain}} + \underbrace{\left(\mu_n^M - \mu_n^T\right) z V_n'(z) + \frac{\sigma_M^2 - \sigma_T^2}{2} z^2 V_n''(z)}_{\text{dynamic gain}}, \tag{11}$$

so that $S_n^*(z) = M$ exactly when $\Delta_n(z) \geq 0$. The static gain compares the flow utility workers obtain across sectors, which is determined by the potential wages in each sector. The dynamic gain captures differences in the human capital dynamics offered by each sector. First, sectors differ in expected skill growth, pinned down by μ_n^M and μ_n^T. These expected gains are valued through the slope of the value function. Second, sectors expose workers to different skill shocks, determined by σ_M^2 and σ_T^2, which are valued through the curvature of the value function. Worker sorting takes a cutoff form in market n when $\Delta_n(z)$ crosses zero only once, from below.

We first introduce two functional-form assumptions for utility and returns in the traditional sector under which we obtain sharp sorting results. Importantly, these are the same functional-form assumptions that we impose in the quantitative analysis in Section 4.

Assumption 1 (Functional forms)**.** Workers have log utility, $u(c) = \log c$, and the traditional technology is $\phi(z) = z^\eta$, with $\eta \in (0,1)$.

Under Assumption 1, we can characterize the sorting cutoff in the static version of our model. Let

$$\hat{z} \equiv (1+\tau)^{\frac{1}{1-\eta}}. \tag{12}$$

Then, from equation (11), we can infer that, absent any dynamic gains, workers with $z \geq \hat{z}$ select into the modern sector, while workers with $z < \hat{z}$ select into the traditional sector. Intuitively, this static cutoff is increasing in τ, since higher payroll taxes depress modern-sector wages and make that sector less attractive to the marginal worker. Similarly, the cutoff is increasing in η, since a higher η raises the marginal productivity of traditional-sector workers and, in turn, their wages. Moreover, because both η and τ are common across the economy, the static cutoff is invariant across markets.

How can the static sorting equilibrium be extended to the dynamic setting? The expression in (11) suggests that, as long as the modern sector provides better learning opportunities than the traditional sector in each market, $Z_n^M \geq Z_n^T$, and the volatility of skill shocks does not differ too much across sectors, the static sorting result should extend to the dynamic learning environment. Assumption 2 introduces a regularity condition on the learning segmentation parameters that helps ensure the former condition holds.

Assumption 2 (Consistent segmentation)**.** The segmentation parameters satisfy $\pi^M + \pi^T \geq 1$.

Assumption 2 rules out learning interactions that are biased toward the opposite sector on net. It holds, in particular, whenever workers in each sector are at least as likely to interact with peers in their own sector as with peers in the other sector, $\pi^M \geq 1/2$ and $\pi^T \geq 1/2$, including the case of random interactions, $\pi^M = \pi^T = 1/2$.[6]

Finally, to control the stationary skill distribution and the vibrancies it generates, we impose joint restrictions on worker turnover, skill volatility, and the entry distribution.

Assumption 3 (Turnover dominates learning)**.** Let $\theta \geq 1$ be the vibrancy parameter in (4), let $m_\psi(q)$ denote the q-th moment of the entry distribution ψ, and let $\sigma \equiv \max\{\sigma_M, \sigma_T\}$. We assume the following:

(i) $\theta^2\sigma^2/2 < \delta$.

(ii) There exists $\varepsilon > 0$ such that $m_\psi(\theta + \varepsilon) < \infty$.

(iii) The θ-th moment of the entry distribution satisfies

$$m_\psi(\theta) \leq \kappa \frac{\left(\delta - \theta^2 \frac{\sigma^2}{2}\right)^{\theta+1}}{(\theta+1)^{\theta+1}\,\gamma^\theta\,\delta}, \tag{13}$$

where $\kappa \in (0, 1]$ is defined in (A5) in the Appendix.

Assumption 3 requires worker turnover to be sufficiently high relative to the learning process and the upper tail of the entry skill distribution.[7] In our quantitative exercise, the entry distribution is Pareto with unit scale and shape parameter ϑ, so that $m_\psi(\theta) = \vartheta/(\vartheta - \theta)$ provided $\vartheta > \theta$. Assumption 3 then reduces to a lower bound on the Pareto shape parameter, $\vartheta \geq \theta R/(R-1)$, where R denotes the right-hand side of (13). Hence, the newborn skill distribution must be sufficiently thin-tailed for a stationary equilibrium to exist. This condition is easier to satisfy when worker turnover δ is high or when the importance of learning from peers, γ, is low.

Assumption 3 also has a natural mathematical interpretation. It is a drift condition in the sense of Meyn and Tweedie (1993): worker turnover pulls the skill distribution toward the entry distribution faster than peer learning spreads it out.

Proposition 1 (Existence of a Sorting Equilibrium)**.** Suppose Assumptions 1–3 hold. Then, there exists $\Sigma > 0$ such that, whenever $|\sigma_M - \sigma_T| < \Sigma$, a stationary equilibrium with positive sorting exists: there are finite cutoffs $\bar{z}_n$ such that $S_n^*(z) = T$ for $z < \bar{z}_n$ and $S_n^*(z) = M$ for $z \geq \bar{z}_n$. Moreover, if learning is sufficiently segmented, $\pi^M > 1/2$ and $\pi^T > 1/2$, then $\bar{z}_n < \hat{z}$ for all n.

Proof. See Appendix A.3. □

Proposition 1 formalizes the main mechanism of the model. Since workers sort across sectors based on their human capital, the modern sector attracts the most skilled workers. This concentration of

[6] Assumption 2 turns out to be the empirically relevant configuration, since our estimates in Section 4, which do not impose this assumption, reveal own-sector bias in both sectors.

[7] Although somewhat technical, each condition has a simple role in ensuring the existence of a stationary equilibrium. Condition (i) guarantees that the stationary skill distribution has a finite θ-th moment. Condition (ii) ensures that this moment changes continuously with the learning environment. Finally, condition (iii) ensures that vibrancies remain bounded in any stationary allocation.

skilled workers makes the modern sector a better learning environment, so forward-looking workers with sufficiently high skill find it optimal to choose that sector. Sorting reinforces itself: skilled workers select into the modern sector, their presence improves learning in that sector, and better learning opportunities foster faster human capital accumulation relative to the traditional sector. Workers with very low levels of human capital, instead, value more the static gains offered by the traditional sector, at the expense of future wage growth.

This logic also explains why the dynamic cutoff lies below the static cutoff when learning is sufficiently segmented. In the static model, workers choose sectors only based on current wages. In the dynamic model, they also value future skill growth. Since the modern sector provides better learning opportunities, some workers enter the modern sector even when their current wage would be higher in the traditional sector. These marginal workers are willing to exchange lower wages today for better learning opportunities that imply higher wages in the future. Therefore, more workers select into the modern sector than static wage comparisons alone would imply. The condition that sectoral skill volatility is not too different ensures that this learning advantage is not overturned by differences in risk.

Having established existence, a natural question is when the equilibrium is unique. Conditional on the vector of vibrancies across markets and sectors, $Z \equiv \{Z_n^M, Z_n^T\}_{n=1}^N$, all remaining equilibrium objects are uniquely determined. Values are pinned down by (7), the cutoff policies are unique because the flow advantage is strictly increasing in $\log z$, the invariant distribution is determined by (9), and the subsidy rate follows from the government budget constraint. Any multiplicity must therefore arise from the finite-dimensional fixed-point problem $Z = T(Z)$. Our next result shows that this fixed point is also unique when the learning externality is not too strong.

Proposition 2 (Uniqueness)**.** Suppose the conditions of Proposition 1 hold. Then, there exists $\bar{\gamma} > 0$ such that, for all $\gamma \in (0, \bar{\gamma})$, the sorting equilibrium of Proposition 1 is the unique stationary equilibrium with vibrancies below a threshold Z_H^* defined in Appendix A.

Proof. See Appendix A.4. □

Proposition 2 says that the sorting equilibrium is unique when peer learning is not too strong for human capital accumulation. When learning from peers is sufficiently strong, however, we cannot rule out multiple equilibria. The key difference across potential equilibria is the level of human capital they sustain. In a high-learning equilibrium, workers expect strong learning in the modern sector, enter it earlier in their careers, and spend more time accumulating skills quickly. This keeps human capital and vibrancy high, validating their initial expectations. In a low-learning equilibrium, workers expect weaker learning, enter the modern sector later, and accumulate skills more slowly, sustaining a lower level of human capital and vibrancy. Across markets, similar forces may determine which location becomes the high-vibrancy hub when fundamentals are similar. The threshold Z_H^* in Proposition 2 rules out precisely these self-fulfilling high-learning configurations.

In our framework, three forces work against this multiplicity. First, idiosyncratic tastes disperse workers across markets. Second, workers continuously exit the labor market, bringing in new workers from the common entry distribution. Third, productivity differences break symmetry across markets. Reassuringly, the predictions we derive next rely only on the sorting structure in Proposition 1, and therefore hold in any sorting equilibrium.

2.6 Model Predictions

The stationary equilibrium delivers two main predictions that organize our empirical analysis. The first is the sorting equilibrium established in Proposition 1. The second is a dynamic modern-sector wage premium. Conditional on the labor market, modern-sector workers experience faster expected wage growth than traditional-sector workers, as formalized in the following lemma.

Lemma 1 (Dynamic modern-sector premium)**.** *Consider a sorting equilibrium as in Proposition 1, and fix a market n. If learning is sufficiently segmented, $\pi^M > 1/2$ and $\pi^T > 1/2$, then there exists $\bar{h} > 0$ such that, for every horizon $h \in (0, \bar{h}]$, the expected difference in log-wage growth between modern- and traditional-sector workers in market n from t to $t+h$ is strictly positive:*

$$\mathbb{E}_t\big[\Delta \log w^M_{n,t+h}\big] - \mathbb{E}_t\big[\Delta \log w^T_{n,t+h}\big] \geq \gamma\big(Z^M_n - \eta\, Z^T_n\big)\, h > 0.$$

Proof. See Appendix A.5. □

Lemma 1 is the main novel testable prediction of our theory. When learning is segmented, workers in both sectors interact more frequently with peers from their own sector. Hence, vibrancies in the stationary sorting equilibrium satisfy $Z^M_n > Z^T_n$. This result reflects the fact that the modern sector attracts more skilled workers, so the modern peer-skill distribution first-order stochastically dominates the traditional one. Consequently, modern-sector workers accumulate human capital faster. Importantly, because the traditional technology is concave, a given increase in human capital raises traditional-sector wages with elasticity $\eta < 1$. Hence, although technological differences across sectors are not necessary for the dynamic premium to arise, they amplify it. A reallocation term, arising from sector switching, reinforces the premium: workers who cross the cutoff from below trade the higher traditional wage for the lower modern wage on the band between $\bar{z}_n$ and $\hat{z}$, which lowers measured traditional wage growth and raises measured modern wage growth.

In the next section, we test Proposition 1 and Lemma 1 in the Chilean data. We first test the sorting prediction using the distribution of estimated worker skill across sectors. We then test the dynamic prediction by estimating, at each horizon h, the average difference in wage growth between modern- and traditional-sector workers.

3 Empirical Analysis

In this section, we test the main model predictions. We begin by describing the data and our definitions of modern and traditional jobs. Our analysis focuses on Chile, where we can exploit rich worker survey data from an important developing economy in which a large fraction of workers still operate in the traditional sector.

3.1 Data

Our main data source is the Chilean *Encuesta de Protección Social* (EPS). The EPS is a comprehensive longitudinal survey designed to gather data on various aspects of social protection. The survey spans five waves conducted in 2002, 2004, 2006, 2009, and 2015.[8] We use two blocks of the survey. First, we use the block containing information on individuals' demographics, such as age and education. Second, we use the block containing individuals' job histories dating back to 1980.[9] The job history includes information on job type, occupation, economic sector, region, weekly hours worked, starting and ending dates, type of contract, pension fund contributions, job category, and the number of workers in the firm. Given our definition of modern and traditional jobs below, we restrict our sample to start in the 2004 wave, the year in which individuals with and without pension affiliation were included, making the survey representative of all workers.

We define modern- and traditional-sector jobs in the data in a way that is consistent with our framework. In the model, modern-sector workers are those employed by firms that comply with labor regulations. Accordingly, we define a modern-sector job as one with a formal labor contract and pension contributions, which maps to the payroll tax in the model. We define a traditional-sector job as any job that does not comply with these labor regulations. In doing so, our definitions of modern and traditional employment coincide with the standard distinction between formal and informal work used in the literature (Ulyssea, 2020b) and typically used by statistical agencies.[10]

The EPS offers four advantages for analyzing employment dynamics among modern and traditional workers. First, the detailed information available for each job allows us to classify workers as modern or traditional based on their contract type and pension fund contributions. Second, the data on disposable monthly income and hours worked allow us to construct hourly wages for jobs starting in 2002.[11] Third, although the survey is conducted only in selected years, the job-history block allows us to reconstruct each worker's employment history since 1980. We aggregate workers' jobs to construct our baseline sample, an unbalanced annual panel with more than 17,000 workers observed between 2002 and 2016.[12] The length and coverage of the panel allow us to track modern and traditional workers over long periods. In particular, we observe 50% of workers in our sample for at least five years and 20% for at least ten years.[13] Finally, although we restrict the analysis to jobs active from 2002 onward because of wage availability, we use workers' job histories since 1980 to measure experience in the modern and traditional sectors separately.[14]

We exclude certain types of workers from our analysis. First, in accordance with Chilean labor regulations, we include male workers aged 15 to 65 and female workers aged 15 to 60, aligning

[8]We exclude the 2012 and 2019 waves from our analysis. The 2012 wave is not representative at the national level, and the questions in 2019 changed because of the COVID-19 pandemic.

[9]When an individual enters the survey, they are asked for their job history since 1980. If, in a specific wave, the individual was already part of the survey, they are asked about their job history since the survey's last wave.

[10]Chilean labor law requires workers to be enrolled in the pension system and contribute 10% of their salary.

[11]We construct wages for 2002 and 2003 retroactively using information from workers' job histories.

[12]For workers with multiple jobs in a given year, we retain the job with the highest total hours worked.

[13]In contrast, Meghir et al. (2015) and Samaniego De La Parra and Fernández Bujanda (2020) use panels that follow workers for nine months over roughly one year in Brazil and five quarters in Mexico, respectively.

[14]We compute experience by dividing cumulative hours worked up to a particular year by the number of hours corresponding to a full-time schedule of 48 hours per week.

Table 1: Summary Statistics

	(1) Modern	(2) Traditional	(3) All
Fraction of workers	0.70	0.30	···
Mean log wage	0.81	0.44	0.70
Std. deviation log wage	0.63	0.69	0.67
Mean weekly working hours	46.00	42.19	44.85
Fraction of male workers	0.63	0.59	0.62
Mean experience (years)	15.24	15.38	15.28
Transitions (by initial status)			
Frac. of modern workers next year	0.97	0.08	···
Frac. of traditional workers next year	0.03	0.92	···
Number of observations	86,646	35,114	121,760
Number of workers	···	···	17,260

Notes: Table 1 displays summary statistics for the baseline sample 2002–2016. We include male workers aged 15 to 65 and female workers aged 15 to 60. We exclude workers without remuneration, and public-sector and armed forces employees. Wage is the real hourly wage in 2004 US dollars. The variable experience corresponds to the equivalent in years of a full-time work schedule of 48 hours per week.

with the country's legal working and retirement ages for men and women, respectively. Second, in our baseline specifications, we omit unpaid workers, as well as public-sector and armed forces employees. Importantly, our data allow us to include self-employed workers and entrepreneurs, who represent a large fraction of traditional-sector workers.[15]

Table 1 displays summary statistics for our baseline sample. Three key points are worth highlighting. First, wages are, on average, higher for modern workers than for traditional workers. Nevertheless, wages among traditional workers are more dispersed than those among modern workers, consistent with previous findings. Second, modern and traditional workers work similar hours per week and have similar years of experience. This similarity supports our modeling choice of abstracting from labor supply decisions and from an explicit allocation of time between working and learning. Third, transition probabilities between the modern and traditional sectors are highly asymmetric. On average, 8% of traditional workers move to the modern sector in the following year, whereas only 3% of modern workers move to the traditional sector. Importantly, these transition probabilities are computed by restricting the sample to active workers, thereby excluding transitions into and out of unemployment. Appendix B provides a more detailed overview of the data and sample construction, while Appendix D reports additional descriptive statistics, including the share of modern workers by age, education, occupation, industry, and firm size.

[15] We provide robustness exercises in which we restrict the sample to salaried workers only.

Figure 1: Wages Over the Life Cycle for Modern and Traditional Workers

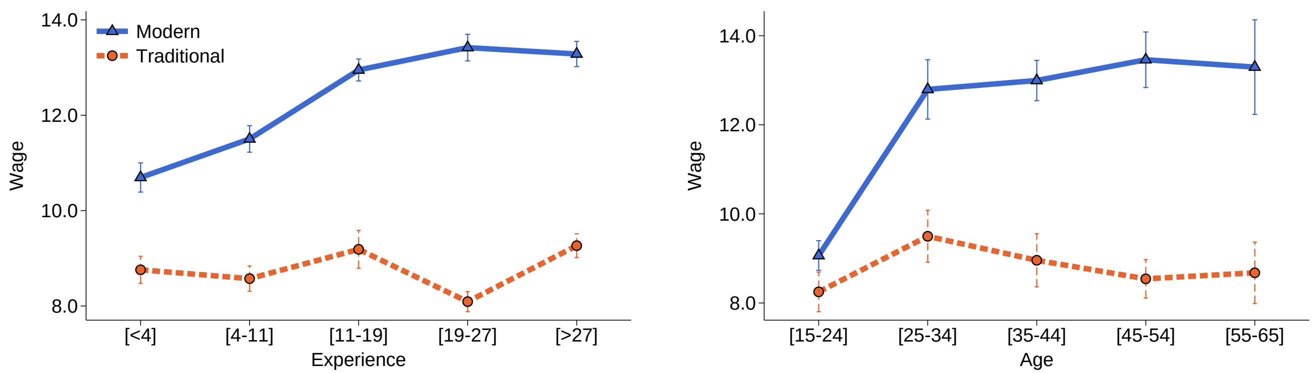

(a) Wage-experience profiles **(b)** Wage-age profiles

Notes: Figure 1 displays wage paths over the life cycle for modern and traditional workers. Panel 1(a) shows the average wage for each experience quintile and panel 1(b) for each 10-year age bin. Vertical dashed lines denote 95 percent confidence intervals.

3.2 Testing the Model's Predictions

This section presents empirical evidence on wages for modern and traditional workers that is consistent with our model. We begin by documenting wage-experience profiles, which reveal different wage growth patterns across sectors. We then test the model's main predictions in two steps. First, we present evidence that high-skill workers sort into the modern sector. Second, we test for the presence of a dynamic modern-sector wage premium.

Figure 1 presents wage-experience and wage-age profiles for modern and traditional workers. The left panel displays the wage-experience profiles. We first classify workers as modern or traditional according to our definition, divide them into five experience bins, and compute the average wage within each bin and sector. The right panel displays wage-age profiles, which are constructed analogously using workers' age. Both panels reveal stark differences in life-cycle wage growth between modern and traditional workers.

Figure 1 shows substantial differences in wage levels and wage growth between modern and traditional workers over the life cycle. Focusing first on the wage-experience profiles, modern workers begin their careers with wages around 20% higher than those of traditional workers. This wage gap then widens over the life cycle, reaching more than 40% by the end of workers' careers. The divergence is mainly driven by wage growth among modern workers, while traditional workers' wages remain mostly flat over time. The wage-age profiles display a similar pattern. Although the wage gap early in the life cycle is smaller, at around 12%, it reaches a similar magnitude by the end of workers' careers. Interestingly, the timing of the divergence differs across the two profiles. In the wage-experience profiles, the gap widens gradually over the life cycle, whereas in the wage-age profiles most of the divergence occurs early.

These life-cycle wage patterns for modern and traditional workers align with recent findings on wage growth across countries. Lagakos et al. (2018) document that wages in developed countries increase more over the life cycle than wages in developing economies. Our findings suggest that the modern sector behaves like a "developed-economy labor market," whereas the traditional sector displays patterns typical of a "developing-economy labor market." In Appendix D, we report the same wage profiles restricting the sample to salaried workers. The patterns remain consistent under this alternative specification.

We interpret these initial findings as motivating evidence for the main mechanism of our model. The initial wage differences are consistent with more productive workers sorting into the modern sector. The subsequent widening of the wage gap over the life cycle is also consistent with modern-sector workers experiencing faster human capital accumulation because of better learning opportunities. In the following subsections, we provide more direct tests of both mechanisms.

3.2.1 Worker Sorting

We investigate worker sorting across the modern and traditional sectors in two ways. First, we examine whether workers' observable characteristics that are potentially related to skill are correlated with their sectoral choices. Perhaps not surprisingly, Figure D2 in the Appendix shows that workers with higher educational attainment are more likely to be employed in the modern sector. The share of modern workers among those with no schooling is slightly above 50%. In contrast, more than 80% of workers with two or more years of college education are employed in the modern sector. To the extent that educational attainment is positively correlated with skill, these patterns support the idea that more skilled workers sort into the modern sector.

Second, we study the extent to which workers with higher unobserved skill are more likely to be employed in the modern sector. To do so, we study the modern-traditional wage gap in levels and assess the role of worker sorting in explaining this gap. We estimate the following regression:

$$\log w_{i,t} = \beta \text{Modern}_{i,t} + \Gamma X_{i,t} + \alpha_t + \alpha_i + \zeta_{i,t}, \tag{14}$$

where $\log w_{i,t}$ is the log wage of worker i at time t, $\text{Modern}_{i,t}$ is an indicator equal to one if worker i is employed in the modern sector in year t and zero if she is employed in the traditional sector, and $X_{i,t}$ is a vector of worker characteristics that includes age, education, gender, occupation, industry, region, firm size, and experience in the modern and traditional sectors. Moreover, α_t and α_i denote time and worker fixed effects, respectively.

The worker fixed effects, α_i, capture time-invariant worker skill that is rewarded in both sectors. Importantly, these fixed effects capture skill differences beyond the observable characteristics included in $X_{i,t}$, such as age, education, and experience in each sector. Our framework predicts that more skilled workers sort into the modern sector. Therefore, through the lens of the model, the distribution of worker fixed effects among modern workers should lie to the right of the corresponding distribution among traditional workers.

Figure 2 presents the distribution of estimated worker fixed effects for modern and traditional workers. We retain one observation per worker and assign each worker to the sector in which she is observed most frequently. The figure provides evidence of worker sorting. Panel 2(a) shows that traditional workers are overrepresented at the bottom of the skill distribution, whereas

Figure 2: Worker Fixed Effects for Modern and Traditional Workers

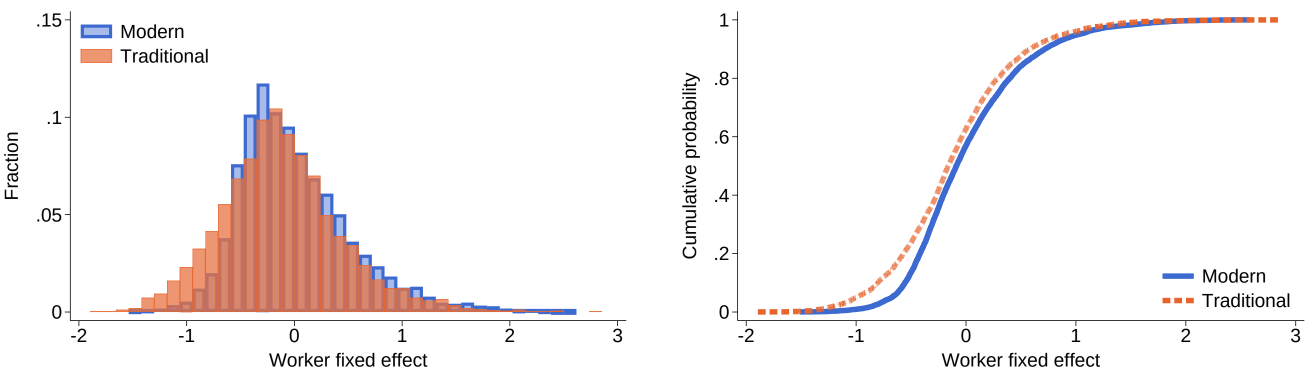

(a) Histogram

(b) Cumulative distribution

Notes: Figure 2 displays the distribution of the worker fixed effects α_i estimated from equation (14), controlling for age, education, gender, occupation, industry, region, firm size, experience in each sector, and time fixed effects. We keep one observation per worker and assign workers to the sector in which we observe them most often. Panel 2(a) shows the histogram and panel 2(b) the empirical cumulative distribution function of the worker fixed effects for modern and traditional workers.

modern workers are concentrated at the top. Panel 2(b) shows that the cumulative distribution of worker fixed effects for modern workers lies everywhere below that of traditional workers. This implies that the modern-sector skill distribution first-order stochastically dominates the traditional-sector distribution. Moreover, the estimated correlation between workers' fixed effects, α_i, and the modern-sector indicator, $\text{Modern}_{i,t}$, is positive, at approximately 0.10, and statistically significant. Hence, consistent with our model, more skilled workers sort into the modern sector.

Table E1 in Appendix E reports the estimates of β in equation (14). Modern workers earn a wage premium even after conditioning on worker fixed effects and observable characteristics. Through the lens of our model, a wage premium among workers with the same skill level provides evidence of diminishing returns to worker skill in the traditional sector.

3.2.2 Dynamic Modern-Sector Premium

We now turn to the main novel prediction of our model: the dynamic modern-sector wage premium. We test this prediction in two steps. First, we examine the short- and medium-run effects of working in the modern sector on future wages. Second, we provide evidence that learning from better-paid peers in the modern sector is a plausible mechanism generating these persistent wage differences between modern- and traditional-sector workers.

We begin by studying how employment in the modern sector relates to future wage growth. To do so, we estimate a variant of (14) that relates workers' future wage growth to their sectoral status and a set of observable and unobservable characteristics. Specifically, we estimate the following relationship separately for different time horizons h:

$$\Delta \log w_{i,t+h} = \beta_h \text{Modern}_{i,t} + \Gamma X_{i,t} + \alpha_t + \alpha_i + \zeta_{i,t}, \tag{15}$$

Figure 3: Modern Sector Dynamic Wage Premium

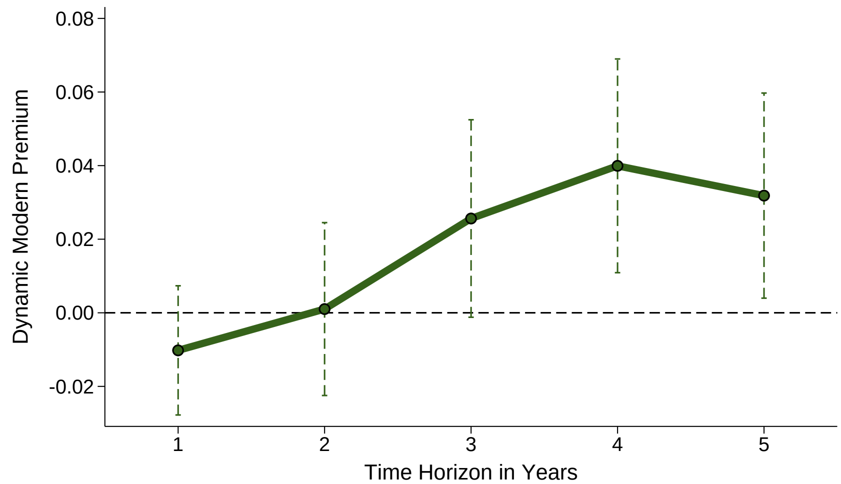

Notes: The figure displays the modern future wage premium based on the estimates of β_h from equation (15) including worker fixed effects. Each dot represents the estimated wage premium at horizon $t+h$: $\exp(\hat{\beta}_h)-1$, for $h = 1, \ldots, 5$. Controls include age, education, gender, occupation, industry, region, experience, wage decile, and time and worker fixed effects. Vertical dotted lines denote 95 percent confidence intervals.

where $\Delta \log w_{i,t+h}$ is the change in worker i's log wage between years t and $t+h$. The vector $X_{i,t}$ includes the same worker characteristics as in (14), together with wage-decile fixed effects. Moreover, α_t and α_i denote time and worker fixed effects, respectively. The parameter of interest is β_h, which captures the average difference in wage growth over h years between modern and traditional workers, conditional on observable characteristics and fixed effects.

Figure 3 presents the estimated future wage premium associated with working in the modern sector across different time horizons. The premium is statistically insignificant at short horizons but increases over time, reaching its peak after four years. At this horizon, modern workers experience wage growth that is approximately 4% higher than that of traditional-sector workers. Crucially, because the specification includes worker fixed effects, identification comes from workers who change sectoral status. This allows us to compare the wage growth trajectories of the same worker during periods of modern and traditional employment and to control for the potential sorting of workers with higher learning ability into the modern sector. Hence, the results suggest that workers who switch from the traditional sector to the modern sector experience cumulative wage gains in subsequent years.

We do not condition on workers remaining in the modern sector in subsequent years. This is consistent with our model, in which human capital is portable across sectors, and it matches the construction of the dynamic premium in Lemma 1, which classifies workers by their sector at the start of the horizon only. In addition, the estimated effects become statistically insignificant after five years. This is natural in our setting, since workers may switch sectors over time in response to idiosyncratic skill shocks.

Which forces drive the dynamic modern-sector wage premium? Following Jarosch et al. (2021) and Herkenhoff et al. (2024), we examine whether interactions with better-paid peers contribute to

Figure 4: Peer Effects on Wage Growth

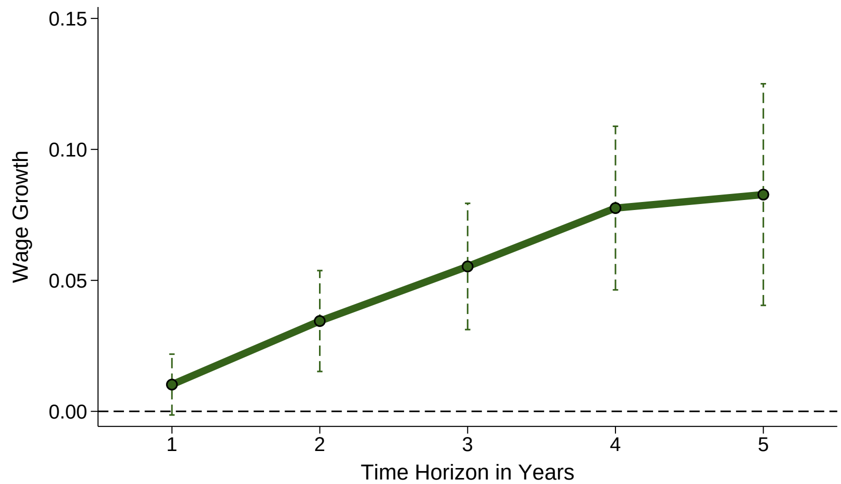

Notes: The figure displays the effect of peer wages on workers' future wage growth based on the estimates of β_h from equation (16). Peers are defined as all other workers in the same Region $\times$ Year $\times$ Industry $\times$ Occupation $\times$ Firm-Size Bracket. Each dot represents the estimated effect at the time horizon $t+h$. Controls include age, education, gender, occupation, industry, region, experience, wage decile, and time fixed effects. Vertical dotted lines denote 95 percent confidence intervals.

workers' wage growth. In our framework, workers interact with others in the same labor market, and access to more skilled peers accelerates human capital accumulation. Accordingly, we define a labor market in the data as a region $\times$ industry $\times$ occupation $\times$ firm-size bracket cell in a given year. For each worker i, we then compute the average wage of all other workers in the same labor market, denoted by $w_{-i,t}$, as a proxy for peer skill. We estimate the following reduced-form equation:

$$\Delta \log w_{i,t+h} = \beta_h \log w_{-i,t} + \Gamma X_{i,t} + \zeta_{i,t}, \tag{16}$$

where β_h captures how exposure to better-paid peers affects a worker's future wage growth, and $X_{i,t}$ contains the same worker-specific controls as in our previous specifications.

Figure 4 presents the estimated effects of peer quality on wage growth across different time horizons. We find strong evidence that workers exposed to better-paid peers experience significantly higher future wage growth. This effect increases with the time horizon, suggesting that peer quality has a cumulative impact on skill accumulation. In terms of magnitude, a one-standard-deviation increase in the average wage of a worker's peers is associated with wages that are approximately 4% higher five years later. These findings align with the literature on learning from coworkers (Jarosch et al., 2021; Herkenhoff et al., 2024) and learning in cities (Crews, 2024; Lhuillier, 2024). They also provide suggestive evidence that the quality of workers' interactions plays an important role in shaping their wage trajectories.

It is natural to consider alternative mechanisms that could drive the dynamic modern-sector premium. Our data allow us to examine whether the peer-learning channel is confounded by two other forces. First, sectors may differ in characteristics other than peer composition that affect wage growth. For instance, consistent with the results of Ma et al. (2024), modern-sector workers may have greater access to on-the-job training, leading to faster human capital accumulation than

Figure 5: Peer Effects on Wage Growth, Robustness

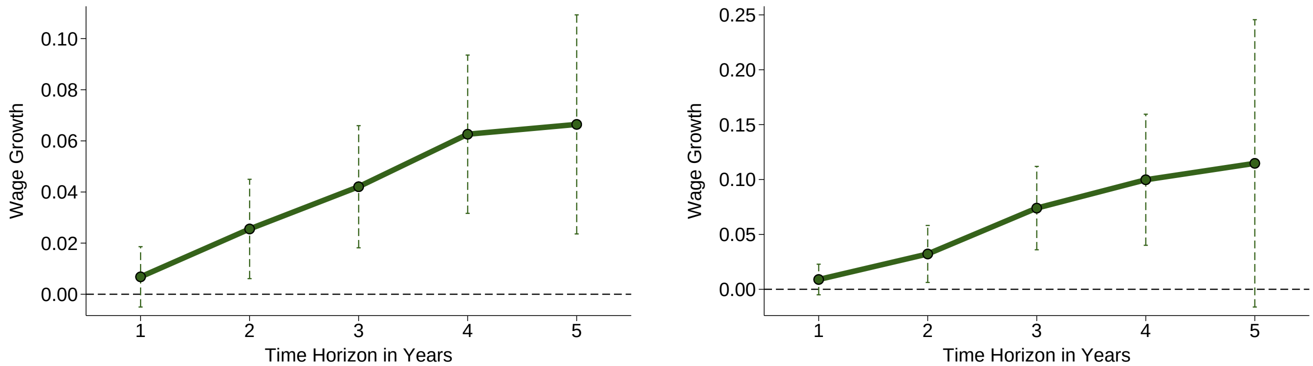

(a) Modern-sector status

(b) Wage-bill growth

Notes: The figure reports estimates of β_h from equation (16) under two robustness specifications. In Panel 5(a) we control for an indicator for modern-sector employment, $\text{Modern}_{i,t}$. In Panel 5(b) we control for the growth of the labor market's total wage bill between $t-2$ and $t-1$, $t-1$ and t, and t and $t+1$. The remaining controls are the same as in Figure 4. Vertical dotted lines denote 95 percent confidence intervals.

traditional-sector workers. To assess whether our peer-learning estimates are confounded by other sector-specific channels, such as training, we estimate a variant of (16) that directly controls for workers' modern-sector status.[16] Panel 5(a) reports the estimates of β_h from this specification. The estimates remain similar to those in Figure 4, suggesting that the peer-learning channel is not driven solely by other sector characteristics that affect human capital accumulation.

Second, an alternative mechanism is that the estimated effects reflect labor-market-level productivity gains that are passed on to workers rather than learning from peers. Following Jarosch et al. (2021), we estimate a version of (16) that controls for growth in the labor market's total wage bill between $t-2$ and $t-1$, $t-1$ and t, and t and $t+1$.[17] Figure 5(b) displays the estimates, which remain positive and increase with the horizon, suggesting that the results are not driven by common shocks to workers' labor markets. Although the standard errors increase at longer horizons, the point estimates are even larger in magnitude.

Having established that peers matter for wage growth, we now examine whether modern-sector workers systematically have access to better peers than traditional-sector workers. Figure 6 compares the distribution of peer wages, $w_{-i,t}$, for workers in the two sectors.

The figure reveals that modern workers indeed have better-paid peers. On average, the peers of modern workers earn wages approximately 20% higher than the peers of traditional workers. In addition, the distribution of peer wages for modern workers first-order stochastically dominates that of traditional workers. Because peer wages average over all workers in a labor market, the two distributions naturally overlap: modern and traditional workers who share the same labor market face similar peer groups. The dominance of the modern-sector distribution therefore reflects the sorting of modern workers into labor markets with better-paid peers. This finding provides the

[16] Perhaps surprisingly, participation in formal training programs appears rare in our data. Only 2% of job spells report participation in an employment or training program.

[17] Recall that our data do not allow us to identify the establishments or firms in which workers are employed.

Figure 6: Distribution of Peer Wages for Modern and Traditional Workers

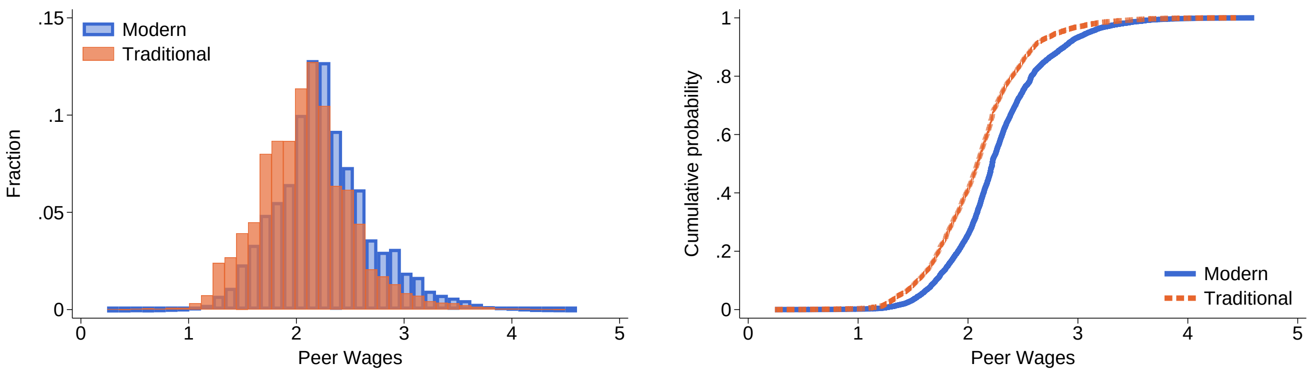

(a) Histogram

(b) Cumulative distribution

Notes: Figure 6 displays the distribution of log peer wages, $\log w_{-i,t}$, for modern and traditional workers. Panel 6(a) shows the histogram and panel 6(b) the empirical cumulative distribution function. Peers are defined as workers in the same Region × Year × Industry × Occupation × Firm-Size Bracket.

missing link in our narrative: modern workers experience higher wage growth partly because they interact with better-paid peers, and these interactions contribute to faster skill accumulation.

We note that this evidence captures differences in peer exposure across labor markets rather than learning segmentation within them. It is rare to observe workers' interactions directly within a labor market, and our data are no exception. Our model addresses this limitation by allowing the frequency of interactions between modern and traditional workers within a labor market to differ. We estimate this learning segmentation in our quantitative analysis and study its implications.

Finally, we provide suggestive evidence supporting our modeling choice for the learning technology. Equation (3) assumes that workers can learn from peers across the entire skill distribution within a labor market, from the least to the most skilled. One way to assess this assumption is to compare the effects of better-paid peers for workers at the top and bottom of the wage distribution. If workers learned only from more skilled peers, we would expect stronger peer effects among low-wage workers, who have a larger pool of more skilled workers from whom to learn. Conversely, if workers learned only from less skilled peers, we would expect stronger effects among high-wage workers. To explore this asymmetry, we estimate the following specification:

$$\Delta \log w_{i,t+h} = \beta_h^+ \, \text{Above}_{i,t} \times \log w_{-i,t} + \beta_h^- \, \text{Below}_{i,t} \times \log w_{-i,t} + \Gamma X_{i,t} + \zeta_{i,t}, \tag{17}$$

where $\text{Above}_{i,t}$ and $\text{Below}_{i,t}$ are indicator variables equal to one when worker i is above or below the mean wage of her peers, respectively.[18]

Table E2 in Appendix E reports the estimates of β_h^+ and β_h^- across different time horizons. Both groups display positive and sustained responses to peer quality at every horizon. While the point estimates are larger for workers above the mean, both sets of coefficients are economically and statistically significant, and they converge at the longest horizons. We interpret this as suggestive

[18]We also include the non-interacted indicator $\text{Above}_{i,t}$ in the vector of controls $X_{i,t}$.

evidence that workers learn from the full pool of peers in their labor market rather than only from a subset of them.

3.2.3 Taking Stock and Alternative Mechanisms

In this section, we provided evidence for the model's main predictions and the mechanism connecting them. Modern-sector workers earn higher wages throughout their careers, and a substantial share of this wage gap reflects the sorting of higher-skilled workers into the modern sector. We also documented a dynamic modern-sector wage premium, with modern workers experiencing faster future wage growth than traditional workers. Consistent with the model, exposure to better-paid peers predicts higher subsequent wage growth, and modern-sector workers are systematically exposed to such peers. These sorting patterns create stronger learning opportunities in the modern sector, contributing to faster human capital accumulation and steeper wage trajectories, while wages in the traditional sector remain relatively flat over the life cycle.

Peer learning, however, may not be the only force shaping human capital accumulation across sectors. Although our peer-effect estimates remain robust after controlling for modern-sector status, more detailed information on firm-provided training, such as that used by Ma et al. (2024), would be necessary to quantify the contribution of on-the-job training to the wage trajectories we document. Traditional-sector workers may also perform tasks that provide weaker incentives to accumulate skills than those typically performed by modern-sector workers. We do not expect this channel to be quantitatively dominant, since all our specifications include industry and occupation fixed effects. Moreover, as shown in Table 1, modern and traditional workers work similar hours. While we abstract from workers' allocation of time between working and learning, standard human capital accumulation models such as Ben-Porath (1967) view hours worked as informative about this tradeoff. Through the lens of these models, the similarity in working hours suggests that workers in the two sectors allocate similar shares of their time to these activities.

Search and matching frictions provide another potential explanation for the different wage trajectories observed in the data. An argument similar to that of Lagakos et al. (2018) regarding differences in life-cycle wage profiles across developed and developing countries applies in our setting. Traditional-sector labor markets may be subject to different search and matching frictions from those in the modern sector, generating flatter wage growth over the medium and long run. The findings of Donovan et al. (2023) suggest that traditional-sector workers may not experience less labor market mobility, but may instead be exposed to riskier jobs and a more precarious job ladder. Under this interpretation, they change jobs more frequently without obtaining the wage gains typically associated with moving up the job ladder. Distinguishing between human capital and search-based explanations is difficult even with detailed panel data such as ours. We therefore view search and matching frictions as a valid and potentially important alternative mechanism. Nevertheless, the relationship we document between peer exposure and subsequent wage growth provides separate support for the peer-learning channel. Quantifying the relative contributions of these mechanisms remains an important avenue for future research.

Taken together, our findings support worker sorting and peer learning as important forces shaping wage trajectories across sectors, while leaving room for complementary mechanisms. In the next section, we quantify the model and assess the aggregate importance of peer learning and learning segmentation for income and welfare.

4 Model Quantification

This section describes the quantification of the model. We first summarize the parameters introduced in the theory and explain the strategies used to estimate them. We then discuss the variation in the data that identifies the parameters and characterize the decentralized equilibrium under the estimated parameter values.

4.1 Setup

Because time is continuous in the model, we interpret each interval $[t, t+1)$ as one year. We average wages and transition probabilities across the modern and traditional sectors over the 2002–2016 period and interpret these averages as representing the economy's steady state. We also adopt the functional-form assumptions for utility and traditional-sector technology stated in Assumption 1 and assume that the entry skill distribution is Pareto with scale parameter normalized to one and shape parameter ϑ.

We define labor markets in a manner consistent with the empirical exercises. The EPS reports information on 14 regions, 10 industries, 10 occupations, and firm size. To make the estimation tractable, we abstract from firm size and define a labor market as a Region $\times$ Industry $\times$ Occupation cell.[19] We then group regions, industries, and occupations into three categories each. For regions, we distinguish among the north, Santiago, and the south. For industries and occupations, we construct high, medium, and low wage groups. Our quantitative exercises therefore include $N = 27$ labor markets. Table E3 in the Appendix describes the composition of each group.[20]

4.2 Estimation

Under our functional-form assumptions, the model contains 13 parameters:

$$\left\{\rho, \tau, \nu, \vartheta, \lambda, \delta, \eta, \theta, \gamma, \pi^M, \pi^T, \sigma_M, \sigma_T\right\},$$

in addition to labor-market productivity, $\{A_n\}_{n=1}^N$, and bilateral migration costs, $\{\xi_{nm}\}_{n,m=1}^N$. We divide these parameters into three groups according to the strategy used to estimate each of them.

External Calibration (3 parameters): ρ, τ, ν

We set workers' discount rate, ρ, to 0.05, a standard value in the literature (Akcigit et al., 2021). We set the payroll tax in the modern sector to $\tau = 0.10$, consistent with Chilean statutory regulations.

[19] Appendix D.3 shows that the main results from our analysis are robust to omitting firm size as a control.

[20] This grouping is necessary because of computational constraints. Without it, the model would contain 1400 labor markets, each requiring us to track a separate skill distribution.

Finally, we set the inverse dispersion parameter governing workers' idiosyncratic preferences across labor markets to $\nu = 1/1.5$, following Traiberman (2019).

Given this value of ν, we estimate bilateral migration costs, $\{\xi_{nm}\}_{n,m=1}^{N}$, nonparametrically using the bilateral migration flows across labor markets observed in the EPS. To do so, we impose symmetric migration costs, $\xi_{nm} = \xi_{mn}$. Appendix C.4 describes the recovery procedure.

Minimum Distance Estimated Parameters (3 parameters): δ, λ, ϑ

We estimate the death rate, δ, from the age distribution implied by the model. Letting $H(a)$ denote the age CDF, the model implies the log-linear relationship

$$\log\left(1 - H(a)\right) = -\delta a.$$

We therefore estimate δ by regressing $\log\left(1 - H^e(a)\right)$ on age a without a constant, where $H^e(a)$ denotes the empirical age CDF.

For the migration rate, λ, we use the worker panel and set it equal to the overall fraction of workers who change labor markets in a given year. In the model, migration opportunities arrive according to a Poisson process with intensity λ, so that over a one-year interval, a fraction $1 - e^{-\lambda} \approx \lambda$ of workers receive at least one opportunity to move. Using the EPS, we identify movers and non-movers and compute λ as the average fraction of workers who move across labor markets between consecutive years.[21]

We estimate the Pareto shape parameter ϑ from the cross-section of entry wages. Because modern-sector wages are proportional to skill, $w_n^M(z) = A_n z/(1+\tau)$, the upper tail of newborn wages within each labor market inherits the Pareto tail index ϑ, up to the market-specific scale factor $A_n/(1+\tau)$. We define modern-sector newborns as formal workers aged 25 or younger with fewer than two years of experience and use each worker's first observed wage. Within each labor market, we rank workers by wage and retain the top quartile. We then estimate the rank-size regression

$$\log\left(\text{rank}_{i,n} - \tfrac{1}{2}\right) = c_n - \vartheta \log w_{i,n} + \zeta_{i,n},$$

where the market fixed effect c_n absorbs differences in the local wage scale, while the coefficient on log wages identifies ϑ. The $-\frac{1}{2}$ rank correction reduces the small-sample bias of the OLS tail-exponent estimator (Gabaix and Ibragimov, 2011).

Our estimation yields $\delta = 0.04$, $\lambda = 0.101$, and $\vartheta = 2.66$. The estimated value of δ implies that approximately 4% of workers exit employment each year and that active workers have an expected remaining work life of about 25 years. This value exceeds Chile's overall mortality rate, which is natural because δ captures not only death but also transitions from employment into unemployment or out of the labor force. Our estimate of λ lies toward the lower end of the range reported by Crews (2024) for the United States. Finally, our estimate of ϑ implies a degree

[21] Because workers who receive a relocation opportunity may optimally remain in their current market, this estimate provides a lower bound on the arrival intensity of relocation opportunities.

of dispersion in entry skills broadly consistent with Hsieh et al. (2019), who calibrate a Fréchet distribution of talent with a shape parameter of 2 to match wage dispersion in the United States.

Simulated Method of Moments (7 parameters): $\eta, \theta, \gamma, \pi^M, \pi^T, \sigma_M, \sigma_T$

We estimate the remaining seven parameters using the Simulated Method of Moments (SMM), jointly with an inversion procedure that recovers the market-specific productivity shifters $\{A_n\}_{n=1}^N$.

The productivity inversion proceeds as follows. Given the previously estimated parameters and a candidate vector for the remaining parameters, we recover the market-specific productivity shifters by exactly matching average wages in each labor market. Formally, the wage equation (1) implies

$$A_n = \frac{\overline{w}_n}{(1+\tau)^{-1} s_n^M \mathbb{E}_n[z|M] + s_n^T \mathbb{E}_n[z^\eta|T]}, \tag{18}$$

where $\overline{w}_n$ is the average wage in market n, s_n^M and s_n^T are the shares of modern and traditional workers in market n, respectively, and $\mathbb{E}_n[z|M]$ and $\mathbb{E}_n[z^\eta|T]$ are their corresponding conditional average marginal products. We use the observed average wage in each labor market to construct the numerator on the right-hand side of (18). Constructing the denominator, in contrast, requires solving the model for a candidate vector of productivities and parameter values to obtain the equilibrium objects entering the expression. We therefore iterate on the vector $\{A_n\}_{n=1}^N$ until convergence, conditional on the parameter vector. This inversion is nested within the SMM estimation routine described below.

Turning to the SMM estimation, we estimate the seven structural parameters $\eta, \theta, \gamma, \pi^M, \pi^T, \sigma_M, \sigma_T$ using ten moments. Four are aggregate cross-sectional moments reported in Table 1: the modern-sector employment share, the one-year transition probabilities across sectors, and the variance of log wages in the modern sector. The remaining six moments are the diagonal elements of the five-year wage-quintile transition matrices within each sector. To construct these moments, we define quintiles of the sector-specific wage distributions and restrict the sample to workers observed in the same sector at both endpoints. We exclude the bottom and top diagonal elements in each sector because the smooth Brownian specification has difficulty matching the high persistence observed at the extremes of the wage distribution.

We deliberately construct the sectoral and wage-quintile transition moments over different horizons. The one-year sector transition probabilities primarily capture diffusion across the sectoral cutoff and are therefore informative about σ_S. In contrast, five-year persistence within sector-specific wage quintiles reflects the cumulative effect of drift over workers' careers and is therefore informative about the parameters governing expected skill growth.

The identification follows naturally from these differences across moments. Persistence within sector-specific wage quintiles helps identify the sectoral drifts, μ^S, and therefore the parameters that determine learning from peers: the learning intensity, γ, the power mean governing vibrancy, θ, and the learning segmentation parameters, π^S. Persistence in the upper wage quintiles is particularly informative about μ^M, while persistence in the lower quintiles is more informative about μ^T. Conditional on the drifts identified by these moments, the one-year sector transition probabilities pin down σ_M and σ_T through the frequency with which skill shocks move workers across the sectoral cutoff. Perla et al. (2021) use a related strategy to estimate the parameters governing firm productivity when it follows a geometric Brownian motion, as in our setting. Finally, the modern-sector employment share and the variance of log wages help identify the technology curvature, η, and the modern-sector volatility, σ_M.

Overall, we use 10 moments to estimate seven parameters. Let $\Theta = (\eta, \theta, \gamma, \pi^M, \pi^T, \sigma_M, \sigma_T)$ denote the vector of parameters to be estimated. We implement the SMM by minimizing the sum of squared symmetric percentage differences between the model-implied moments, $\Psi^m(\Theta)$, and their empirical counterparts, Ψ^d:

$$\min_{\Theta} \sum_{i=1}^{10} \left(\frac{\Psi_i^m(\Theta) - \Psi_i^d}{0.5\left(\Psi_i^m(\Theta) + \Psi_i^d\right)} \right)^2 .$$

We search over the parameter space using the TikTak global optimization algorithm of Arnoud et al. (2019).[22] At each iteration of the optimization routine, we invert the equilibrium mapping in (18) to recover $\{A_n\}_{n=1}^N$ nonparametrically.

Table 2 reports the estimates. Panel A presents the estimated SMM parameters. We find strong diminishing returns in the traditional sector, with η well below one. We also estimate the power-mean parameter governing sectoral vibrancy to be 1.77. This value is somewhat lower than the estimate reported by Crews (2024) for the United States, who focus on interactions within cities and incorporate dynamic agglomeration forces. The difference likely reflects both our narrower definition of labor markets and the absence of agglomeration forces in our framework. Our estimates also imply a sharply asymmetric degree of learning segmentation across the two sectors. For modern workers, π^M is close to 1/2, so their learning interactions are essentially unbiased. Compared with a random-interactions benchmark, a modern worker is only about 5 percent more likely to learn from another modern worker than from a traditional worker. Traditional workers, by contrast, exhibit a strong own-sector bias, with π^T well above 1/2. They are roughly two and a half times more likely to learn from a worker in their own sector than from one in the modern sector. Finally, we estimate skill volatility to be similar across the two sectors, although somewhat higher for modern workers.[23]

Panel B compares the moments in the data with their model counterparts. Overall, the model fits the 10 moments well using only seven parameters. Among the aggregate moments, it closely matches the one-year sector transition probabilities and the variance of log wages in the modern sector, although it falls slightly short of reproducing the modern-sector employment share. Despite its parsimonious specification for skill dynamics in both sectors, the model also performs well in matching the sector-specific transition probabilities across wage quintiles.

[22] We use a Sobol sequence of 5,000 starting points and a simplex method for local optimization, initialized from the 50 best candidates.

[23] Although we do not impose the restrictions in Assumptions 2 and 3 during estimation, the resulting estimates satisfy the parameter restrictions required by the sufficient conditions for the sorting equilibrium.

Table 2: SMM estimation results

Panel A: Parameter Estimates		
Parameter	Description	Estimate
η	Decreasing returns, traditional	0.520
θ	Power-mean, vibrancy	1.770
γ	Peer-learning intensity	0.001
π^M	Learning segmentation, modern	0.512
π^T	Learning segmentation, traditional	0.719
σ_M	Volatility of log skill, modern	0.136
σ_T	Volatility of log skill, traditional	0.096

Panel B: Targeted Moments		
Moment	Data	Model
Modern-sector employment share	0.70	0.65
Variance of log wages, modern sector	0.39	0.42
Modern-to-modern transition	0.97	0.95
Traditional-to-traditional transition	0.92	0.91
Modern $q_2 \to q_2$ transition	0.30	0.33
Modern $q_3 \to q_3$ transition	0.37	0.36
Modern $q_4 \to q_4$ transition	0.48	0.50
Traditional $q_2 \to q_2$ transition	0.37	0.44
Traditional $q_3 \to q_3$ transition	0.33	0.35
Traditional $q_4 \to q_4$ transition	0.39	0.36

Notes: Panel A reports the SMM parameter estimates obtained by minimizing the weighted distance between the model and data moments. Panel B displays the empirical moments computed from the EPS and their model counterparts at the estimated parameters.

4.3 Over-identification Exercises and Stationary Equilibrium

This subsection presents a set of over-identification and model-fit exercises. We use nontargeted moments to assess the identification of the estimated parameters and then discuss key qualitative properties of the stationary equilibrium under those estimates.

Figure 7 presents our over-identification exercises, comparing two important nontargeted moments in the model and the data. Figure 7(a) first reports wage-experience profiles for modern and traditional workers. We normalize average wages in each experience bin by the wage level in the first bin, so the figure shows how wages evolve over the life cycle for each group in the model and the data. Figure D11 presents the corresponding comparison in levels, without normalizing entry wages. In that figure, the data series coincide with those reported in Figure 1(a).

The model performs well overall. Although we do not target any moments related to life-cycle wage growth, it matches the wage profiles of both modern and traditional workers reasonably well, both qualitatively and quantitatively. For modern workers, the model closely tracks wage growth through 19 years of experience. Beyond that point, however, it does not reproduce the plateau observed in the data and therefore overpredicts wage growth in the last two experience bins. For traditional workers, the model tracks wage growth closely across all experience bins. As Figure

Figure 7: Life Cycle Wage Growth and Dynamic Modern Premium: Model vs Data

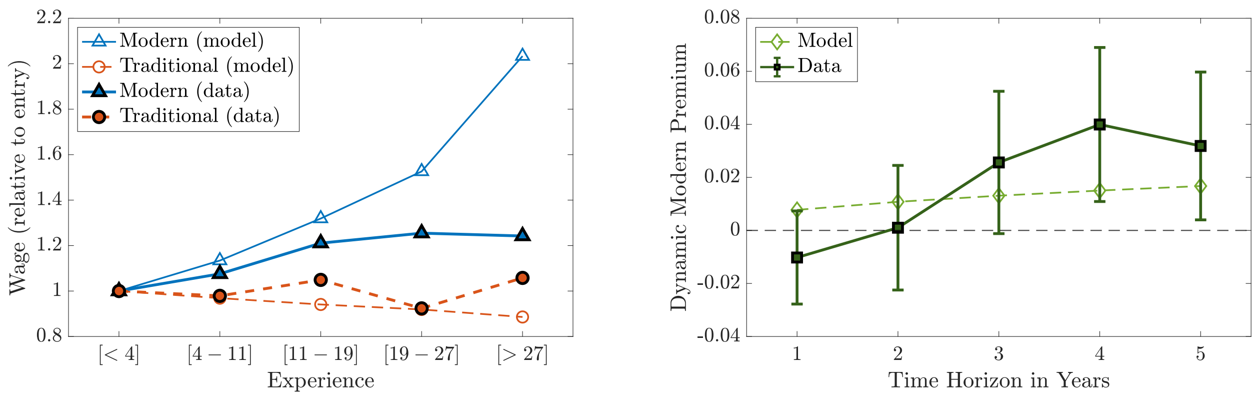

(a) Life-cycle wage growth

(b) Dynamic modern premium

Notes: Figure 7 compares nontargeted moments in the model and in the data. Panel 7(a) displays average wages by experience for modern and traditional workers, with each series normalized by its own entry level. Model averages are computed over the same experience-quintile bins as in Figure 1, weighting ages by surviving sector mass. Panel 7(b) displays the dynamic modern premium: the model series is the raw sectoral gap in expected wage growth, $\mathbb{E}[\Delta \log w_{t+h} \mid M] - \mathbb{E}[\Delta \log w_{t+h} \mid T]$, and the data series reports the estimates of β_h from equation (15). Vertical bars denote 95 percent confidence intervals.

D11 shows, this fit also holds in levels. Even without normalizing entry wages, the model closely replicates both the level and growth of traditional-sector wages. For modern workers, by contrast, the model predicts wages above those observed in the data throughout the life cycle.

Figure 7(b) turns to the dynamic modern-sector wage premium. The model series reports the difference in expected wage growth between modern and traditional workers over horizons of one to five years, which corresponds to the model counterpart of the estimated coefficients β_h in equation (15). As before, none of these moments are targeted in the estimation. The model reproduces the two main features of the data. Qualitatively, the premium is positive and increases with the time horizon. Quantitatively, the model-implied premium lies within the 95 percent confidence intervals of the empirical estimates at every horizon. The main discrepancy appears at short horizons. In the data, the premium is close to zero during the first two years and emerges only afterward, whereas in the model modern-sector workers begin to pull ahead immediately.

Taken together, we view these results as evidence that the model can replicate the wage dynamics observed in the data, both qualitatively and quantitatively. We now turn to the stationary equilibrium under the estimated parameters, focusing on how workers sort across sectors and on the learning environments offered by different labor markets.

Figure 8 illustrates key properties of the stationary equilibrium. Figure 8(a) first shows the skill distribution of workers in the median market in terms of productivity, A_n.[24] The y-axis denotes the share of workers at each skill level within the market, while the vertical dotted line marks the log of the modern-sector cutoff, $\bar{z}_n$. Consistent with Proposition 1, the estimated stationary equilibrium features sorting across sectors, with higher-skill workers employed primarily in the

[24] Appendix Figure D12 displays the skill distributions for all markets.

Figure 8: Decentralized Equilibrium

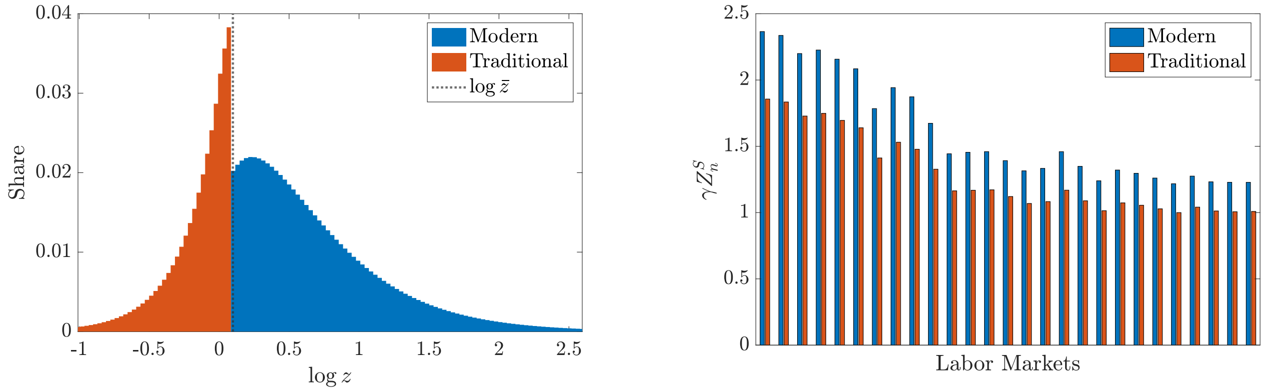

(a) Skill distribution, median market

(b) Learning intensity

Notes: Figure 8 illustrates the stationary equilibrium at the estimated parameters. Panel 8(a) displays the stationary distribution of workers over log skill by sector in the median market by productivity A_n, expressed as a share of the market's workers. The dotted vertical line denotes the modern-sector cutoff log $\bar{z}$. Panel 8(b) displays the learning drifts γZ_n^S by market and sector, normalized by the smallest drift across markets and sectors. Markets are sorted by productivity, with the most productive market on the left.

modern sector and lower-skill workers in the traditional sector.

The figure also shows a jump in the distribution immediately to the right of the modern-sector cutoff. This jump reflects the higher volatility of idiosyncratic skill shocks in the modern sector relative to the traditional sector. Modern workers just above the cutoff experience larger skill fluctuations, which may push them farther up the skill distribution or below the cutoff, inducing them to switch into the traditional sector. By contrast, traditional workers just below the cutoff experience less volatile shocks and therefore move across skill levels less frequently. As a result of this asymmetry in skill volatility, workers pool just below the modern-sector cutoff. This pattern is not unique to the median market and appears across all labor markets, as shown in Figure D12.

Second, Figure 8(b) displays estimated average skill growth across the economy. The figure reports the drifts γZ_n^M and γZ_n^T in (3) across markets and sectors. We order markets from most to least productive and normalize all drifts by the smallest one.

The figure reveals substantial heterogeneity in average skill growth across markets and sectors. Modern-sector workers in every market accumulate skills faster than traditional-sector workers in any market, and within markets their human capital growth rates are about 20% higher. Average human capital accumulation is not monotonic in market productivity because markets also differ in bilateral migration costs. Markets with higher migration costs attract fewer workers, since forward-looking individuals value the option to relocate in response to future labor-market preference shocks, which can weaken local learning opportunities. As a result, workers in more productive markets with higher migration costs may accumulate less human capital than workers in less productive markets with lower migration costs.

5 Counterfactual Analysis

With the estimated model, we conduct two counterfactual exercises to explore the role of peer learning in economic development in the Chilean context. First, we consider a policy exercise that studies the aggregate effects of changing the costs of operating in the modern sector. Specifically, we consider counterfactual economies in which we vary the payroll tax τ. Changes in τ affect the skill composition of workers across sectors and, in turn, the learning opportunities available to workers in each sector. Second, we study alternative specifications of the learning technology. In particular, we consider counterfactual economies with different configurations of the learning segmentation parameters, π^M and π^T, and trace out how the degree of learning segmentation faced by modern and traditional workers affects aggregate income and welfare.

Do we expect learning segmentation to always be a barrier to economic development? The answer, perhaps surprisingly, is no. Workers impose a learning externality on others. When they choose labor markets and sectors, they do not internalize that these decisions affect other workers' learning opportunities. Eliminating learning segmentation altogether can actually reduce the learning opportunities of the most skilled workers, because they are now exposed to less skilled peers, creating a crowding-out effect. At the same time, eliminating segmentation increases the learning opportunities of traditional-sector workers, who become more exposed to higher-skilled counterparts. Whether, in the aggregate, removing learning segmentation raises or lowers income and welfare is therefore a quantitative question. Importantly, this crowding-out effect also appears in semi-endogenous growth models such as Buera and Oberfield (2016), who show that in a world with free trade, idea diffusion can reduce growth in some countries.

5.1 Reducing the Cost of Operating in the Modern Sector

In our first counterfactual exercise, we study how changes in modern-sector regulation affect peer composition and aggregate outcomes. We implement this exercise by varying the payroll tax around its baseline value of $\tau = 0.10$, considering four counterfactual economies with payroll taxes 5 and 10 percentage points above and below the baseline, corresponding to $\tau = 0.15$, $\tau = 0.20$, $\tau = 0.05$, and $\tau = 0$. We focus on the effects of these changes on four aggregate outcomes relative to the baseline economy: the share of modern workers, income per capita, the labor productivity gap between the modern and traditional sectors, and the consumption-equivalent welfare change coming from workers' learning. This last object captures the change in the continuation value from learning, corresponding to the skill-drift term $\mu_n^S z \partial_z V_n$ in (7). This is precisely the margin through which workers value the peer composition of their sector.

We focus on the learning channel when comparing welfare across counterfactual economies. One could instead consider the full welfare change, incorporating all the components of workers' value. However, changes in payroll taxes induce redistribution through the government wage subsidy, so aggregate welfare comparisons depend on how gains and losses are weighted across workers with different skill levels. Focusing on the learning component isolates the welfare effects generated by changes in peer composition, which is the mechanism at the core of our paper. Table E4 in the Appendix provides a full welfare decomposition for each value of τ, weighting workers equally.

Table 3: Aggregate Effects of Changing the Payroll Tax, τ

		Change from baseline (%)		
(1)	(2)	(3)	(4)	(5)
τ	Share Modern	Income	Sector Gap	CE Learning
0.20	0.50	-2.95	5.19	-0.36
0.15	0.57	-1.32	2.02	-0.18
0.10	0.65	···	···	···
0.05	0.71	0.97	-0.71	0.20
0.00	0.77	1.58	-0.23	0.37

Notes: Table 3 reports the effects of changing the payroll tax, τ, relative to the baseline stationary equilibrium with $\tau = 0.10$. Column (2) shows the modern-sector employment share, column (3) the change in income per capita, column (4) the change in the labor productivity gap between the modern and traditional sectors, and column (5) the consumption-equivalent welfare change coming from the learning channel. All changes are reported in percentage terms.

Table 3 reports the aggregate effects of changing the cost of operating in the modern sector. The table compares steady states across different values of τ. The first two columns report the payroll tax and the share of modern workers in the economy, respectively. Lower payroll taxes increase the modern-sector employment share. However, because of the curvature of the traditional-sector production technology, the least productive workers still find it optimal to remain in the traditional sector even when payroll taxes are reduced to zero.

Column 3 of Table 3 shows the change in income per capita, which declines monotonically with the payroll tax. Lowering the cost of operating in the modern sector increases aggregate income by 1.58% when payroll taxes are eliminated. Conversely, raising the payroll tax to 0.20 reduces income per capita by 2.95%. These changes are driven by two forces. First, workers reallocate immediately across sectors with different production technologies, generating a static effect on aggregate income. Second, this reallocation changes workers' learning opportunities and therefore the evolution of human capital over time, leading to a different long-run skill distribution and an additional dynamic effect on income. Figure 10 below decomposes these two margins.

Productivity gaps between the modern and traditional sectors respond systematically to changes in payroll taxes, as shown in Column 4. The key mechanism is worker selection. When payroll taxes increase, marginal workers leave the modern sector for the traditional sector. Because these workers are less productive than the average modern worker but more productive than the average traditional worker, average productivity rises in both sectors, with a larger increase in the modern sector, so the productivity gap widens. When payroll taxes fall, the opposite occurs. Marginal workers enter the modern sector, lowering average productivity in both sectors, with a larger decline in the modern sector and therefore a narrower productivity gap.

Finally, the last column of Table 3 reports the welfare effects generated through peer learning. We find that workers gain on average when the cost of working in the modern sector falls. In consumption-equivalent terms, the welfare gains from improved learning opportunities reach 0.37%

Figure 9: Heterogeneous Welfare Gains from Peer Learning with No Payroll Taxes

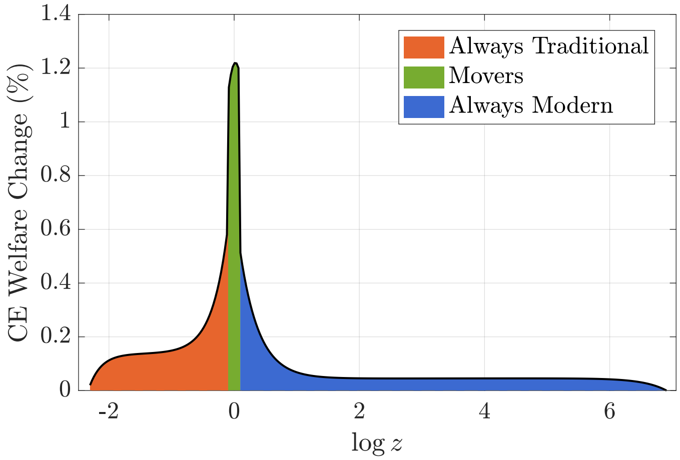

Group	Share	CE Learning
Always Traditional	0.20	0.35
Movers	0.16	1.19
Always Modern	0.65	0.17

Notes: Figure 9 decomposes the welfare gains from peer learning in the counterfactual economy with $\tau = 0$. In the left panel, the x-axis denotes log skill and the y-axis denotes consumption-equivalent welfare gains from the learning channel. The shaded areas divide workers into three groups: always-traditional workers (orange), movers (green), and always-modern workers (blue). The right panel reports the baseline population share of each group and the corresponding mass-weighted average consumption-equivalent welfare gain from learning.

when payroll taxes are completely eliminated, while increasing the payroll tax to 0.20 generates learning-related welfare losses of 0.36%. These effects arise because lower payroll taxes induce marginal workers to enter the modern sector, where they face better learning opportunities.

However, the aggregate welfare effect of completely removing payroll taxes in the modern sector masks substantial heterogeneity across workers. The policy changes sectoral composition and creates three groups that are affected differently. First, movers are marginal workers who switch from the traditional to the modern sector after the policy change. Second, the policy also affects workers who remain in their original sector, the "always traditional" and "always modern" workers. These groups may gain or lose through the peer-learning channel depending on how peer composition changes and on how much workers value future human capital accumulation.[25] Therefore, the aggregate welfare effect reported in the last column averages across workers who are affected differently by the policy. We decompose these heterogeneous effects below.

Figure 9 decomposes the welfare gains from learning when payroll taxes are completely eliminated across workers with different skill levels. The x-axis denotes workers' log skill, while the y-axis denotes the consumption-equivalent welfare gains from the learning channel. The shaded areas map the three groups described above into the skill distribution: always-traditional workers lie below both average modern-sector cutoffs, movers lie between the baseline and counterfactual cutoffs, and always-modern workers lie above both. The table next to the figure reports the baseline population share of each group and its average welfare gain from learning.

The policy has heterogeneous effects on workers depending on their skill. First, the largest welfare gains are concentrated among movers. By switching into the modern sector, these workers gain access to better learning opportunities, generating welfare gains of around 1.2% on average. Movers

[25]This valuation is captured by $V'(z)$, which measures the value of an additional unit of human capital.

also benefit from a higher valuation of human capital. Eliminating payroll taxes raises modern-sector wages, increasing the value of accumulating skills as future increases in z translate into higher future earnings. Both improved learning opportunities and a higher valuation of human capital therefore contribute to the large welfare gains experienced by this group.

Second, workers who remain in the modern sector also experience welfare gains, although these are the smallest in the economy, averaging 0.17%. Similar to movers, these gains are driven primarily by a higher valuation of human capital. Learning opportunities in the modern sector, by contrast, are largely unchanged. The estimated value of θ places relatively more weight on higher-skilled workers in the peer distribution, so the influx of less-skilled workers has little quantitative effect on modern-sector vibrancy. Thus, although one might initially expect the entry of lower-skilled workers to worsen learning opportunities for incumbent modern workers, this effect is quantitatively negligible under the estimated parameters.

Third, workers who remain in the traditional sector experience welfare gains of around 0.35% on average. Unlike those of modern-sector incumbents, these gains reflect both channels in roughly equal measure. On the one hand, learning opportunities in the traditional sector improve. Because traditional workers partly learn from modern-sector peers, the expansion of the modern sector raises traditional-sector vibrancy and increases skill growth in the average market. On the other hand, traditional workers also place a higher value on accumulating human capital. Eliminating the payroll tax raises modern-sector wages and lowers the skill threshold for entering that sector, making a future switch more valuable. This increases the marginal value of skill even for workers who remain below the cutoff. Thus, low-skilled workers benefit from the policy despite never entering the modern sector themselves, both because the larger modern sector improves their learning environment and because the human capital they accumulate becomes more valuable.

Finally, the effects of raising payroll taxes are roughly symmetric. Increasing τ to 0.20 generates mirror-image welfare losses, concentrated among workers who switch from the modern to the traditional sector. Figure D13 in Appendix D shows this pattern.

5.1.1 Transitional Dynamics

The previous analysis focused on comparisons across steady states. We now extend the analysis to study transition dynamics for the case in which payroll taxes are completely eliminated. Computing these transitions is challenging because workers interact through the skill distributions across sectors and labor markets. As a result, at every instant along the transition path, we need to solve for a fixed point in several infinitesimal equilibrium objects. To address this problem, we build on Bilal and Goyal (2026), who extend the Sequence Space Jacobian (SSJ) method of Auclert et al. (2021) to continuous time. We defer the details of the implementation to Appendix C.6.

Figure 10 reports the transition paths for the share of modern workers, income per capita, and the learning-channel welfare gains. The modern-sector share responds almost immediately to the reform. Because workers can freely switch sectors, removing the payroll tax makes the modern sector attractive right away to a large group of workers who were previously close to the cutoff. As a result, the modern-sector share jumps from 0.65 to 0.80 on impact, temporarily overshooting its

Figure 10: Transitional Dynamics After Eliminating Payroll Taxes

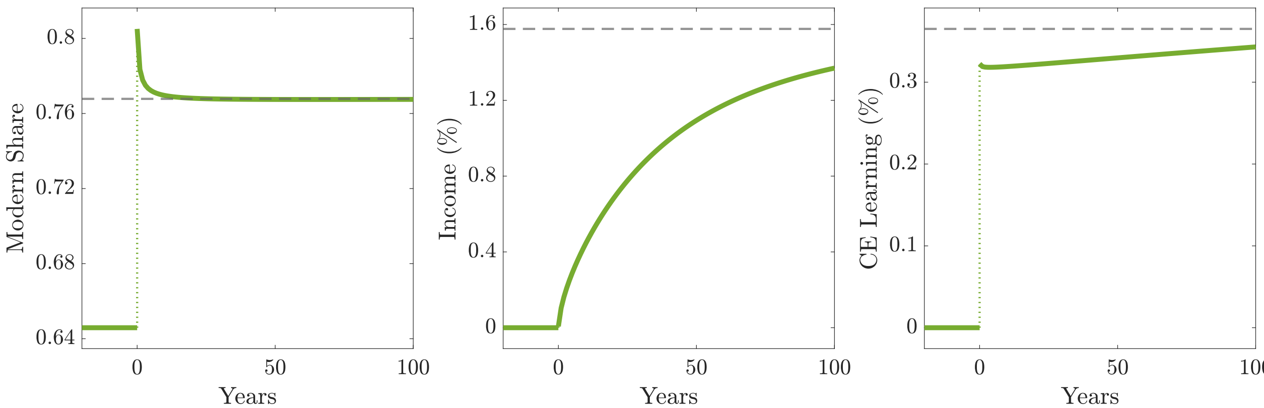

Notes: Figure 10 displays the transition paths following an unanticipated permanent elimination of the payroll tax at $t = 0$. The panels report the share of modern workers, income per capita as a percent deviation from the baseline stationary equilibrium, and the consumption-equivalent welfare change from the learning channel. Dashed horizontal lines indicate the new stationary equilibrium with $\tau = 0$. Transition paths are computed over a 300-year horizon, while the figure displays the first 100 years.

long-run level of 0.77, with 90% of the adjustment completed within six years. The overshooting reflects the shape of the baseline skill distribution. Slower learning in the traditional sector leaves many workers concentrated just below the modern-sector cutoff, and these workers switch as soon as the tax is removed. Over time, this concentration fades as workers accumulate more human capital in the modern sector and new low-skill workers enter the economy.

Income per capita, by contrast, responds much more slowly. Even though many workers switch sectors immediately after the reform, this reallocation has almost no effect on income on impact. Most of the long-run increase in income comes instead from workers gradually accumulating more human capital as their learning opportunities improve. Income closes half of the gap to the new steady state after 26 years and 90% of the gap after roughly 120 years. This slow transition reflects the feedback between peer learning and the skill distribution. Better peers raise skill growth, but peer quality itself improves only gradually as workers accumulate human capital, making the adjustment much more persistent than demographic turnover alone would imply.

Finally, the learning-channel welfare gains respond immediately to the reform. They jump to 0.32% on impact, about 88% of the long-run effect. Unlike income, welfare moves right away because workers value the better learning opportunities they expect to receive in the future. The gains then rise gradually to their long-run level of 0.37% as the modern sector expands and peer composition improves across labor markets.

5.2 Changing the Learning Technology for Traditional Workers

In our second counterfactual exercise, we directly equalize the learning opportunities of modern and traditional workers by changing the learning technology. Formally, we change the learning segmentation parameter for traditional workers such that $\pi^T = 1 - \pi^M$. Under this restriction, modern and traditional workers face the same vibrancy in every labor market and therefore the same learning opportunities. At the estimated parameters, this counterfactual is close to a random-

Figure 11: Heterogeneous Welfare Gains from Peer Learning with Equal Learning Technology

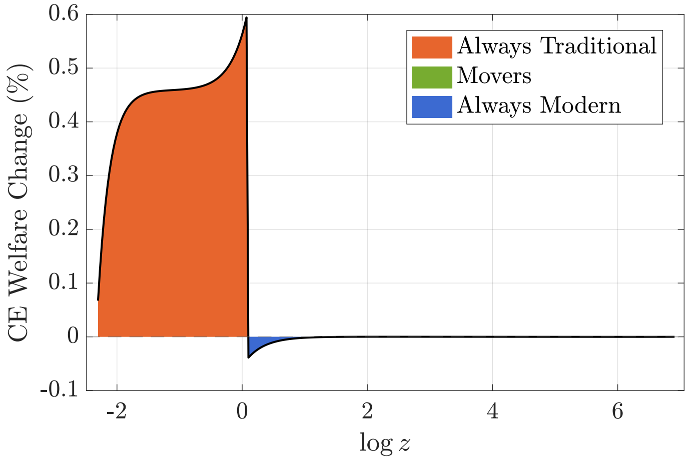

Group	Share	CE Learning
Always Traditional	0.35	0.52
Movers	0.02	-0.04
Always Modern	0.63	-0.01

Notes: Figure 11 decomposes the welfare gains from peer learning in the counterfactual economy with $\pi^T = 1 - \pi^M$. In the left panel, the x-axis denotes log skill and the y-axis denotes consumption-equivalent welfare gains from the learning channel. The shaded areas divide workers into three groups: always-traditional workers (orange), movers (green), and always-modern workers (blue). The right panel reports the baseline population shares and the mass-weighted average consumption-equivalent welfare gain from learning.

interactions benchmark, with learning parameters $\pi^M = 0.51$ and $\pi^T = 0.49$. Thus, traditional-sector workers move from a learning technology strongly biased toward interactions with other traditional workers to one in which they learn almost equally from workers in both sectors.

We first describe the heterogeneous welfare effects across workers. Figure 11 shows that equalizing learning opportunities across sectors generates welfare gains for workers who always remain in the traditional sector. Workers in this group gain 0.52%, in consumption-equivalent terms, as their learning opportunities improve significantly. In contrast, workers who remain in the modern sector are largely unaffected by the new environment, with only those close to the cutoff experiencing small welfare losses. As Figure 12 below shows, the share of modern workers remains nearly constant, declining by only 2 percentage points. Therefore, only a very small fraction of workers move from the modern to the traditional sector, and the associated welfare losses are negligible.

Turning to the aggregate effects, Figure 12 illustrates the transitional dynamics and highlights the new steady-state values. As noted above, the share of modern workers decreases by 2 percentage points when learning opportunities are equalized across the two groups. The figure shows, however, that the share of modern workers falls more sharply on impact and then gradually recovers before converging to its new long-run value. The initial decline reflects the fact that the thresholds, $\bar{z}_n$, jump on impact, as workers' forward-looking values adjust immediately when the learning technology changes. Subsequently, some traditional workers accumulate human capital more rapidly because they face better learning opportunities and transition into the modern sector, explaining the gradual recovery.

The responses of aggregate income and aggregate welfare gains from learning are small under the new learning environment. Income declines slightly on impact, reflecting the immediate movement of marginal workers from the modern to the traditional sector. Because these workers operate

Figure 12: Transitional Dynamics After Equalizing Learning Technologies

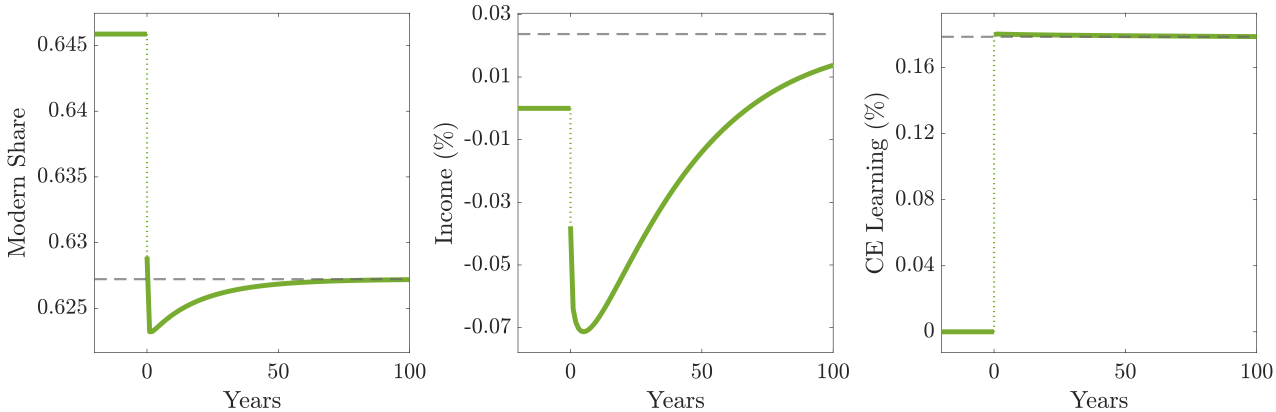

Notes: Figure 12 displays the transition paths following an unanticipated permanent equalization of the learning technologies, $\pi^T = 1 - \pi^M$, at $t = 0$. The panels report the share of modern workers, income per capita as a percent deviation from the baseline stationary equilibrium, and the consumption-equivalent welfare change from the learning channel. Dashed horizontal lines indicate the new stationary equilibrium with equal learning technologies. Transition paths are computed over a 300-year horizon, while the figure displays the first 100 years.

an inferior technology given their skill level, income per capita falls. Subsequently, workers in the traditional sector accumulate human capital at a faster pace, leading income to recover and eventually increase by 0.02% in the new steady state. In contrast, welfare gains from learning from peers jump on impact by 0.18% and remain at this new long-run level thereafter.

5.3 Discussion

Why do the two counterfactual exercises imply such different responses? At first glance, one might expect the counterfactual that equalizes learning technologies across sectors to generate larger effects. Equalizing learning opportunities directly improves the learning environment of all workers initially in the traditional sector. In contrast, removing τ improves learning opportunities primarily for workers who switch from the traditional to the modern sector. Hence, a much larger group of workers is directly exposed to better learning opportunities in the former exercise.

There is, however, an important difference between the two exercises. When learning opportunities improve by lowering the cost of operating in the modern sector, human capital also becomes more valuable in the economy. Removing τ increases the share of modern workers by 12 percentage points and raises income per capita by 1.6%. As more workers operate the superior modern technology, wages increase, and so does the value of accumulating human capital. Workers therefore have stronger incentives to accumulate skills and transition into the modern sector. Hence, the increase in income is fundamentally dynamic. Lowering τ raises the return to human capital, which strengthens incentives to accumulate skills and gradually increases aggregate income.

In contrast, equalizing learning opportunities by changing the learning technology makes working in the modern sector less attractive. Once workers can access the same learning opportunities in both sectors, traditional workers have weaker incentives to transition into the modern sector and instead remain traditional, where they operate a smaller-scale technology. The welfare gains from improved learning opportunities are nevertheless sizable, increasing by 0.18%, compared with 0.37% when τ is eliminated. Thus, equalizing learning technologies generates approximately half of the welfare-through-learning gains from eliminating τ, despite directly improving learning opportunities for a larger group of workers. The reason is that traditional workers facing the improved learning technology value additional human capital less than workers in the economy without payroll taxes, where the returns to accumulating human capital are higher. Taken together, these results highlight an important complementarity between access to better learning opportunities and the returns to accumulating human capital.

6 Conclusion

This paper has studied how learning segmentation shapes economic development. We build a heterogeneous-agent model in which workers sort across labor markets and between modern and traditional sectors while accumulating skills through learning from others. The model predicts that higher-skill workers select into the modern sector and that modern-sector workers experience faster wage growth. We empirically document this dynamic modern-sector premium using Chilean panel data and provide evidence that it reflects learning from better-paid peers. Our counterfactual exercises show that improving learning opportunities for traditional-sector workers can generate meaningful welfare gains, but that the effects on aggregate income depend crucially on the returns to accumulating human capital. Lowering the cost of operating in the modern sector improves workers' learning opportunities while also raising the value of learning itself. This encourages workers to enter the modern sector, generating long-run income gains. In contrast, directly changing the learning technology in the traditional sector produces welfare gains but little aggregate income growth because it weakens workers' incentives to transition into the modern sector. A central message of the paper is therefore that learning opportunities and the returns to human capital are complementary forces in economic development. Policies that improve learning are most effective when workers also have incentives to use those skills with better technologies.

Our framework, inevitably, abstracts from other potentially important mechanisms. Perhaps the most important is labor-market frictions. Understanding how search, matching, and job mobility interact with human capital accumulation in developing economies would provide a natural extension of our analysis. A second promising avenue is to give firms a more active role. Firms in developing countries may also improve their technologies by imitating suppliers or competitors. As a result, technology adoption may depend crucially on the markets in which firms operate. Finally, our framework can be used to study optimal policy in dual economies with peer learning. Throughout the paper, we emphasize that workers do not internalize how their sectoral choices affect the learning opportunities of others. This local externality creates scope for policy interventions.

References

Achdou, Y., Han, J., Lasry, J.-M., Lions, P.-L., and Moll, B. (2022). Income and Wealth Distribution in Macroeconomics: A Continuous-Time Approach. *The Review of Economic Studies*, 89(1):45–86.

Akcigit, U., Akgunduz, Y. E., Alp, H., Quintero, J. M., and Cilasun, S. M. (2024). Good Firms, Bad Policies: The Dynamics of Informality and Industry Policy in Shaping Economic Growth.

Akcigit, U., Alp, H., and Peters, M. (2021). Lack of Selection and Limits to Delegation: Firm Dynamics in Developing Countries. *American Economic Review*, 111(1):231–275.

Akcigit, U., Caicedo, S., Miguelez, E., Stantcheva, S., and Sterzi, V. (2018). Dancing with the Stars: Innovation Through Interactions.

Amaral, P. and Rivera-Padilla, A. (2024). Cross-country income dispersion, human capital, and technology adoption. MPRA Paper 121157, University Library of Munich.

Arnoud, A., Guvenen, F., and Kleineberg, T. (2019). Benchmarking global optimizers. Working Paper 26340, National Bureau of Economic Research.

Auclert, A., Bardóczy, B., Rognlie, M., and Straub, L. (2021). Using the Sequence-Space Jacobian to Solve and Estimate Heterogeneous-Agent Models. *Econometrica*, 89(5):2375–2408.

Ben-Porath, Y. (1967). The Production of Human Capital and the Life Cycle of Earnings. *Journal of Political Economy*, 75(4, Part 1):352–365. Publisher: The University of Chicago Press.

Bilal, A. and Goyal, S. (2026). Some Pleasant Sequence-Space Arithmetic in Continuous Time. Working Paper.

Bobba, M., Flabbi, L., and Levy, S. (2022). Labor Market Search, Informality, and Schooling Investments. *International Economic Review*, 63(1):211–259.

Buera, F. J. and Oberfield, E. (2016). The Global Diffusion of Ideas.

Crews, L. (2024). A Dynamic Spatial Knowledge Economy.

Dix-Carneiro, R., Goldberg, P. K., Meghir, C., and Ulyssea, G. (2021). Trade and Informality in the Presence of Labor Market Frictions and Regulations.

Donovan, K., Lu, W. J., and Schoellman, T. (2023). Labor Market Dynamics and Development*. *The Quarterly Journal of Economics*, 138(4):2287–2325.

Duarte, M. and Restuccia, D. (2019). Relative prices and sectoral productivity. *Journal of the European Economic Association*, 18(3):1400–1443.

Engbom, N. (2022). Labor Market Fluidity and Human Capital Accumulation.

Engbom, N., Malmberg, H., Porzio, T., Rossi, F., and Schoellman, T. (2025). Economic development according to chandler. Technical report, National Bureau of Economic Research.

Gabaix, X. and Ibragimov, R. (2011). Rank — 1/2: A simple way to improve the ols estimation of tail exponents. *Journal of Business and Economic Statistics*, 29(1):24–39.

Gollin, D. (2014). The lewis model: A 60-year retrospective. *Journal of Economic Perspectives*, 28(3):71–88.

Gollin, D. and Rogerson, R. (2025). Structural change and macro development: beyond the one-sector growth model. *Oxford Review of Economic Policy*, 41(2):291–312.

Hashimoto, H. and Tsuchiya, T. (2014). Convergence rate of stability problems of SDEs with (dis-)continuous coefficients. arXiv:1401.4542.

Herkenhoff, K., Lise, J., Menzio, G., and Phillips, G. M. (2024). Production and Learning in

Teams. *Econometrica*, 92(2):467–504.

Herrendorf, B., Rogerson, R., and Ákos Valentinyi (2014). Chapter 6 - growth and structural transformation. In Aghion, P. and Durlauf, S. N., editors, *Handbook of Economic Growth*, volume 2 of *Handbook of Economic Growth*, pages 855–941. Elsevier.

Herrendorf, B. and Schoellman, T. (2018). Wages, human capital, and barriers to structural transformation. *American Economic Journal: Macroeconomics*, 10(2):1–23.

Hsieh, C.-T., Hurst, E., Jones, C. I., and Klenow, P. J. (2019). The allocation of talent and U.S. economic growth. *Econometrica*, 87(5):1439–1474.

Jarosch, G., Oberfield, E., and Rossi-Hansberg, E. (2021). Learning From Coworkers. *Econometrica*, 89(2):647–676.

Lagakos, D. (2016). Explaining cross-country productivity differences in retail trade. *Journal of Political Economy*, 124(2):579–620.

Lagakos, D., Moll, B., Porzio, T., Qian, N., and Schoellman, T. (2018). Life Cycle Wage Growth across Countries. *Journal of Political Economy*, 126(2):797–849. Publisher: The University of Chicago Press.

Lewis, W. A. (1954). Economic development with unlimited supplies of labour. *The Manchester School*, 22(2):139–191.

Lhuillier, H. (2024). Should I Stay or Should I Grow?

Lopez Garcia, I. (2015). Human Capital and Labor Informality in Chile: A Life-Cycle Approach.

Lopez-Martin, B. (2019). Informal Sector Misallocation. *Macroeconomic Dynamics*, 23(8):3065–3098. Publisher: Cambridge University Press.

Lucas, R. E. and Moll, B. (2014). Knowledge Growth and the Allocation of Time. *Journal of Political Economy*, 122(1):1–51. Publisher: The University of Chicago Press.

Lucas, Jr., R. E. (2004). Life earnings and rural-urban migration. *Journal of Political Economy*, 112(S1):S29–S59.

Ma, X., Nakab, A., and Vidart, D. (2024). Human Capital Investment and Development: The Role of On-the-Job Training. *Journal of Political Economy Macroeconomics*, 2(1):107–148. Publisher: The University of Chicago Press.

Meghir, C., Narita, R., and Robin, J.-M. (2015). Wages and Informality in Developing Countries. *American Economic Review*, 105(4):1509–1546.

Meyn, S. P. and Tweedie, R. L. (1993). Stability of Markovian processes III: Foster–Lyapunov criteria for continuous-time processes. *Advances in Applied Probability*, 25(3):518–548.

Perla, J. and Tonetti, C. (2014). Equilibrium Imitation and Growth. *Journal of Political Economy*, 122(1):52–76.

Perla, J., Tonetti, C., and Waugh, M. E. (2021). Equilibrium Technology Diffusion, Trade, and Growth. *American Economic Review*, 111(1):73–128.

Perry, G. E., Arias, O., Fajnzylber, P., Maloney, W. F., Mason, A., and Saavedra-Chanduvi, J. (2007). *Informality: Exit and Exclusion.* The World Bank.

Samaniego De La Parra, B. and Fernández Bujanda, L. (2020). Increasing the Cost of Informal Workers: Evidence from Mexico.

Schwartzman, M. (2025). From street markets to shopping malls: The transformation of the service sector. Steg working paper, CEPR.

Traiberman, S. (2019). Occupations and import competition: Evidence from denmark. *American Economic Review*, 109(12):4260–4301.

Ulyssea, G. (2018). Firms, Informality, and Development: Theory and Evidence from Brazil. *American Economic Review*, 108(8):2015–2047.

Ulyssea, G. (2020a). Formal and Informal Firm Dynamics.

Ulyssea, G. (2020b). Informality: Causes and Consequences for Development. *Annual Review of Economics*, 12(1):525–546.

Appendix

A Theory Appendix

This appendix develops the properties used in Section 2.5. We first study worker values and sectoral sorting for given learning environments. We then establish the stationary-distribution bounds needed to construct an equilibrium. The last three subsections address existence, uniqueness, and the dynamic wage premium.

Throughout, we restrict attention to stationary equilibria in which the value functions are twice continuously differentiable in log skill, except possibly at the sectoral cutoffs, where they are continuously differentiable.

A.1 Worker Values and Sectoral Sorting

For notational convenience, $x = \log z$ and $v_n(x) = V_n(e^x)$. Primes on v_n therefore denote derivatives with respect to log skill. We begin with a fixed vibrancy vector and finite worker values, and do not impose equilibrium consistency at this stage.

The first lemma bounds the slope of each value function and establishes convexity.

Lemma 2 (Shape of the value function)**.** *Fix vibrancies $\{Z_n^S\}$ with finite induced values, and suppose Assumption 1 holds. Then, for every n:*

(a) v_n is strictly increasing, with slopes bounded by $\eta/(\rho+\delta) \le v_n' \le 1/(\rho+\delta)$,

(b) v_n is convex.

Proof. Both parts compare workers who start with different skill levels and follow the same feasible plan. A plan specifies sector choices and choices at relocation opportunities, adapted to the Wiener path, arrival times, and taste draws. Neither sectoral access nor relocation opportunities depend on initial skill, so the plan is feasible for both workers. It need not be optimal for both.

(a) Fix $x_1 > x_0$ and a feasible plan from initial market n. Let both workers follow this plan under the same shocks. They visit the same markets and sectors, so their log-skill increments in (3) are identical. Thus, for every $t \ge 0$,

$$x(t; x_1) - x(t; x_0) = x_1 - x_0.$$

Under the functional forms described in Assumption 1, their instantaneous wages along the plan are

$$\begin{aligned} \log\big((1+b)w_n^T(e^x)\big) &= \log(1+b) + \log A_n + \eta x, \\ \log\big((1+b)w_n^M(e^x)\big) &= \log(1+b) + \log A_n - \log(1+\tau) + x. \end{aligned}$$

Thus the wage difference lies between $\eta(x_1 - x_0)$ and $x_1 - x_0$ across the entire trajectory, and hence, the effective discount rate $\rho + \delta$ bounds the expected payoff difference from this fixed plan between $\eta(x_1 - x_0)/(\rho+\delta)$ and $(x_1 - x_0)/(\rho+\delta)$.

Apply the lower bound to plans approaching the optimum at x_0 and the upper bound to plans approaching the optimum at x_1. Taking the corresponding suprema gives

$$\frac{\eta(x_1 - x_0)}{\rho + \delta} \leq v_n(x_1) - v_n(x_0) \leq \frac{x_1 - x_0}{\rho + \delta}.$$

The lower bound is positive, so v_n is strictly increasing. Dividing by $x_1 - x_0$ gives the stated slope bounds.

(b) Fix x_0, x_1 and $0 \leq \alpha \leq 1$, and let $x_\alpha = \alpha x_1 + (1-\alpha)x_0$. Follow the same feasible plan from each initial skill, using the same shocks. Along this plan, log skill shifts one for one with its initial value, so $x(t; x_\alpha) = \alpha x(t; x_1) + (1-\alpha)x(t; x_0)$. Log wages are affine in log skill, while mobility costs and taste payoffs do not depend on initial skill. The expected discounted payoff from this plan at x_α is therefore the same convex combination of its payoffs at x_1 and x_0. Because the set of feasible plans is common to all three initial skills, taking suprema gives

$$v_n(x_\alpha) \leq \alpha v_n(x_1) + (1-\alpha)v_n(x_0).$$

Thus v_n is convex. □

We next consider how sorting affects the learning environments within a market.

Definition 1. *An allocation in market n is sorted at $\bar{z}_n$ if $N_n^T(z) = 0$ for every $z > \bar{z}_n$, and $N_n^M(z) = 0$ for every $z < \bar{z}_n$.*

We first take sorting as given and rank the resulting vibrancies. We then show when worker choices produce a sorted allocation.

Lemma 3 (Sorting ranks learning environments)**.** *Suppose the allocation in market n is sorted at some $\bar{z}_n$ and there is consistent segmentation. Then g_n^M first-order stochastically dominates g_n^T, and hence $Z_n^M \geq Z_n^T$ for every θ. If both sectors are populated, and $\pi^M + \pi^T > 1$, then both inequalities are strict.*

Proof. If one sector is empty, the peer distributions in (5) are the same. Now suppose both sectors are populated, and let $\hat{g}_n^S = N_n^S / L_n^S$ denote their within-sector densities. Sorting places the support of $\hat{g}_n^T$ to the left of $\hat{g}_n^M$, so $\hat{g}_n^M$ first-order stochastically dominates $\hat{g}_n^T$. The effective peer distributions in (5) can then be written as

$$g_n^S = \omega^S \hat{g}_n^M + (1-\omega^S)\hat{g}_n^T,$$

where

$$\omega^M = \frac{\pi^M L_n^M}{\pi^M L_n^M + (1-\pi^M)L_n^T}, \qquad \omega^T = \frac{(1-\pi^T)L_n^M}{(1-\pi^T)L_n^M + \pi^T L_n^T}.$$

Consistent segmentation implies $\omega^M \geq \omega^T$. Thus g_n^M first-order stochastically dominates g_n^T.

For $\theta \geq 1$, first-order stochastic dominance gives

$$\int_0^\infty z^\theta g_n^M(z)\,\mathrm{d}z \geq \int_0^\infty z^\theta g_n^T(z)\,\mathrm{d}z.$$

Taking the positive power $1/\theta$ gives $Z_n^M \geq Z_n^T$. If $\pi^M + \pi^T > 1$, the mixture-weight inequality is strict. Since the two populated sectors have different skill distributions, both the stochastic dominance and the vibrancy ranking are then strict whenever the relevant moments are finite. □

Define

$$Z_H^* \equiv \frac{\delta - \theta^2\sigma^2/2}{(\theta+1)\gamma}, \qquad \sigma \equiv \max\{\sigma_M, \sigma_T\}. \tag{A1}$$

Assumption 3 makes $Z_H^* > 0$. We use it as an upper bound on conjectured vibrancies. Appendix A.2 shows that the stationary allocations considered there generate vibrancies within this bound.

Lemma 4 (Labor supply is a cutoff)**.** *Consider market n, and fix vibrancies with $Z_n^T \leq Z_n^M \leq Z_H^*$. Suppose $\sigma_M = \sigma_T$, and let Assumption 1 hold. Then there exists $\bar{z}_n$ such that market n is sorted at $\bar{z}_n$. Moreover, the cutoff satisfies*

$$\underline{z} \leq \bar{z}_n \leq \hat{z}, \qquad \underline{z} \equiv \exp\left(\frac{\log(1+\tau) - \gamma Z_H^*/(\rho+\delta)}{1-\eta}\right), \tag{A2}$$

with $\bar{z}_n < \hat{z}$ whenever $Z_n^M > Z_n^T$.

Proof. Equal volatilities eliminate both the difference in Itô corrections in (6) and the curvature term in (11). Log utility removes the common subsidy and productivity terms from the sector comparison. The flow advantage therefore becomes

$$\Delta_n(e^x) = (1-\eta)x - \log(1+\tau) + \gamma(Z_n^M - Z_n^T)v_n'(x). \tag{A3}$$

The static term is linear in x, with slope $1-\eta$. The dynamic term is nondecreasing because v_n is convex and $Z_n^M \geq Z_n^T$. Thus $\Delta_n(e^x)$ is continuous and strictly increasing, with derivative at least $1-\eta$ wherever it exists.

Lemma 2 also bounds the dynamic term:

$$0 \leq \gamma(Z_n^M - Z_n^T)v_n'(x) \leq \frac{\gamma Z_H^*}{\rho+\delta}.$$

The linear static term therefore determines the sign of the flow advantage in the two tails. Since the advantage is continuous and strictly increasing, it crosses zero exactly once.

The same bound locates the crossing. Consider $x < \log \underline{z}$. Then

$$\Delta_n(e^x) \leq (1-\eta)x - \log(1+\tau) + \frac{\gamma Z_H^*}{\rho+\delta} < 0,$$

so $\bar{z}_n \geq \underline{z}$. At the static cutoff, write $\hat{x} = \log \hat{z} = \log(1+\tau)/(1-\eta)$. The static term vanishes, giving

$$\Delta_n(\hat{z}) = \gamma(Z_n^M - Z_n^T)v_n'(\hat{x}) \geq 0,$$

and therefore $\bar{z}_n \leq \hat{z}$. If $Z_n^M > Z_n^T$, the lower slope bound $v_n' \geq \eta/(\rho+\delta) > 0$ makes the last inequality strict, so $\bar{z}_n < \hat{z}$. ☐

A.2 Stationary Distributions and Vibrancy Bounds

Fix a vibrancy vector bounded by Z_H^* and consider a stationary allocation induced by its policies. We bound market populations and the aggregate skill moment in turn. These bounds control the denominators and numerators of the peer-skill moments.

Positive entry into every market keeps the denominators in (5) away from zero. The next lemma makes this population bound uniform over all conjectured vibrancies below Z_H^* and their induced stationary allocations.

Lemma 5 (Uniform population floor)**.** *Let Assumption 1 hold, and fix any vibrancy vector satisfying $Z_n^S \leq Z_H^*$ for all n and S. Then the stationary populations induced by the associated policies satisfy $L_n \geq \underline{L}$ for every n, where*

$$\begin{aligned} \underline{L} &\equiv \frac{\delta}{\delta+\lambda}\frac{e^{-\nu\bar{\Delta}}}{N}, \\ \bar{\Delta} &\equiv \frac{1}{\rho+\delta}\left[\max_{n,m}|\log A_n - \log A_m| + \frac{\gamma Z_H^*}{\rho+\delta} + \frac{\lambda}{\nu}\log N\right]. \end{aligned} \tag{A4}$$

Proof. The proof has two steps. First, we bound the value difference between any pair of markets. We then use that bound to show that each market has at least $\underline{L}$ workers in a stationary allocation.

Fix $\varepsilon \in (0,1]$ and choose (x,n,m) maximizing $v_n(x) - v_m(x) - \varepsilon x^2$ over log skill and all ordered pairs of markets. Lemma 2 implies that the value functions grow at most linearly, whereas the quadratic penalty dominates in both tails, so the maximum is attained. Because the penalty is the same for every pair of markets, n has the highest value and m the lowest value at x. At this point,

$$v_n'(x) - v_m'(x) = 2\varepsilon x, \qquad v_n''(x) - v_m''(x) \leq 2\varepsilon.$$

Subtracting the Bellman equation for m from that for n gives

$$\begin{aligned} (\rho+\delta)(v_n(x) - v_m(x)) = \; &\max_S\left\{\log\left((1+b)w_n^S(e^x)\right) + \gamma Z_n^S v_n'(x) + \frac{\sigma_S^2}{2}v_n''(x)\right\} \\ &- \max_S\left\{\log\left((1+b)w_m^S(e^x)\right) + \gamma Z_m^S v_m'(x) + \frac{\sigma_S^2}{2}v_m''(x)\right\} \\ &+ \lambda\left[\frac{1}{\nu}\log\left(\sum_{k=1}^N e^{\nu(v_k(x)-\xi_{nk})}\right) - v_n(x)\right] \\ &- \lambda\left[\frac{1}{\nu}\log\left(\sum_{k=1}^N e^{\nu(v_k(x)-\xi_{mk})}\right) - v_m(x)\right]. \end{aligned}$$

We bound the sector terms at a common sector. Let S attain the maximum for market n. The maximum for market m is at least its payoff in that same sector, so the difference between the first two lines is no greater than

$$\log A_n - \log A_m + \gamma(Z_n^S - Z_m^S)v_m' + \gamma Z_n^S(v_n' - v_m') + \frac{\sigma_S^2}{2}(v_n'' - v_m'').$$

The wage difference is $\log A_n - \log A_m$ in either sector. Lemma 2 and $0 \leq Z_n^S, Z_m^S \leq Z_H^*$ bound the two learning terms above by $\gamma Z_H^*/(\rho+\delta)$ and $2\gamma Z_H^* \varepsilon |x|$, respectively. The curvature term is at most $\varepsilon\sigma^2$, since the same σ_S^2 multiplies the curvature difference across markets.

We next bound the mobility terms. Since $v_k \leq v_n$ for every k at x, equation (2) and the nonnegative mobility costs give

$$\frac{1}{\nu}\log\left(\sum_{k=1}^{N} e^{\nu(v_k - \xi_{nk})}\right) - v_n \leq \frac{\log N}{\nu}.$$

Since staying in market m is feasible,

$$\frac{1}{\nu}\log\left(\sum_{k=1}^{N} e^{\nu(v_k - \xi_{mk})}\right) - v_m \geq 0.$$

The difference between the mobility terms is therefore at most $(\lambda/\nu)\log N$. Combining these bounds and using the definition of $\bar{\Delta}$ gives

$$(\rho+\delta)(v_n - v_m) \leq (\rho+\delta)\bar{\Delta} + 2\gamma Z_H^* \varepsilon|x| + \varepsilon\sigma^2.$$

The slope bounds in Lemma 2 first give $2\varepsilon|x| = |v_n' - v_m'| \leq (1-\eta)/(\rho+\delta)$. The right-hand side above is therefore bounded independently of ε, and $v_n - v_m \leq C$ for some finite constant C. Moreover, the penalized maximum is at least zero, since $n = m$ and $x = 0$ give zero. Hence

$$\varepsilon x^2 \leq v_n - v_m \leq C, \qquad 2\varepsilon|x| \leq 2\sqrt{C\varepsilon}.$$

Returning to the Bellman comparison with this sharper bound yields

$$(\rho+\delta)(v_n - v_m) \leq (\rho+\delta)\bar{\Delta} + 2\gamma Z_H^* \sqrt{C\varepsilon} + \varepsilon\sigma^2.$$

Now fix any log skill y and markets i, j. By the choice of (x, n, m),

$$v_i(y) - v_j(y) - \varepsilon y^2 \leq v_n(x) - v_m(x) - \varepsilon x^2 \leq \bar{\Delta} + \frac{2\gamma Z_H^*\sqrt{C\varepsilon} + \varepsilon\sigma^2}{\rho+\delta}.$$

Letting ε tend to zero gives $v_i(y) - v_j(y) \leq \bar{\Delta}$. Reversing i and j shows that $|v_i(y) - v_j(y)| \leq \bar{\Delta}$ for every skill and pair of markets.

Newborns pay no mobility cost. Dividing the numerator and denominator of (10) by $e^{\nu v_n}$ and using the value bound gives

$$\begin{aligned}\Pi_n(z) &= \frac{e^{\nu V_n(z)}}{\sum_{m=1}^N e^{\nu V_m(z)}} \\ &= \frac{1}{\sum_{m=1}^N e^{\nu(V_m(z)-V_n(z))}} \\ &\geq \frac{e^{-\nu\bar{\Delta}}}{N},\end{aligned}$$

so the entry inflow into market n is at least $\delta e^{-\nu\bar{\Delta}}/N$. Outflow cannot exceed $(\lambda+\delta)L_n$ because a worker can leave only at a relocation opportunity or at death. Stationarity requires inflow and outflow to balance. Hence

$$(\lambda+\delta)L_n \geq \frac{\delta e^{-\nu\bar{\Delta}}}{N}.$$

This gives $L_n \geq \underline{L}$. □

Skill moments and the vibrancy cap

The population floor controls the denominator of each effective peer distribution. Before stating the vibrancy bound, we distinguish between conjectured and generated vibrancies. Given a conjecture $Z \in \mathbb{R}_+^{2N}$, consider any stationary allocation induced by the associated worker policies. Whenever the relevant moments are finite, let $T(Z)$ denote the vibrancies generated by this allocation:

$$T_n^S(Z) \equiv \left(\int_0^\infty z^\theta g_n^S(z;Z)\,\mathrm{d}z\right)^{1/\theta}.$$

Thus Z determines the learning drifts used in the worker problem, while $T(Z)$ is computed from the stationary allocation that those drifts generate. The next lemma shows that conjectures below Z_H^* generate finite vibrancies that also remain below Z_H^*.

Lemma 6 (Vibrancy cap)**.** *Define*

$$\kappa \equiv \frac{\underline{L}}{c_\pi}, \qquad c_\pi \equiv \max_{S\in\{M,T\}} \frac{\max\{\pi^S,\, 1-\pi^S\}}{\min\{\pi^S,\, 1-\pi^S\}}, \tag{A5}$$

and let

$$\bar{Z} \equiv \left[\frac{c_\pi}{\underline{L}}\frac{(\theta+1)\delta m_\psi(\theta)}{\delta-\theta^2\sigma^2/2}\right]^{1/\theta},$$

with $\underline{L}$ given by (A4).[26] *Let Assumption 3 hold, and fix any conjecture $Z \in \mathbb{R}_+^{2N}$ satisfying $Z_n^S \leq Z_H^*$ for every n and S. Then any stationary allocation induced by the associated policies has finite generated vibrancies satisfying $T_n^S(Z) \leq \bar{Z} \leq Z_H^*$ for every n and S.*

Proof. Fix such a conjecture and a stationary allocation induced by its policies. We begin by bounding the aggregate θ-moment of the skill distribution. Let $\mathcal{L}$ denote the full generator of

[26] The constant c_π is finite for interior segmentation, $\pi^S \in (0,1)$.

the worker process. At a point assigned to sector S in market n, skill accumulation contributes $(\theta\gamma Z_n^S + \theta^2\sigma_S^2/2)z^\theta$ to $\mathcal{L}z^\theta$. Mobility contributes zero because it does not change skill. Death and rebirth replace z^θ with its entry expectation $m_\psi(\theta)$ at rate δ. Therefore

$$\mathcal{L}z^\theta = \left(\theta\gamma Z_n^S + \frac{\theta^2\sigma_S^2}{2}\right) z^\theta + \delta\big[m_\psi(\theta) - z^\theta\big].$$

Since $Z_n^S \le Z_H^*$ and $\sigma_S \le \sigma$, we obtain

$$\begin{aligned} &\mathcal{L}z^\theta \le -cz^\theta + d, \\ &\quad c \equiv \delta - \theta\gamma Z_H^* - \frac{\theta^2\sigma^2}{2} = \frac{\delta - \theta^2\sigma^2/2}{\theta+1} > 0, \\ &\quad d \equiv \delta m_\psi(\theta). \end{aligned} \tag{A6}$$

The drift condition gives the aggregate stationary moment bound

$$\int_0^\infty z^\theta \sum_{k=1}^N N_k(z)\,\mathrm{d}z \le \frac{(\theta+1)\delta m_\psi(\theta)}{\delta - \theta^2\sigma^2/2}.^{27} \tag{A7}$$

Now consider the effective peer distribution in market n and sector S. The numerator and denominator of (5) satisfy

$$\begin{aligned} \pi^S N_n^S(z) + (1-\pi^S)N_n^{-S}(z) &\le \max\{\pi^S, 1-\pi^S\}N_n(z), \\ \pi^S L_n^S + (1-\pi^S)L_n^{-S} &\ge \min\{\pi^S, 1-\pi^S\}L_n. \end{aligned}$$

Dividing these inequalities and using $L_n \ge \underline{L}$ gives

$$g_n^S(z) \le \frac{c_\pi}{L_n} N_n(z) \le \frac{c_\pi}{\underline{L}} N_n(z).$$

Therefore,

$$\begin{aligned} \big[T_n^S(Z)\big]^\theta &= \int_0^\infty z^\theta g_n^S(z)\,\mathrm{d}z \\ &\le \frac{c_\pi}{\underline{L}} \int_0^\infty z^\theta N_n(z)\,\mathrm{d}z \\ &\le \frac{c_\pi}{\underline{L}} \int_0^\infty z^\theta \sum_{k=1}^N N_k(z)\,\mathrm{d}z \\ &\le \frac{c_\pi}{\underline{L}} \frac{(\theta+1)\delta m_\psi(\theta)}{\delta - \theta^2\sigma^2/2}. \end{aligned}$$

The second inequality adds the nonnegative skill densities from the other markets, and the last inequality uses (A7). The right-hand side is $\bar{Z}^\theta$, so $T_n^S(Z) \le \bar{Z}$. By the definition of Z_H^*, the bound

[27] The bound follows from Theorem 4.3(ii) of Meyn and Tweedie (1993) applied to (A6).

$\bar{Z} \leq Z_H^*$ holds precisely when

$$\frac{c_\pi}{\underline{L}} \frac{(\theta+1)\delta m_\psi(\theta)}{\delta - \theta^2\sigma^2/2} \leq \left(\frac{\delta - \theta^2\sigma^2/2}{(\theta+1)\gamma} \right)^\theta .$$

All factors are positive. Multiplying both sides by $\frac{\underline{L}}{c_\pi} \frac{\delta - \theta^2\sigma^2/2}{(\theta+1)\delta}$ and using $\kappa = \underline{L}/c_\pi$ gives

$$m_\psi(\theta) \leq \kappa \frac{(\delta - \theta^2\sigma^2/2)^{\theta+1}}{(\theta+1)^{\theta+1}\gamma^\theta \delta}.$$

This is (13). Assumption 3 therefore implies $T_n^S(Z) \leq \bar{Z} \leq Z_H^*$ for every market and sector. □

Remark 1 (Matching conditions)**.** Under a cutoff policy, $N_n^T(z) = N_n(z)$ for $z < \bar{z}_n$ and $N_n^M(z) = N_n(z)$ for $z > \bar{z}_n$. The stationary KFE is therefore a two-region system. For a piecewise regular stationary density, the weak KFE gives the matching conditions

$$\sigma_T^2 N_n^T(\bar{z}_n^-) = \sigma_M^2 N_n^M(\bar{z}_n^+), \qquad J_n^T(\bar{z}_n^-) = J_n^M(\bar{z}_n^+).$$

The first condition matches the diffusion-weighted densities, while the second conserves probability flux across the cutoff. When $\sigma_M = \sigma_T$, the density is continuous, although the change in learning drift can produce a kink. When the volatilities differ, the density may jump. The finite-volume scheme in Appendix C approximates these conditions without imposing equality of the two densities.

A.3 Existence of a Sorting Equilibrium

Proof of Proposition 1. We first take $\sigma_M = \sigma_T = \sigma$ and set $b = 0$. The construction starts from conjectured vibrancies, solves the worker problem, and computes the vibrancies generated by the resulting stationary allocation. An equilibrium requires these generated vibrancies to equal the conjecture.

The set of conjectures is

$$\mathcal{K} \equiv \left\{ (Z_n^M, Z_n^T)_{n=1}^N : 0 \leq Z_n^T \leq Z_n^M \leq Z_H^* \right\}.$$

This is a compact convex subset of $\mathbb{R}^{2N}$. We show that the map T defined above is well defined on $\mathcal{K}$, that $\mathcal{K}$ is closed under T, and that T is continuous. The subsidy can be recovered afterward because, with log utility, a proportional rebate adds a common constant to values and leaves choices unchanged.

Well-defined. We first show that every $Z \in \mathcal{K}$ determines a unique, finite vector $T(Z) \in \mathbb{R}^{2N}$. There are two steps. First, we establish finite worker values and obtain their policies. Second, we show that these policies generate a unique stationary allocation with finite implied vibrancies.

Fix $Z \in \mathcal{K}$. Under any feasible plan, log skill starting at x satisfies

$$x(t;Z) = x + \int_0^t \gamma Z_{n_s}^{S_s}\,\mathrm{d}s + \sigma W_t, \qquad \mathbb{E}|x(t;Z)| \le |x| + \gamma Z_H^* t + \sigma\sqrt{t}.$$

Flow utility is affine in log skill within each sector, and expected taste payoffs at relocation opportunities are finite. Discounting bounds the payoff of every feasible plan from above by $C(1+|x|)$, uniformly over $Z \in \mathcal{K}$. A feasible plan that remains in its initial market supplies a corresponding lower bound. Taking the supremum over plans therefore gives a finite value function satisfying $|v_n(x;Z)| \le C(1+|x|)$. Lemma 2 now applies: its common-plan comparison makes the value function Lipschitz and convex in log skill. With equal sectoral volatilities, Lemma 4 gives a unique sectoral cutoff $\bar{z}_n(Z) \in [\underline{z}, \hat{z}]$ in each market. Values and cutoffs determine the relocation, entry, and sectoral policies.

Under these policies, the mixture of newborn worker paths over exponentially distributed ages defines a stationary law. At birth, skill is drawn from ψ and the market from $\Pi_n(z)$. Two workers given a common death clock, newborn skill and market draws, and subsequent shocks agree after their first death, so this law is unique. Its density solves (9) under the fixed policies, with the matching conditions in Remark 1. Lemma 5 bounds market populations away from zero, making the denominators in (5) positive. Lemma 6 bounds the stationary skill moment, making the moments in (4) finite. The allocation therefore determines one finite vector $T(Z)$.

The set $\mathcal{K}$ is closed under T. Fix $Z \in \mathcal{K}$. The stationary allocation is sorted, so Lemma 3 gives $T_n^T(Z) \le T_n^M(Z)$. Lemma 6 gives $T_n^S(Z) \le Z_H^*$, and vibrancies are nonnegative. Hence $T(Z) \in \mathcal{K}$.

Continuity. Let $\{Z_j\}_j$ be a sequence in $\mathcal{K}$ with $Z_j \to Z$. We show that $T(Z_j) \to T(Z)$ by comparing, in order, the worker values, the cutoffs, the stationary allocations, and their implied vibrancies.

Fix any feasible plan and use the same market and sector choices, Wiener path, relocation opportunities, and taste draws under Z_j and Z. Under the common volatility σ, the Brownian terms in the two log-skill paths cancel:

$$x(t;Z_j) - x(t;Z) = \gamma \int_0^t \left((Z_j)_{n_s}^{S_s} - Z_{n_s}^{S_s}\right)\,\mathrm{d}s, \qquad |x(t;Z_j) - x(t;Z)| \le \gamma t \|Z_j - Z\|_\infty.$$

Log wages have slope at most one in log skill. Mobility costs and taste draws under the common plan are unchanged. Comparing discounted payoffs and then taking suprema over the same set of feasible plans gives

$$\sup_{n,x} |v_n(x;Z_j) - v_n(x;Z)| \le \frac{\gamma}{(\rho+\delta)^2}\|Z_j - Z\|_\infty \longrightarrow 0.$$

Next fix a market n and write $x_n = \log \bar{z}_n(Z)$. Given any $\varepsilon > 0$, choose $a, b \in \mathbb{R}$ such that $x_n - \varepsilon < a < x_n < b < x_n + \varepsilon$. We compare the value slopes at these two fixed points. For $y = a, b$, convexity gives, for every $h > 0$,

$$\frac{v_n(y; Z_j) - v_n(y-h; Z_j)}{h} \le v_n'(y; Z_j) \le \frac{v_n(y+h; Z_j) - v_n(y; Z_j)}{h}.$$

Taking lower and upper limits as $j \to \infty$ and using the uniform convergence of values yields

$$\frac{v_n(y; Z) - v_n(y-h; Z)}{h} \le \liminf_{j\to\infty} v_n'(y; Z_j) \le \limsup_{j\to\infty} v_n'(y; Z_j) \le \frac{v_n(y+h; Z) - v_n(y; Z)}{h}.$$

Letting $h \downarrow 0$ and using the smoothness of $v_n(\cdot; Z)$ gives $v_n'(y; Z_j) \to v_n'(y; Z)$ at a and b.

By (A3), the flow advantages at a and b converge to those under Z. Lemma 4 makes the limiting advantage negative at a and positive at b. The same signs hold for all sufficiently large j, so the unique crossing under Z_j lies between these points. Thus $a < \log \bar{z}_n(Z_j) < b$ eventually. Since ε was arbitrary, $\bar{z}_n(Z_j) \to \bar{z}_n(Z)$. Sector choices therefore converge at every log skill other than x_n. The relocation and birth-market probabilities converge uniformly in log skill because the logit formulas are Lipschitz in the values, which converge uniformly.

It remains to pass from policies to stationary allocations. Put $\mu_j = \gamma Z_j$ and $\mu = \gamma Z$, and write $x_k(\mu_j) = \log \bar{z}_k(Z_j)$ and $x_k(\mu) = \log \bar{z}_k(Z)$. For either drift vector, define the policy-induced drift of log skill by

$$\beta_k(x; \mu) = \begin{cases} \mu_k^T, & x < x_k(\mu), \\ \mu_k^M, & x \ge x_k(\mu). \end{cases}$$

The same definition applies to μ_j. The convergence of the cutoffs and of Z_j implies that $\beta_k(x; \mu_j) \to \beta_k(x; \mu)$ at every $x \ne x_k(\mu)$, while $|\beta_k| \le \gamma Z_H^*$ for every j.

Fix an age $t > 0$. Under a common reference law, draw initial log skill from the entry distribution, draw the initial market uniformly, and let $x(s) = x(0) + \sigma W_s$. At Poisson relocation opportunities, choose the next market uniformly. Let $n(s)$ be the resulting market path. Brownian motion spends zero time at each of the finitely many limiting cutoffs. Bounded convergence therefore gives

$$\mathbb{E} \int_0^t \left| \beta_{n(s)}(x(s); \mu_j) - \beta_{n(s)}(x(s); \mu) \right|^2 \, \mathrm{d}s \longrightarrow 0.$$

Under this reference law, the likelihood of a worker path induced by μ_j has two parts: a bounded-drift change-of-measure factor and ratios for the newborn-market and relocation choices. The displayed limit and Itô isometry make the stochastic integrals in the first factor converge. Boundedness of β does the same for their quadratic terms. For the choice ratios, the logit probabilities converge at every opportunity, and there are almost surely only finitely many before t. Each ratio is at most N. Bounded drifts give a uniform moment bound for the first factor, while the number of Poisson opportunities has exponential moments. Hölder's inequality then makes the likelihoods uniformly integrable. They converge in L^1, so the finite-age worker laws converge in total variation.

Integrating these laws against the exponential age distribution gives convergence of the stationary laws. At every positive age, nondegenerate diffusion places no mass at a cutoff, so the moving sector assignments also converge. Lemma 5 keeps the denominators in (5) uniformly positive. Assumption 3 also allows an exponent $\theta + \varepsilon$ with finite entry moment and

$$\delta - (\theta + \varepsilon)\gamma Z_H^* - \frac{(\theta + \varepsilon)^2 \sigma^2}{2} > 0.$$

The drift argument in Lemma 6 then gives a uniform bound on this higher stationary moment, so z^θ is uniformly integrable. Passing to the limit in the sectoral moments and their denominators yields $T(Z_j) \to T(Z)$.

The map T is therefore a continuous self-map of the compact convex set $\mathcal{K}$. Brouwer's fixed point theorem gives $Z^* \in \mathcal{K}$ such that $T(Z^*) = Z^*$.

The government budget. At this fixed point, set

$$b^* = \frac{\displaystyle\sum_{n=1}^{N} \int_0^\infty \tau w_n^M(z) N_n^M(z)\,\mathrm{d}z}{\displaystyle\sum_{n=1}^{N} \sum_{S \in \{M,T\}} \int_0^\infty w_n^S(z) N_n^S(z)\,\mathrm{d}z}.$$

The integrals are finite because (A7), with $\theta \geq 1$, bounds the first moment. The denominator is positive. The numerator is nonnegative and is positive when $\tau > 0$, since the stationary allocation has positive modern-sector mass.

Under logarithmic utility, this rebate raises all worker values by

$$\frac{\log(1 + b^*)}{\rho + \delta}.$$

The common shift leaves the sector comparison unchanged. It also leaves relocation and entry probabilities unchanged, since these depend on value differences. In the HJB, the shift cancels between the log-sum-exp continuation value and the current value at a relocation opportunity. Thus the allocation used to construct Z^* remains optimal at b^*. Together, this allocation and the rebate satisfy conditions *(i)–(vi)* of the equilibrium definition.

Unequal sectoral volatilities (sketch). When $\sigma_M \neq \sigma_T$, the flow advantage in log skill is

$$\Delta_n(e^x) = (1 - \eta)x - \log(1 + \tau) + \gamma(Z_n^M - Z_n^T)v_n'(x) + \frac{\sigma_M^2 - \sigma_T^2}{2} v_n''(x).$$

The Itô correction in the level drift cancels the corresponding term in v_n'. We sketch why the remaining curvature term does not change the cutoff policy when the two volatilities are close.

On any interval where sector S is optimal, differentiating its HJB equation gives

$$\frac{\sigma_S^2}{2}v_n'''(x)+\gamma Z_n^S v_n''(x)=(\rho+\delta)v_n'(x)-\frac{\mathrm{d}}{\mathrm{d}x}\log w_n^S(e^x)\\ -\lambda\left(\sum_m m_{nm}(e^x)v_m'(x)-v_n'(x)\right).$$

Lemma 2 bounds every value slope, the wage slope is either η or 1, and the relocation probabilities sum to one. The right-hand side is therefore bounded. Convexity also gives $v_n''\geq 0$ and

$$\int_x^{x+1} v_n''(s)\,\mathrm{d}s=v_n'(x+1)-v_n'(x)\leq\frac{1-\eta}{\rho+\delta}.$$

When both volatilities stay in a fixed compact subset of $(0,\infty)$, we use a uniform bound on v_n'' and on its variation across switching points. For a constant C independent of $Z\in\mathcal{K}$, it follows that, wherever the flow advantage is differentiable,

$$\frac{\mathrm{d}}{\mathrm{d}x}\Delta_n(e^x)\geq 1-\eta-\frac{C}{2}|\sigma_M^2-\sigma_T^2|.$$

Under this curvature bound, the advantage is strictly increasing when the volatility gap is sufficiently small. Since v_n' and v_n'' are bounded, its linear static term determines its sign as x tends to either tail. Thus it crosses zero exactly once in each market.

The sorting and moment bounds used above continue to apply with $\sigma=\max\{\sigma_M,\sigma_T\}$. To complete the fixed-point argument, the stationary law must also vary continuously as the cutoff and sectoral volatilities change. This is a stability property for diffusions with discontinuous coefficients, of the type studied by Hashimoto and Tsuchiya (2014), and it must respect the matching conditions in Remark 1. If this continuity holds, T remains a continuous self-map of $\mathcal{K}$, and Brouwer's theorem gives a sorting equilibrium.

Finally, suppose $\pi^M>1/2$ and $\pi^T>1/2$. At equal volatilities, Lemma 3 and positive mass in both sectors give $Z_n^M>Z_n^T$. Hence $\Delta_n(\hat{z})>0$ and $\bar{z}_n<\hat{z}$. Joint continuity of the equilibrium construction in the volatilities would preserve this strict inequality for sufficiently small volatility gaps. □

A.4 Uniqueness

Proof of Proposition 2. Take $\sigma_M=\sigma_T=\sigma$ and $\gamma>0$. We first show that every equilibrium satisfying the vibrancy cap is sorted when γ is small. This allows us to represent every such equilibrium as a fixed point of the map constructed in Proposition 1. We then write this map in terms of learning drifts and compare the allocations generated by two different drift vectors. The comparison shows that the drift map is a contraction when γ is small.

Every capped equilibrium is sorted. Consider any stationary equilibrium with $Z_n^S\leq Z_H^*$. At an equilibrium, the conjectured and generated vibrancies coincide, so $Z=T(Z)$. Lemma 6 therefore gives $Z_n^S = T_n^S(Z) \le \bar{Z}$. The bound $\bar{Z}$ does not change with γ. To see this, recall that $\underline{L}$ depends on γ only through γZ_H^*, which is fixed by (A1). This is the reason for introducing $\bar{Z}$. It allows us to make the learning term in the sector comparison small by taking γ small.

Write $\hat{x} = \log \hat{z}$ and $r = \rho + \delta$. By Lemma 2, $0 < v_n' \le 1/r$. It follows from (A3) that any zero of the flow advantage satisfies

$$|x - \hat{x}| \le \frac{\gamma \bar{Z}}{r(1-\eta)}.$$

Thus, for all sufficiently small γ, every possible zero lies in a fixed compact interval around $\hat{x}$.

We next bound the curvature of the value function on this interval. Under equal volatilities, the Bellman equation can be written as

$$\frac{\sigma^2}{2} v_n''(x) = r v_n(x) - \max_S \left\{ \log\left((1+b) w_n^S(e^x)\right) + \gamma Z_n^S v_n'(x) \right\} \\ - \lambda \left[\frac{1}{\nu} \log\left(\sum_{k=1}^{N} e^{\nu(v_k(x) - \xi_{nk})} \right) - v_n(x) \right].$$

The value-growth estimate used in Proposition 1 bounds v_n on the compact interval, and Lemma 2 bounds v_n'. Flow wages are also bounded there. Finally, Lemma 5 bounds the same-skill differences between market values, which bounds the mobility term. Hence there is a constant C_0, independent of γ, such that

$$|v_n''(x)| \le C_0$$

at every possible zero of the flow advantage.

Differentiating (A3) now gives

$$\frac{\mathrm{d}}{\mathrm{d}x} \Delta_n(e^x) = 1 - \eta + \gamma (Z_n^M - Z_n^T) v_n''(x) \ge 1 - \eta - \gamma \bar{Z} C_0.$$

This lower bound does not require $Z_n^M \ge Z_n^T$. For sufficiently small γ, the flow advantage is strictly increasing wherever it could vanish. The learning term is bounded, while the static term tends to opposite signs in the two tails. The flow advantage therefore crosses zero exactly once. The equilibrium is sorted, and Lemma 3 then gives $Z_n^T \le Z_n^M$.

The drift map. As in the existence proof, write $\mu_n^S = \gamma Z_n^S$ for the drift of log skill and define

$$\mathcal{D} \equiv \left\{ \mu \in \mathbb{R}^{2N} : 0 \le \mu_n^T \le \mu_n^M \le \gamma Z_H^* \text{ for every } n \right\}.$$

The set $\mathcal{D} = \gamma \mathcal{K}$ is a closed subset of $\mathbb{R}^{2N}$ and is therefore complete under the sup norm. Its upper bound does not depend on γ, since γZ_H^* is fixed by (A1). Define

$$\widetilde{T}(\mu) = \gamma T(\mu/\gamma).$$

Proposition 1 shows that T maps $\mathcal{K}$ into itself. Hence $\widetilde{T}$ maps $\mathcal{D}$ into itself. The preceding argument also shows that the drift vector of every capped equilibrium belongs to $\mathcal{D}$.

To prove uniqueness, it remains to show that the generated vibrancies are Lipschitz in the drift vector with a constant that does not depend on γ. In particular, we show that there is a constant C such that

$$\|T(\mu/\gamma) - T(\widetilde{\mu}/\gamma)\|_\infty \le C\,\|\mu - \widetilde{\mu}\|_\infty$$

for any $\mu, \widetilde{\mu} \in \mathcal{D}$. We first compare values and policies. We then compare the stationary populations and moments they generate. The final step compares the resulting peer moments.

Fix $\mu, \widetilde{\mu} \in \mathcal{D}$ and write

$$d = \|\mu - \widetilde{\mu}\|_\infty .$$

Let v and $\widetilde{v}$ be the corresponding value functions. Use the same feasible plan and the same shocks in the two worker problems. At time t, the two log-skill trajectories differ by at most td. Log wages have slope at most one, so comparing discounted payoffs and then taking suprema over plans gives

$$\|v - \widetilde{v}\|_\infty \le \frac{d}{r^2}.$$

We next compare the value slopes. Subtract the two Bellman equations. The sectoral maximum cannot change by more than the largest change in the return from a fixed sector.[28] For each sector, the drift term satisfies

$$\begin{aligned}\left|\mu_n^S v_n' - \widetilde{\mu}_n^S \widetilde{v}_n'\right| &\le \mu_n^S \left|v_n' - \widetilde{v}_n'\right| + \left|\mu_n^S - \widetilde{\mu}_n^S\right| \left|\widetilde{v}_n'\right| \\ &\le \gamma Z_H^* \left|v_n' - \widetilde{v}_n'\right| + \frac{d}{r}.\end{aligned}$$

The log-sum-exp mobility value is Lipschitz under the sup norm. Combining the sectoral and mobility terms gives

$$\|v'' - \widetilde{v}''\|_\infty \le \frac{2}{\sigma^2}\left[(r + 2\lambda)\|v - \widetilde{v}\|_\infty + \gamma Z_H^* \|v' - \widetilde{v}'\|_\infty + \frac{d}{r}\right].$$

The difference-quotient inequality then gives

$$\|v' - \widetilde{v}'\|_\infty^2 \le 4\|v - \widetilde{v}\|_\infty \|v'' - \widetilde{v}''\|_\infty \le Cd\left(d + \|v' - \widetilde{v}'\|_\infty\right).$$

Dividing by d^2 when $d > 0$ bounds $\|v' - \widetilde{v}'\|_\infty / d$ by the positive root of a fixed quadratic inequality. The result is immediate when $d = 0$. Hence

$$\|v' - \widetilde{v}'\|_\infty \le Cd,$$

where C is independent of γ because γZ_H^* is fixed.

We can now compare the policies. Let $I = [\log \underline{z}, \hat{x}]$, the common cutoff interval in Lemma 4. The change in the flow advantage comes from the sectoral drifts and the value slope. Lemma 2 and

[28] For any two finite collections, $|\max_S a_S - \max_S \widetilde{a}_S| \le \max_S |a_S - \widetilde{a}_S|$.

the bound $\|v' - \widetilde{v}'\|_\infty \le Cd$ give

$$\sup_{x\in I} |\Delta_n(e^x;\mu) - \Delta_n(e^x;\widetilde{\mu})| \le Cd.$$

Both flow advantages cross zero with slope at least $1-\eta$. Write $x_n(\mu) = \log \bar{z}_n(\mu)$ for the log cutoff generated by μ. Then

$$|x_n(\mu) - x_n(\widetilde{\mu})| \le Cd.$$

The logit formulas and the value comparison also imply that the relocation and newborn-market probabilities differ by at most Cd.

Stationary allocations. We next show that each sectoral population and each sectoral θ-moment changes by at most Cd. These are the numerators and denominators from which T is constructed. The comparison has two parts. We first bound the mass reassigned when a cutoff moves. We then compare the two stationary distributions while assigning sectors according to the second cutoff policy.

For each market k, write $x_k = x_k(\mu)$, $\widetilde{x}_k = x_k(\widetilde{\mu})$, and define the interval between the two cutoffs by

$$J_k \equiv [\min\{x_k, \widetilde{x}_k\}, \max\{x_k, \widetilde{x}_k\}].$$

Consider first the interval J_n. Under the first drift vector, the bounded-drift trajectory $x(t;\mu)$ has a density, after summing over markets, bounded by $Ct^{-1/2}$ for $0 < t \le 1$ and by C for $t \ge 1$. The same estimate holds for $x(t;\widetilde{\mu})$.[29] Mixing these finite-age densities with weights $\delta e^{-\delta t}$ gives a uniform bound on both stationary densities. Since all cutoffs belong to I, where $1+e^{\theta x}$ is bounded, the stationary population and θ-moment on J_n are at most

$$C|J_n| \le Cd.$$

We now hold the second sectoral assignment fixed and compare the stationary distributions generated by the two policies. Let $\mathbb{E}_\mu$ and $\mathbb{E}_{\widetilde{\mu}}$ denote expectations under these stationary distributions. Fix a market n and a sector S, and let f select either its population or its θ-moment under the second cutoff policy. For example, the modern-sector moment uses

$$f_k(x) = e^{\theta x} \mathbb{1}_{\{k=n\}} \mathbb{1}_{\{x \ge \widetilde{x}_n\}}.$$

The traditional-sector moment uses the opposite cutoff indicator, and the two population comparisons replace $e^{\theta x}$ by 1.

Recall that $\beta_k(x;\mu)$ is the policy-induced log-skill drift defined in the existence proof. To compare these expectations, follow the policies induced by $\widetilde{\mu}$ and let $\phi_k(x)$ be the expected accumulation

[29] Convolving with the Gaussian transition density gives $\|q_t\|_\infty \le Ct^{-1/2} + C\gamma Z_H^* \int_0^t \|q_s\|_\infty (t-s)^{-1/2}\,\mathrm{d}s$ for the finite-age density q_t. Iteration gives the stated bound on $(0,1]$, and restarting the estimate over the last unit of time gives the bound for later ages.

of f before the next death:

$$\phi_k(x) = \mathbb{E}^{\widetilde{\mu}}_{k,x}\left[\int_0^\infty e^{-\delta t} f_{n(t)}\big(x(t;\widetilde{\mu})\big)\,\mathrm{d}t\right].$$

This auxiliary function is different from the worker value. The value function maximizes discounted utility, while ϕ evaluates one population statistic under a fixed policy. If $m_{kj}(x;\widetilde{\mu})$ is the relocation probability under the second policy, then ϕ satisfies

$$\delta\phi_k = f_k + \frac{\sigma^2}{2}\phi_k'' + \beta_k\phi_k' + \lambda\sum_j m_{kj}(\phi_j - \phi_k),$$

where the dependence of β_k and m_{kj} on $\widetilde{\mu}$ is suppressed in the display.

We first apply this equation to bounded smooth approximations of the cutoff policy and f. The drift bound and the condition

$$\delta - \theta\gamma Z_H^* - \frac{\theta^2\sigma^2}{2} > 0$$

give

$$|\phi_k(x)| \le C(1 + e^{\theta x}).$$

The equation also bounds the weighted second derivative of ϕ in terms of its weighted first derivative. A difference quotient over a sufficiently short interval allows the first-derivative term to be absorbed, giving[30]

$$|\phi_k'(x)| \le C(1 + e^{\theta x}).$$

We then pass from the smooth approximations to the cutoff policy and indicator used above, taking the derivative bound to carry over to this limit uniformly over cutoff locations in I.

Let $\mathcal{L}_\mu$ and $\mathcal{L}_{\widetilde{\mu}}$ denote the full generators under the two policies, including death and rebirth. The definition of ϕ and stationarity under the second policy give the Poisson equation

$$f - \mathbb{E}_{\widetilde{\mu}}[f] = -\mathcal{L}_{\widetilde{\mu}}\phi.$$

Stationarity under the first policy gives $\mathbb{E}_\mu[\mathcal{L}_\mu\phi] = 0$. Taking $\mathbb{E}_\mu$ of the Poisson equation therefore yields

$$\mathbb{E}_\mu[f] - \mathbb{E}_{\widetilde{\mu}}[f] = \mathbb{E}_\mu\left[(\mathcal{L}_\mu - \mathcal{L}_{\widetilde{\mu}})\phi\right].$$

This identity separates the comparison into changes in learning drifts, relocation probabilities, and newborn-market probabilities.

The entry skill distribution ψ is fixed. Only the newborn-market probabilities $\Pi_n(z;\mu)$ and $\Pi_n(z;\widetilde{\mu})$ change, and the logit comparison bounds their difference by Cd. The growth bound on ϕ and the finite entry moment therefore bound the rebirth contribution by Cd. The same argument, using the relocation logits and the stationary moment bound, controls the relocation contribution.

[30] If $H = \sup_{k,x}|\phi_k'(x)|/(1+e^{\theta x})$, the difference-quotient argument gives $H \le C(\ell^{-1} + \ell) + C\gamma Z_H^*\ell H$. Choose $\ell > 0$ so that the last coefficient is less than one.

It remains to compare the policy-induced learning drifts. In market k,

$$|\beta_k(x;\mu) - \beta_k(x;\widetilde{\mu})| \le d + \gamma Z_H^* \mathbb{1}_{\{x\in J_k\}}.$$

The first term contributes at most Cd by the bound on ϕ_k' and the stationary moment bound. The second term is present only between the cutoffs, where the population and θ-moment are also bounded by Cd. It follows that

$$|\mathbb{E}_\mu[f] - \mathbb{E}_{\widetilde{\mu}}[f]| \le Cd.$$

The function f assigns sectors using the second cutoff policy. Replacing this indicator with the first cutoff policy changes the first expectation only between the two cutoffs, adding at most Cd. Thus every sectoral population and every sectoral θ-moment changes by at most Cd.

The contraction. Fix a market and a sector. Write A and B for the numerator and denominator of its peer-skill moment in (5), and write $\widetilde{A}$ and $\widetilde{B}$ for the corresponding objects under the second drift vector. The stationary comparison gives

$$|A - \widetilde{A}| \le Cd, \qquad |B - \widetilde{B}| \le Cd.$$

Lemma 5 keeps B and $\widetilde{B}$ bounded away from zero, while (A7) gives a common upper bound for A and $\widetilde{A}$.

We also need the ratios A/B and $\widetilde{A}/\widetilde{B}$ to be bounded away from zero. By the proof of Lemma 5, newborns choose market n with probability at least $e^{-\nu\bar{\Delta}}/N$. Among those who have not received a relocation opportunity, expected z^θ does not fall because learning drifts are nonnegative. Mixing over ages gives

$$\int_0^\infty z^\theta N_n(z)\,\mathrm{d}z \ge \frac{\delta}{\delta+\lambda}\frac{e^{-\nu\bar{\Delta}}}{N} m_\psi(\theta) = \underline{L} m_\psi(\theta).$$

The mixture weights in (5) therefore imply

$$\frac{A}{B}, \frac{\widetilde{A}}{\widetilde{B}} \ge \frac{\underline{L} m_\psi(\theta)}{c_\pi} > 0.$$

Comparing the two ratios term by term gives

$$\left|\frac{A}{B} - \frac{\widetilde{A}}{\widetilde{B}}\right| \le \frac{|A-\widetilde{A}|}{B} + \frac{\widetilde{A}}{B\widetilde{B}}|B-\widetilde{B}| \le Cd.$$

On this range, $s \mapsto s^{1/\theta}$ has bounded derivative because $\theta \ge 1$. Hence

$$\|T(\mu/\gamma) - T(\widetilde{\mu}/\gamma)\|_\infty \le Cd.$$

By the definition of $\widetilde{T}$,

$$\left\|\widetilde{T}(\mu) - \widetilde{T}(\widetilde{\mu})\right\|_\infty \le \gamma C \left\|\mu - \widetilde{\mu}\right\|_\infty.$$

Thus $\widetilde{T}$ is a contraction whenever $\gamma C < 1$. Banach's fixed-point theorem gives a unique fixed point μ^* in the complete set $\mathcal{D}$. Because $\gamma > 0$, this fixed point corresponds to a unique vibrancy vector $Z^* = \mu^*/\gamma$ satisfying $T(Z^*) = Z^*$. Every capped stationary equilibrium has already been shown to generate a drift vector in $\mathcal{D}$. The fixed point therefore gives the only capped stationary equilibrium. The government budget determines the associated rebate. $\square$

A.5 The Dynamic Wage Premium

Proof of Lemma 1. Fix a market n, and write $x_n = \log \bar{z}_n$ and $\hat{x} = \log \hat{z}$. We compare wage growth among workers in each sector at date t who are observed again at $t + h$. Death is independent of skill and sector, so conditioning on survival does not change either cohort's distribution at date t.

We first establish that the stationary allocation places workers immediately on both sides of the cutoff. Let $q_n(x) = e^x N_n(e^x)$ be the density of log skill in market n. On either side of x_n, its stationary equation is

$$\frac{\sigma_S^2}{2} q_n'' - \gamma Z_n^S q_n' - (\lambda + \delta) q_n = -r_n(x),$$

where $r_n(x) \geq 0$ collects relocation and newborn inflows. The weak stationary equation requires continuity at x_n of both $\sigma_S^2 q_n$ and the probability flux. Suppose that $q_n(x_n^-) = 0$. The first matching condition also gives $q_n(x_n^+) = 0$. Since the density is nonnegative, its left derivative at the cutoff is nonpositive and its right derivative is nonnegative. Flux continuity forces both derivatives to be zero. Solving the equation above outward from zero value and zero slope gives a nonpositive density on either side, because the inflow enters with a minus sign. The density must therefore vanish throughout the market. This contradicts the positive market population in Lemma 5. Thus both one-sided densities at the cutoff are positive.

Consider next a worker who receives no relocation opportunity during $[t, t+h]$. Her change in log skill is a drift bounded by a constant times h, plus the martingale

$$M_h = \int_0^h \sigma_{S_{t+s}} \, \mathrm{d}W_s.$$

Both volatilities are positive. Uniformly over starting skills, $\mathbb{E}M_h = 0$, its second moment is bounded below by a positive multiple of h, and its fourth moment is bounded above by a constant times h^2. These bounds imply that there are $a, p > 0$ such that $M_h < -a\sqrt{h}$ and $M_h > a\sqrt{h}$ each have probability at least p. Indeed, the moment bounds keep $\mathbb{E}|M_h|/\sqrt{h}$ away from zero. The positive and negative parts have equal expectations, and Cauchy–Schwarz then bounds each tail probability away from zero.

For sufficiently small h, a modern worker starting between x_n and $x_n + a\sqrt{h}/2$ therefore has probability at least p of finishing below x_n. Because the density immediately to the right of the cutoff is positive, at least $C\sqrt{h}$ modern workers start in this interval. The share of the initial modern cohort finishing in the traditional sector is therefore at least $C\sqrt{h}$, for a possibly different positive constant C. The same argument applies to traditional workers starting just below the cutoff.

We also need an upper bound on crossings to account for changes in learning drift. A worker starting a fixed distance from x_n can cross it in time s only after an unusually large skill shock. The exponential martingale bound makes that probability exponentially small in $1/s$. Near x_n, the stationary density is bounded. Integrating over starting skills shows that the share of either initial cohort on the other side of the cutoff at time $t+s$ is $O(\sqrt{s})$. Consequently, the expected time spent learning in the other sector over $[t, t+h]$ is $O(h^{3/2})$. The martingale has mean zero for each initial cohort, and hence its mean log-skill growth, conditional on no relocation opportunity, is

$$\gamma Z_n^S h + O(h^{3/2}).$$

It remains to translate crossings into wages. Put $G_n(x) = \log w_n^T(e^x) - \log w_n^M(e^x) = (1-\eta)(\hat{x} - x)$. Since $x_n < \hat{x}$, the wage gap $G_n(x_n)$ is strictly positive. For a worker who remains in market n, the wage-growth identity is

$$\Delta \log w_n = \begin{cases} X_h - X_0 + G_n(X_h)\mathbb{1}_{\{X_h < x_n\}}, & \text{if initially modern,} \\ \eta(X_h - X_0) - G_n(X_h)\mathbb{1}_{\{X_h > x_n\}}, & \text{if initially traditional,} \end{cases}$$

where X_s denotes log skill at date $t+s$. This identity compares each worker's final wage with the wage schedule of her initial sector. It does not condition the learning term on remaining in that sector.

For a modern worker who finishes below the cutoff, $G_n(X_h) \geq G_n(x_n) > 0$. The crossing bound therefore adds at least a positive multiple of $\sqrt{h}$ to mean modern-cohort wage growth. For a traditional worker who finishes between x_n and $\hat{x}$, the term $-G_n(X_h)$ lowers her wage growth and reinforces the difference between cohorts. A traditional worker finishing beyond $\hat{x}$ has the opposite wage adjustment, but must travel the fixed distance $\hat{x} - x_n > 0$ in time h. The expected contribution of those events is exponentially small.

Finally, the probability of at least one relocation opportunity is $O(h)$. Its contribution to expected wage growth is also $O(h)$. Wages selected in any two markets differ by a bounded amount at a given skill: below all cutoffs every market uses the traditional schedule, and above all cutoffs every market uses the modern schedule. The cutoffs lie in a bounded interval, where the wage differences are bounded as well. Conditional on an opportunity arriving, bounded drifts and volatilities give expected absolute skill displacement of order $\sqrt{h}$. Thus the opportunity paths contribute at most $O(h)$ to either cohort's expected wage growth.

Combining within-sector growth, cutoff crossings, and relocation gives, for some $C, C' > 0$ and all sufficiently small h,

$$\mathbb{E}_t\left[\Delta \log w_{n,t+h}^M\right] - \mathbb{E}_t\left[\Delta \log w_{n,t+h}^T\right] \geq \gamma(Z_n^M - \eta Z_n^T)h + C\sqrt{h} - C'h.$$

The positive $\sqrt{h}$ term exceeds $C'h$ when h is small. Both sectors are populated, so Lemma 3 gives $Z_n^M > Z_n^T$ under strict segmentation. Since $\eta < 1$ and $\gamma > 0$, there is $\bar{h} > 0$ such that, for every $h \in (0, \bar{h}]$,

$$\mathbb{E}_t\left[\Delta \log w_{n,t+h}^M\right] - \mathbb{E}_t\left[\Delta \log w_{n,t+h}^T\right] \geq \gamma(Z_n^M - \eta Z_n^T)h > 0.$$

□

B Data Appendix

This appendix describes the survey underlying our empirical analysis and the construction of our baseline sample.

B.1 Overview of the EPS

The *Encuesta de Protección Social* (EPS) is a longitudinal survey of the Chilean population commissioned by the Undersecretariat of Social Security (*Subsecretaría de Previsión Social*) of the Ministry of Labor. It was the first panel survey conducted in Chile and was created to study participation in the pension system, particularly the frequency with which workers contribute. Its early rounds were an important input into the design of the 2008 Chilean pension reform. The first four waves were designed and fielded by the Centro de Microdatos of the Universidad de Chile, in collaboration with researchers at the University of Pennsylvania and the University of Michigan. The EPS was conducted in 2002, 2004, 2006, 2009, 2012, and 2015, with additional waves collected after our sample period.

The 2002 round sampled individuals from the administrative register of pension-system affiliates and is therefore representative only of that population. In 2004, the EPS added new affiliates and individuals who were not affiliated with the pension system. From that round onward, it is representative of the Chilean population aged 18 and older, excluding the armed forces and police, who participate in a separate pension system. Each round interviews roughly 14,500 to 17,000 individuals. Respondents are followed over time, and those who miss a round can reenter the survey in later waves. The EPS also provides survey weights that adjust for nonresponse and align the sample with official population projections. We use these weights in all statistics.

The key feature of the EPS for our analysis is its retrospective labor-history module. Respondents provide a complete dated history of their labor-market activities, recorded as spells of employment, unemployment, or inactivity. For each employment spell, they report the start and end month, occupational category, type of contract, pension contributions, average monthly net earnings, usual weekly hours worked, occupation, industry, firm size, and region of work.[31] In the 2002 round, respondents report all activities since January 1980. In later rounds, returning respondents update their labor histories, while new respondents report their full histories.

We exclude the 2012 round from our analysis. Fieldwork fell substantially short of the target sample, nonresponse was non-random, and an official evaluation commissioned by the Undersecretariat concluded that the round should not be used for statistical inference. This exclusion does not create a gap in the labor histories because the 2015 round updates respondents' histories back to January 2009.

[31] Spell-level earnings are collected from the 2004 round onward.

B.2 Sample Construction

We use two blocks from the 2002, 2004, 2006, 2009, and 2015 rounds: the demographics module and the labor-history module. We first harmonize both blocks across rounds. Education is mapped into five categories using a crosswalk across the wave-specific classifications. Because reported ages are not always consistent across rounds, we impute each worker's birth year as the mode of interview year minus reported age. We also harmonize regions of work to the thirteen-region classification that preceded the 2007 administrative reform, and occupations and industries to the one-digit classifications used in the 2004 round.

From the labor histories, we keep employment spells and classify each job as modern or traditional. A job is traditional when the worker reports either not contributing to a pension fund or not having a labor contract, and modern otherwise. We drop observations with invalid or inconsistent dates, missing weekly hours, or more than 168 reported hours per week. In the 2004 and 2006 rounds, we also drop jobs starting after the survey year to avoid double counting across rounds.

We then aggregate the spell records into an annual panel. We first expand each spell into worker-month observations and aggregate them to the job-year level. For workers holding multiple jobs in a year, we keep the job with the highest hours worked. We construct wages by dividing monthly net earnings by usual weekly hours, deflate them to 2004 Chilean pesos using the Chilean CPI, and convert them to US dollars using the 2004 average exchange rate. For the summary statistics, we express wages in hourly terms by further dividing by the average number of weeks in a month. We trim hours and wages at the 1st and 99th percentiles and drop negligible reported incomes, which we treat as data errors. Because spell-level earnings are available from the 2004 round onward, wages can be constructed for jobs active from 2002 onward. We measure experience separately in each sector using the full job histories since 1980, converting cumulative hours worked into equivalent years under a full-time schedule of 48 hours per week.

We then select our baseline sample. We keep male workers aged 15 to 65 and female workers aged 15 to 60. We exclude unpaid workers, public-sector and armed forces employees, jobs with an unreported region of work, and observations without a valid wage. The resulting sample is an unbalanced annual panel of workers observed between 2002 and 2016, summarized in Table 1.

C Computational Appendix

This appendix describes the algorithm we use to compute the stationary equilibrium, based on finite-difference methods in the spirit of Achdou et al. (2022). Throughout, we work with log skill, $x \equiv \log z$. By (3), log skill follows a Brownian motion with constant drift within each market and sector,

$$\bar{\mu}_n^S = \gamma\, Z_n^S, \qquad S \in \{M, T\}, \tag{C1}$$

where the vibrancies Z_n^S are given by (4), evaluated at the stationary peer-skill distributions (5). The bar distinguishes the drift of *log* skill from the level drift μ_n^S in (6), which includes the Itô correction $\sigma_S^2/2$. Since $\gamma \geq 0$ and $Z_n^S \geq 0$, these drifts are nonnegative, a sign restriction we exploit in the discretization below. We discretize x on a uniform grid $\{x_j\}_{j=1}^J$ with spacing Δx and approximate the continuous-time model by a discrete-time model with period length Δt. Our implementation uses $J = 300$ nodes spanning $z \in [0.1, 1000]$ and $\Delta t = 0.003$ years.

The algorithm has three nested components. Given drifts and a subsidy rate, Appendix C.1 solves the workers' problem (7) using Howard's policy iteration, delivering values and sector cutoffs. Given values, cutoffs, and drifts, Appendix C.2 solves the stationary KFE (9) as a single sparse linear system. Appendix C.3 then closes the model by expressing the stationary equilibrium as a fixed point in the $2N$ vibrancies and solving it by damped iteration over the map generated by the two inner solvers. Finally, Appendix C.6 describes how we compute transitional dynamics.

C.1 Solving the HJB Equation

Fix drifts (C1) and a subsidy rate b. In logs, the stationary envelope HJB equation (7) becomes

$$(\rho + \delta)\, V_n(x) = \max_{S \in \{M,T\}} \left\{ u_n^S(x) + \bar{\mu}_n^S\, \partial_x V_n(x) + \frac{\sigma_S^2}{2}\, \partial_{xx} V_n(x) \right\} + \mathcal{M}_n[V](x), \tag{C2}$$

where $u_n^S(x) = \log\big((1+b)\, w_n^S(e^x)\big)$ is flow utility under the wage schedules (1),[32] and $\mathcal{M}_n[V](x)$ is the mobility option value (2), with time arguments omitted.

We approximate (C2) by the Bellman equation of a discrete-time Markov chain on the grid. Over a period of length Δt, a worker in sector S of market n discounts the future by the survival-adjusted factor $\beta \equiv 1 - \Delta t\,(\rho + \delta)$ and transitions to neighboring nodes with probabilities

$$p_+^{n,S} = \frac{\Delta t}{\beta} \left(\frac{\bar{\mu}_n^S}{\Delta x} + \frac{\sigma_S^2}{2\Delta x^2} \right), \qquad p_-^S = \frac{\Delta t}{\beta}\, \frac{\sigma_S^2}{2\Delta x^2}, \qquad p_0^{n,S} = 1 - p_+^{n,S} - p_-^S, \tag{C3}$$

which we collect in a row-stochastic tridiagonal matrix P_n^S. At the two boundary nodes, the outward move is suppressed, so the grid boundaries are reflecting. We upwind the drift forward because $\bar{\mu}_n^S \geq 0$. All three probabilities are nonnegative provided $\Delta t\,\big(\rho + \delta + \bar{\mu}_n^S/\Delta x + \sigma_S^2/\Delta x^2\big) \leq 1$,

[32] In the implementation, the logarithm is guarded by a linear extension below a small consumption floor (10^{-4}); the floor never binds on the equilibrium wage schedules.

which is satisfied by our time step. The resulting discrete Bellman equation is

$$V_n(x_j) = \max_{S\in\{M,T\}} \left\{\Delta t\, u_n^S(x_j) + \beta \left[P_n^S V_n\right]_j\right\} + \Delta t\, \mathcal{M}_n[V](x_j), \tag{C4}$$

which converges to (C2) as the grid spacing and time step shrink.

We solve (C4) by Howard's policy iteration on the $N \times J$ state space. Given a candidate envelope V^k, the policy step assigns to each node the sector with the larger Bellman return,

$$S_n^k(x_j) = \operatorname*{argmax}_{S\in\{M,T\}} \left\{\Delta t\, u_n^S(x_j) + \beta \left[P_n^S V_n^k\right]_j\right\},$$

where the mobility term drops out because it is common to both sectors.

Given this policy, the evaluation step solves the linear system implied by (C4),

$$(1+\Delta t\,\lambda)\, V_n^{k+1}(x_j) - \beta \left[P_n^{S^k} V_n^{k+1}\right]_j = \Delta t\, u_n^{S^k}(x_j) + \frac{\Delta t\,\lambda}{\nu} \log\left(\sum_{m=1}^{N} e^{\nu\left(V_m^k(x_j)-\xi_{nm}\right)}\right), \tag{C5}$$

which evaluates the log-sum-exp inside $\mathcal{M}_n[V]$ at the lagged iterate while treating its own-value term, $-\lambda V_n$, implicitly. Each evaluation step requires a single sparse solve over the NJ stacked states. We alternate between the policy and evaluation steps until values converge in the sup norm, using a tolerance of 10^{-5}.

Relative to direct iteration on (C4), Howard's policy iteration replaces many small value updates with exact solves under candidate policies and converges in a small number of iterations. From a cold start, we initialize values at the annuitized modern flow value, $V^0 = u^M/(\rho+\delta)$. Inside the equilibrium loop of Appendix C.3, we instead warm-start from the values obtained in the previous iteration.

Given the converged envelope, sector-specific values follow from one application of each sector's Bellman operator,

$$V_n^S = \Delta t\, u_n^S + \beta\, P_n^S V_n + \Delta t\, \mathcal{M}_n[V], \qquad S \in \{M,T\},$$

with $V_n = \max\{V_n^M, V_n^T\}$ node by node. The labor supply policy is determined by the sign change of $\Delta_n \equiv V_n^M - V_n^T$. Letting j denote the first node at which the policy switches from the traditional to the modern sector, linear interpolation gives

$$\bar{x}_n = x_j - \frac{\Delta_n(x_j)}{\Delta_n(x_{j+1}) - \Delta_n(x_j)}\, \Delta x. \tag{C6}$$

If one sector is selected everywhere, we assign the cutoff to the corresponding end of the grid.

C.2 Solving the Kolmogorov Forward Equation

Given values, cutoffs, and drifts, the stationary distribution solves (9) with $\partial_t N_n^S = 0$. Under the cutoff policy, sector choice is a deterministic function of the worker's state. It therefore suffices to solve for the aggregate densities $N_n(x)$ and recover the sectoral densities as

$$N_n^M(x) = N_n(x)\,\mathbb{1}\{x > \bar{x}_n\}, \qquad N_n^T(x) = N_n(x)\,\mathbb{1}\{x \le \bar{x}_n\}.$$

We discretize the Brownian part of (9) in conservative form using a finite-volume scheme. Each grid node represents a cell that exchanges mass with its neighbors through common faces, with each face flux added to one cell and subtracted from the other. Mass conservation therefore holds cell by cell, including at the cutoff face where the drift and diffusion coefficients jump. The scheme approximates the flux and diffusion-weighted density matching conditions in Remark 1. It does not impose continuity of density when sectoral volatilities differ.

For this reason, we do not construct the forward operator by transposing the HJB matrices of Appendix C.1. The transposed scheme assigns the cutoff face the coefficients of a single node, misrepresenting the flux precisely where the coefficients jump. The conservative scheme instead imposes flux continuity by construction.

Concretely, drop the market index and let cell j carry the coefficients $(\bar{\mu}_j, \sigma_j^2)$ of its sector, modern if and only if $x_j > \bar{x}_n$. Conditional on receiving neither a mobility nor a death shock over the period, an event with probability $1 - \Delta t\,(\lambda + \delta)$, mass crosses the face between cells j and $j+1$ upward and downward with probabilities

$$q_j^+ = s\left(\frac{\bar{\mu}_j + \bar{\mu}_{j+1}}{2\,\Delta x} + \frac{\sigma_j^2}{2\Delta x^2}\right), \qquad q_j^- = s\,\frac{\sigma_{j+1}^2}{2\Delta x^2}, \qquad s \equiv \frac{\Delta t}{1 - \Delta t\,(\lambda + \delta)}, \tag{C7}$$

so the drift is transported using the face-averaged $\bar{\mu}$ and forward-only upwinding, while each cell diffuses across a face at the rate implied by its own σ^2. We impose zero flux at the ends of the grid. Collecting these probabilities yields a column-stochastic tridiagonal matrix Q_n for each market. Every column sums to one, so any mass leaving a cell is exactly transferred to an adjacent cell.

The stationary distribution then satisfies the discrete-time balance

$$\boldsymbol{N} = \big(1 - \Delta t\,(\lambda + \delta)\big)\,Q\,\boldsymbol{N} + \Delta t\,\lambda\,\boldsymbol{M}(V)\,\boldsymbol{N} + \Delta t\,\delta\,\boldsymbol{\psi}, \tag{C8}$$

where $\boldsymbol{N} \in \mathbb{R}^{NJ}$ stacks the market densities and $Q = \mathrm{diag}(Q_1, \ldots, Q_N)$. The mobility operator reallocates mass across markets at fixed skill according to the logit shares of Section 2,

$$[\boldsymbol{M}(V)\boldsymbol{N}]_n(x_j) = \sum_{k=1}^{N} m_{kn}(x_j)\,N_k(x_j),$$

while the entry vector has components

$$[\boldsymbol{\psi}]_n(x_j) = \psi(x_j)\,\Pi_n(x_j),$$

with Π_n denoting the newborn location probabilities in (10).

Equation (C8) is a sparse linear system in $\boldsymbol{N}$, which we solve with a single factorization; no time iteration is required. Moreover, Q and $\boldsymbol{M}(V)$ are column-stochastic, Π_n sums to one across markets, and ψ is normalized to integrate to one on the grid. Summing (C8) over all states implies that the stationary distribution integrates to one exactly, so no renormalization is required.

C.3 Solving for the Stationary Equilibrium

The outer loop combines the two solvers into a stationary equilibrium as defined in Section 2.4. The key observation, anticipated in the discussion of uniqueness preceding Proposition 2, is that conditional on the vector of vibrancies $Z = \{Z_n^M, Z_n^T\}_{n=1}^N$, all remaining equilibrium objects are pinned down sequentially. Wages follow from optimal labor demand, condition (i), in closed form from (1). Values and the cutoff policy follow from the workers' dynamic problem, condition (ii), computed as in Appendix C.1. The stationary distribution follows from the distribution dynamics, condition (iv), computed as in Appendix C.2. Finally, the subsidy rate follows from budget balance, condition (v):

$$b = \tau \, \frac{\sum_{n=1}^N \int w_n^M(z)\, N_n^M(z)\,\mathrm{d}z}{\sum_{n=1}^N \sum_{S\in\{M,T\}} \int w_n^S(z)\, N_n^S(z)\,\mathrm{d}z}. \tag{C9}$$

Labor market clearing, condition (vi), holds by construction: firms absorb all workers at the posted wages, while the unit-mass condition is preserved exactly by the KFE scheme.

The remaining equilibrium condition is learning consistency, condition (iii). The vibrancies implied by the computed sectoral distributions through (4) and (5) must coincide with those workers take as given when solving their problem. A stationary equilibrium is therefore a fixed point $Z = T(Z)$ of the finite-dimensional map $T : \mathbb{R}_+^{2N} \to \mathbb{R}_+^{2N}$ that, given vibrancies, computes the remaining equilibrium objects and returns the implied vibrancies. We solve this fixed point by damped successive approximation on T, or equivalently, by (C1), by iterating on the drifts $\bar{\mu}_n^S = \gamma Z_n^S$:

Step 0. Initialize. Set $N_n^0(x) = \psi(x)/N$, so newborn skills are spread evenly across markets, with a common sector cutoff at the grid midpoint; alternatively, warm-start from a previously computed equilibrium. Compute Z^0 from (4) and (5), set $\bar{\mu}^0 = \gamma Z^0$, and compute b^0 from (C9).

Step 1. Worker problem. Given $(\bar{\mu}^r, b^r)$, solve (C4) to obtain values V^r and cutoffs $\bar{x}^r$.

Step 2. Distribution. Solve (C8) at $(\bar{\mu}^r, \bar{x}^r, V^r)$ to obtain $\widetilde{N}$. Relax toward the previous iterate, $N^{r+1} = \omega_N \widetilde{N} + (1-\omega_N)\, N^r$, and split the resulting distribution into sectors at $\bar{x}^r$.

Step 3. Learning consistency. Compute $\widetilde{Z}$ from (4) and (5) at N^{r+1} and obtain the implied drifts $\gamma\widetilde{Z}$.

Step 4. Convergence. If $\max_{n,S} \left|\gamma \widetilde{Z}_n^S - \bar{\mu}_n^{S,r}\right| / \bar{\mu}_n^{S,r}$ is below tolerance, stop. Otherwise, set $\bar{\mu}^{r+1} = \omega\,\gamma\widetilde{Z} + (1-\omega)\,\bar{\mu}^r$, update b^{r+1} from (C9), and return to Step 1, warm-starting the value solver at V^r.

The two relaxations ($\omega = \omega_N = 0.2$; convergence tolerance 10^{-2}) temper the feedback loop at the core of the model. A larger modern sector raises Z_n^M, which increases $\bar{\mu}_n^M$ and, in turn, attracts more workers into the modern sector. Undamped iteration can overshoot through this feedback and spuriously absorb the traditional sector. At convergence, conditions (i)–(vi) hold simultaneously up to the stated tolerance. Finally, as discussed after Proposition 2, we probe for multiple equilibria by re-running the algorithm from different initial distributions.

C.4 Recovering Migration Costs

We recover the bilateral migration costs $\{\xi_{nm}\}_{n,m=1}^N$ from migration flows observed in the EPS. We first construct year-to-year transitions between consecutive survey years and compute survey-weighted flows between every origin and destination market, averaging these flows over the sample period. Dividing each flow by the total mass of workers from its origin market, including those who stay, yields the empirical migration shares $\hat{m}_{nm}$.

The mobility shares of Section 2 imply that, for a worker in market n,

$$X_{nm} \equiv \log \hat{m}_{nm} - \log \hat{m}_{nn} = \nu\,(V_m - V_n) - \nu\,\xi_{nm}, \tag{C10}$$

where we impose the normalization $\xi_{nn} = 0$. Taking the corresponding expression for the reverse flow and adding the two equations eliminates the value terms:

$$X_{nm} + X_{mn} = -\nu\,(\xi_{nm} + \xi_{mn}).$$

Assuming symmetric migration costs, $\xi_{nm} = \xi_{mn}$, we recover

$$\xi_{nm} = -\frac{X_{nm} + X_{mn}}{2\nu}, \tag{C11}$$

using the calibrated taste dispersion ν.

Two qualifications are worth noting. First, we do not recover skill-specific migration costs. Although mobility shares in the model depend on skill through workers' values, we pool workers across skill levels when constructing the empirical shares and recover a single migration cost for each market pair. Second, market pairs with no observed flows in either direction are assigned an infinite migration cost, ruling out migration between them in the model.

C.5 Construction of Model Moments

The estimation in Section 4 matches ten moments, all computed directly from the stationary equilibrium, so no simulation is required. Two of these moments are cross-sectional. The modern-sector employment share is given by the mass of workers above the sectoral cutoffs, $\sum_n \int N_n^M(z)\,\mathrm{d}z$, where total population is normalized to one. The variance of modern log wages is the variance of $\log w_n^M(z)$ under the modern-sector distribution $N_n^M(z)$. Both moments are computed directly from the stationary distribution obtained in Appendix C.2.

The transition moments track individual workers over time and therefore require the law of motion of a worker's state, (n, x). On the NJ-state grid, this law of motion is summarized by the generator

$$\mathcal{Q} \;=\; \frac{Q - I}{\Delta t} \;+\; \lambda\big(\boldsymbol{M}(V) - I\big) \;-\; \delta I, \tag{C12}$$

where the three terms capture the per-year rates of learning through drift and diffusion, migration across labor markets, and death, respectively. The generator is evaluated at the stationary equilibrium using the operators defined in Appendix C.2.

Death is absorbing in (C12). The newborn who replaces an exiting worker is a different individual in the panel, so the rebirth inflow that appears in the KFE is excluded here. For any mass vector $\boldsymbol{\nu}$ of workers, $e^{h\mathcal{Q}}\boldsymbol{\nu}$ gives their distribution across states h years later, scaled by the surviving share $e^{-\delta h}$. Because the sector is a property of the grid cell, with modern cells above the stationary cutoff and traditional cells below it, sector and wage classifications at any two dates use the same time-invariant labels.

The sector transition probabilities condition on survival. Let $\mathbf{1}_S$ indicate the cells assigned to sector S and let $\boldsymbol{N}^S$ denote the stationary mass in those cells. The probability that a worker who starts in sector S is in sector S' after h years, conditional on surviving, is

$$P^h_{SS'} \;=\; \frac{\mathbf{1}'_{S'}\, e^{h\mathcal{Q}}\, \boldsymbol{N}^S}{\mathbf{1}'\, e^{h\mathcal{Q}}\, \boldsymbol{N}^S}, \tag{C13}$$

where $\mathbf{1}$ sums over all cells, so the denominator removes the uniform survival factor. The moment vector includes the one-year staying probabilities, P^1_{MM} and P^1_{TT}.

The within-sector wage-quintile transitions mirror their construction in the data. Quintiles are defined separately within each sector's wage distribution, and the sample is restricted to workers observed in the same sector at both endpoints. Let $\mathbf{1}^S_i$ indicate the sector-S cells in the i-th quintile of the sector's stationary wage distribution, and let $\boldsymbol{N}^S_i$ denote the stationary mass in those cells. The five-year transition probability from quintile i to quintile j, conditional on surviving and being in sector S at both endpoints, is

$$P^{5,S}_{ij} \;=\; \frac{(\mathbf{1}^S_j)'\, e^{5\mathcal{Q}}\, \boldsymbol{N}^S_i}{\sum_{j'}(\mathbf{1}^S_{j'})'\, e^{5\mathcal{Q}}\, \boldsymbol{N}^S_i}, \tag{C14}$$

where the denominator retains only the mass of workers who remain in sector-S cells after five years. The moment vector uses the interior diagonal elements, $P^{5,S}_{22}$, $P^{5,S}_{33}$, and $P^{5,S}_{44}$, for each sector, giving six moments. We exclude the corner elements for the reasons discussed in Section 4.

C.6 Transitional Dynamics via the Sequence-Space Jacobian

We compute the perfect-foresight transitions generated by the two permanent shocks considered in Section 5: eliminating the payroll tax and equalizing the learning technology for traditional workers. We solve for these transitions to first order in sequence space, following the continuous-time formulation of Bilal and Goyal (2026). Both reforms are unanticipated and permanent.

Following the convention in Auclert et al. (2021) for permanent shocks, we therefore linearize the equilibrium conditions around the terminal steady state, whose objects we denote with an asterisk. The transition is then expressed as a path of deviations from this terminal equilibrium. At the time of the reform, the economy is still distributed according to the baseline stationary equilibrium, so the initial deviation is $\Delta N_0 = N^0 - N^*$. These deviations converge to zero along the transition path. We truncate the computation at $T = 300$ years and use the remaining deviation at the terminal date as a diagnostic for the accuracy of the truncation.

The only aggregate sequences we need to solve for are the $2N$ vibrancy paths, $\Delta Z = \{\Delta Z_n^S(t)\}$. Vibrancies play a dual role in the equilibrium. On the one hand, they enter the individual worker problem through the learning drift in (C1). On the other hand, they are determined by the cross-sectional distribution of workers through the CES aggregator in (4). In this sense, vibrancies play the role of the price sequences in Auclert et al. (2021). No other aggregate sequence needs to be solved for. Wages depend only on parameters and market productivities, while the subsidy rate shifts flow utility uniformly across states and therefore does not affect workers' decisions.

Writing $\Delta V(\Delta Z)$ for the value deviations implied by the backward block and $\Delta N(\Delta Z; \Delta N_0)$ for the distribution deviations implied by the forward block, equilibrium requires the vibrancies generated by the resulting cross-sectional distribution to coincide with the conjectured paths:

$$\Delta Z_t^{\text{impl}}\big(\Delta V, \Delta N\big) - \Delta Z_t = 0, \qquad t = 0, \ldots, T-1. \tag{C15}$$

We construct the linearized blocks using exact derivatives of the discretized steady-state operators described in Appendices C.1 and C.2. This approach preserves the adjoint relation between the backward and forward blocks at the discrete level. Let Φ denote the one-year worker-level transition operator at the terminal equilibrium, incorporating learning, migration, and death—that is, $\Phi = e^{\mathcal{Q}}$, with the generator (C12) evaluated at the terminal equilibrium—and let Φ' denote its adjoint. Throughout this appendix, primes denote adjoint operators. Newborn entry remains at its terminal value, except for the behavioral response of location choice that we introduce below. We also define Φ_V as the discounted counterpart of Φ under the discount rate ρ. Because death is already incorporated into Φ, together these two components imply that workers' values discount at rate $\rho + \delta$.

We first consider the backward block. Changes in vibrancy affect the Bellman equation through the learning drift. Hence, the value response to a change in vibrancy is given by the discounted expected marginal value of the resulting increase in skill growth:

$$\Delta V_t = \sum_{a \geq 0} \Phi_V^a \, G_V \, \Delta Z_{t+a}, \qquad \big(G_V \, \Delta Z\big)_n(x) \equiv \gamma \, \partial_x V_n^*(x) \, \Delta Z_n^{S_n^*(x)}, \tag{C16}$$

where $S_n^*(x)$ denotes the terminal sector assignment. We compute the full set of kernels with a single linear backward pass. We next linearize the sector-indifference condition of Appendix C.1 around the terminal cutoffs. The resulting cutoff response is

$$\Delta \bar{x}_t = C_V \, \Delta V_t + C_Z \, \Delta Z_t, \tag{C17}$$

where the first term captures how changes in workers' values affect the sector choice, while the second captures the direct effect of changes in vibrancy on the dynamic gains from each sector.

We then turn to the forward block. The distribution deviation evolves according to the linearized Kolmogorov forward equation,

$$\Delta N_{t+1} = \Phi\, \Delta N_t + G_N\, \Delta Z_t + B\, \Delta V_t, \tag{C18}$$

where G_N and B capture two forces affecting the evolution of the distribution. The operator G_N moves the terminal distribution in response to changes in the learning drift through the derivative of the conservative flux in (C7). The operator B captures behavioral reallocation through changes in migration-destination and newborn-location choice probabilities induced by changes in workers' values. Both operators also incorporate the cutoff response in (C17), which changes the sector assignment, and therefore the learning technology, of workers at the cutoff.

The final block maps the distribution back into implied vibrancies. Changes in the distribution affect vibrancy through the CES gradients of (4), which we collect in the matrix E, as well as through the reassignment of workers around the sectoral cutoff:

$$\Delta Z_t^{\text{impl}} = E'\, \Delta N_t + G_{\bar{x}}\, \Delta \bar{x}_t. \tag{C19}$$

Combining (C16)–(C18) with (C19) turns the equilibrium condition in (C15) into a linear system in ΔZ. We construct its Jacobian, $\mathcal{J} = \partial \Delta Z^{\text{impl}} / \partial \Delta Z$, using the fake-news algorithm of Auclert et al. (2021).

In particular, the expectation vectors $E_a = (\Phi')^a E$ propagate the output functionals forward, while the distribution impulses $D_q = B\, \Phi_V^q\, G_V + \mathbb{1}\{q = 0\}\, G_N$ collect the forward response to vibrancy news arriving at horizon q. Their inner products give the fake-news matrix, $\mathcal{F}_{a,q} = E_a'\, D_q$, from which the standard recursion delivers $\mathcal{J}$. We additionally include the contemporaneous response operating through the within-period cutoff, given by $G_{\bar{x}} C_V \Phi_V^q G_V$ and $G_{\bar{x}} C_Z$. The equilibrium path then solves

$$(I - \mathcal{J})\, \Delta Z = R, \qquad R_a = E_a'\, \Delta N_0, \tag{C20}$$

where R captures the autonomous propagation of the initial distribution gap.

With $N = 27$ markets, two sectors, and a horizon of $T = 300$ years, (C20) is a single dense linear system of size $2NT = 16{,}200$. We aggregate time into one-year periods and construct the annual transition operators using twelve implicit Euler substeps, with the required factorization computed only once.

D Additional Figures

D.1 Descriptive Statistics

This section reports additional descriptive statistics on the share of modern workers in Chile. We confirm previously well-established patterns for the Chilean economy:

1. The share of modern workers follows an inverse U-shaped pattern over the life cycle.

2. The share of modern workers increases with educational attainment.

3. The share of modern workers increases with firm size.

Then, we report the share of modern workers by occupation and economic sector.

Figure D1: Share of Modern Workers by Age

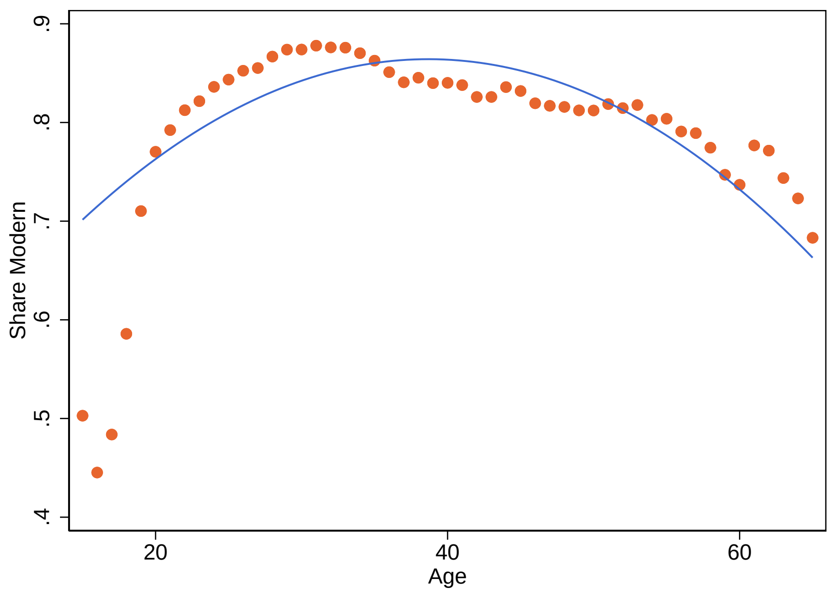

Notes: Figure D1 displays the average share of modern workers at each age, together with a quadratic fit. We restrict our sample to salaried workers, excluding self-employed workers, entrepreneurs, workers without remuneration, and public-sector and armed forces employees.

Figure D2: Share of Modern Workers by Educational Attainment

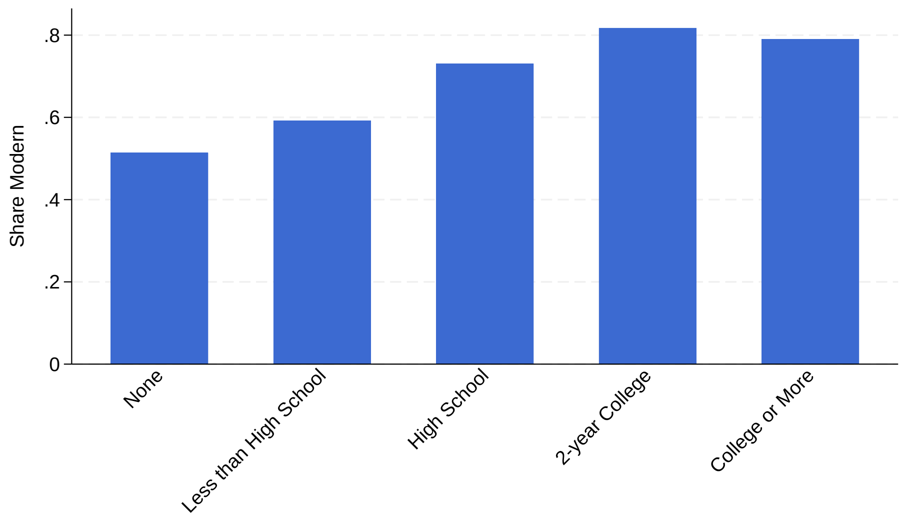

Notes: Figure D2 displays the share of modern workers by education group. We consider all workers in our baseline sample, including self-employed workers and entrepreneurs.

Figure D3: Share of Modern Workers by Firm Size

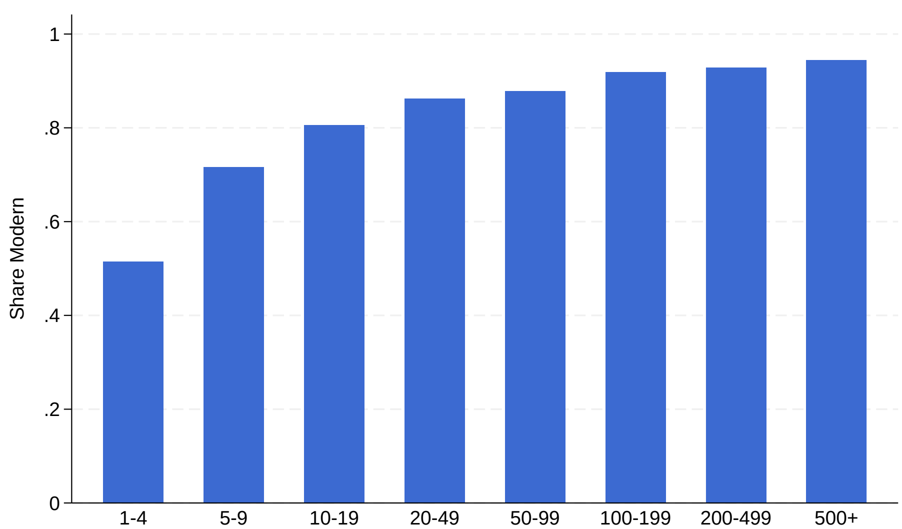

Notes: Figure D3 displays the share of modern workers by firm size. Bars denote firm size groups, and labels denote the range of employees in each group. We restrict our sample to salaried workers, excluding self-employed workers, entrepreneurs, workers without remuneration, and public-sector and armed forces employees.

Figure D4: Share of Modern Workers by Occupation

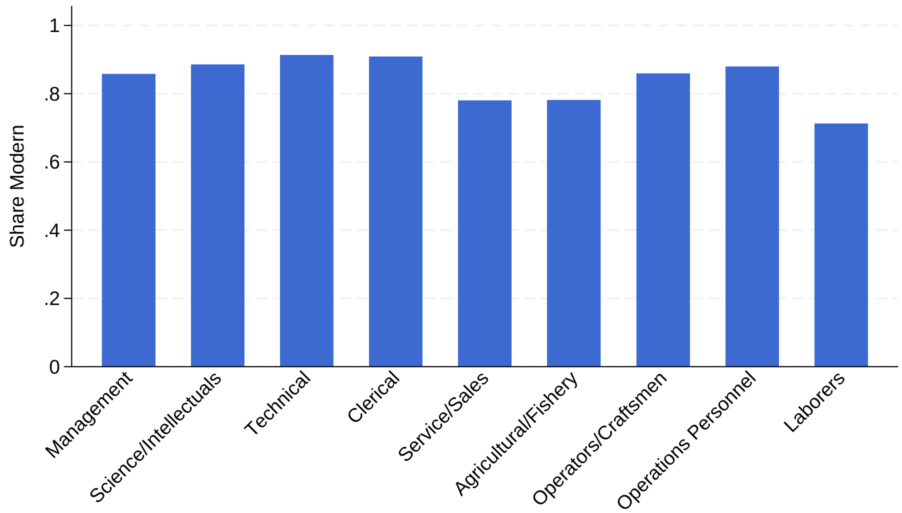

Notes: Figure D4 displays the share of modern workers by occupation. We restrict our sample to salaried workers, excluding self-employed workers, entrepreneurs, workers without remuneration, and public-sector and armed forces employees.

Figure D5: Share of Modern Workers by Sector

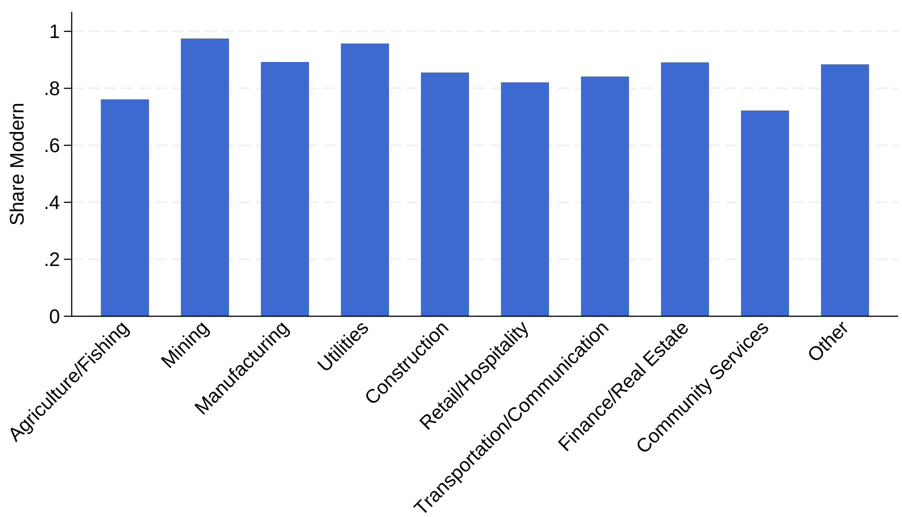

Notes: Figure D5 displays the share of modern workers by economic sector. We restrict our sample to salaried workers, excluding self-employed workers, entrepreneurs, workers without remuneration, and public-sector and armed forces employees.

D.2 Modern and Traditional Wage Dynamics

In this section, we report wage-experience and wage-age profiles for modern and traditional workers, restricting the sample to salaried workers.

Figure D6: Wages Over the Life Cycle for Modern and Traditional Workers, Salaried Workers

(a) Wage-experience profiles **(b)** Wage-age profiles

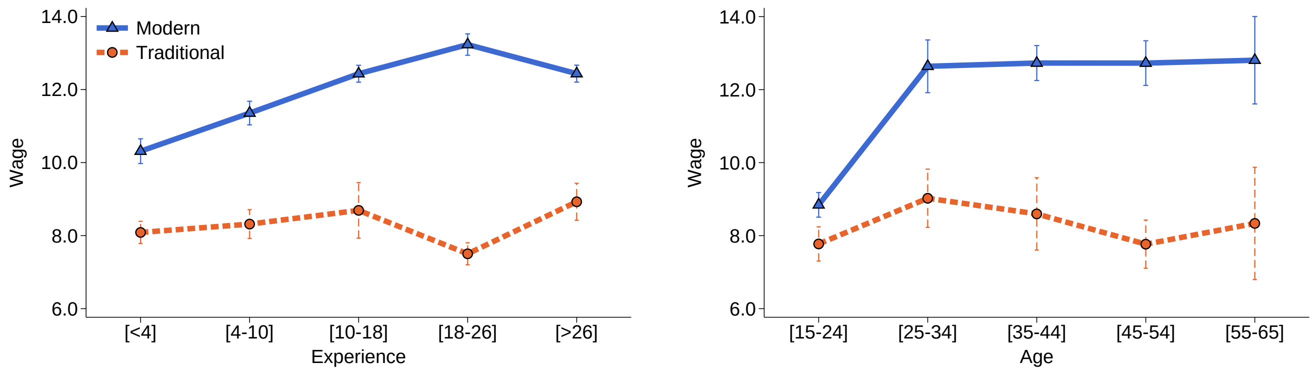

Notes: Figure D6 displays average wages by experience quintile (panel (a)) and by 10-year age bin (panel (b)) for modern and traditional workers. We restrict our sample to salaried workers, excluding self-employed workers and entrepreneurs. Vertical dashed lines denote 95 percent confidence intervals.

D.3 Robustness: Omitting Firm Size

In this section, we show that the main results of our empirical analysis are robust to omitting firm size. We re-estimate the specifications underlying Figures 2, 3, 4, and 5, excluding the firm-size bracket both from the set of controls and from the definition of workers' labor markets, which become Region $\times$ Year $\times$ Industry $\times$ Occupation cells.

Figure D7: Worker Fixed Effects for Modern and Traditional Workers, Omitting Firm Size

(a) Histogram

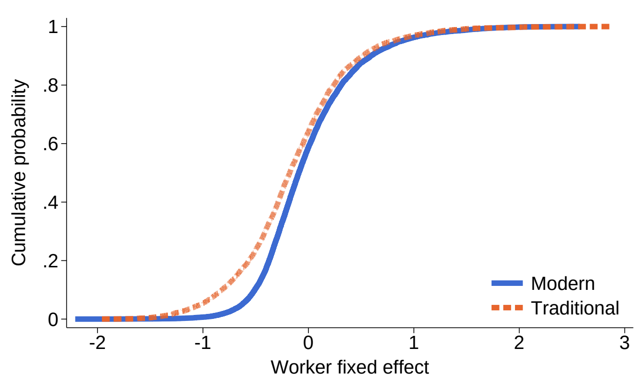

(b) Cumulative distribution

Notes: Figure D7 replicates Figure 2 omitting firm size from the set of controls. Worker fixed effects α_i are estimated from equation (14), controlling for age, education, occupation, industry, region, experience in each sector, and time fixed effects. We keep one observation per worker and assign workers to the sector in which we observe them most often.

Figure D8: Modern Sector Dynamic Wage Premium, Omitting Firm Size

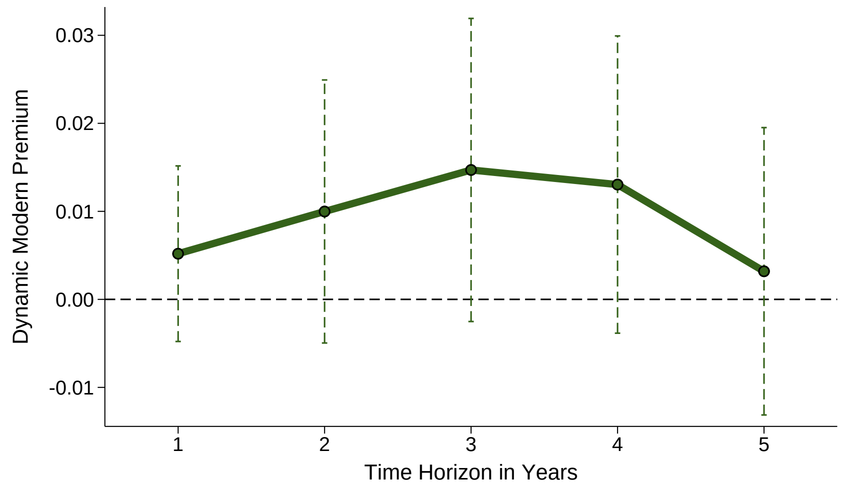

Notes: Figure D8 replicates Figure 3 omitting firm size from the set of controls. Each dot represents the estimated wage premium at horizon $t + h$: $\exp(\hat{\beta}_h) - 1$, for $h = 1, \ldots, 5$, from equation (15) including worker fixed effects. Controls include age, education, gender, occupation, industry, region, experience, wage decile, and time and worker fixed effects. Vertical dotted lines denote 95 percent confidence intervals.

Figure D9: Peer Effects on Wage Growth, Omitting Firm Size

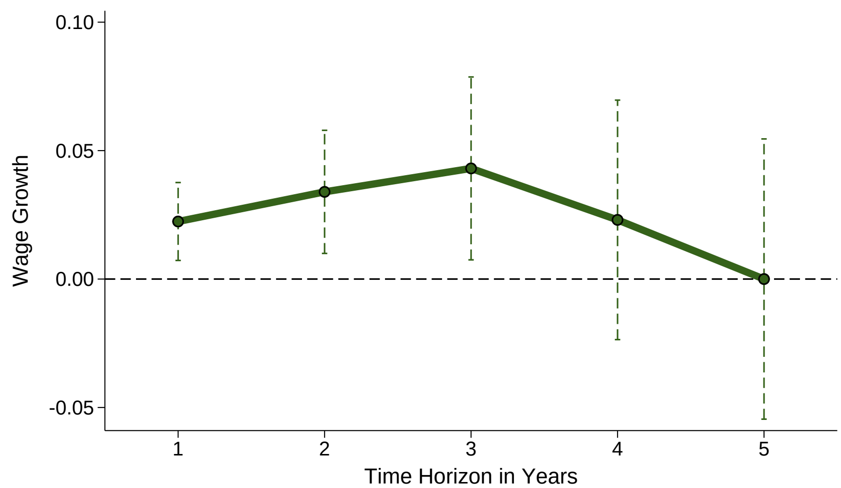

Notes: Figure D9 replicates Figure 4 omitting the firm-size bracket from the definition of peer groups. Peers are defined as all other workers in the same Region × Year × Industry × Occupation cell. Each dot represents the estimated effect of peer wages on workers' future wage growth at the time horizon $t + h$, based on the estimates of β_h from equation (16). Controls include age, education, gender, occupation, industry, region, experience, wage decile, and time fixed effects. Vertical dotted lines denote 95 percent confidence intervals.

Figure D10: Peer Effects on Wage Growth Robustness, Omitting Firm Size

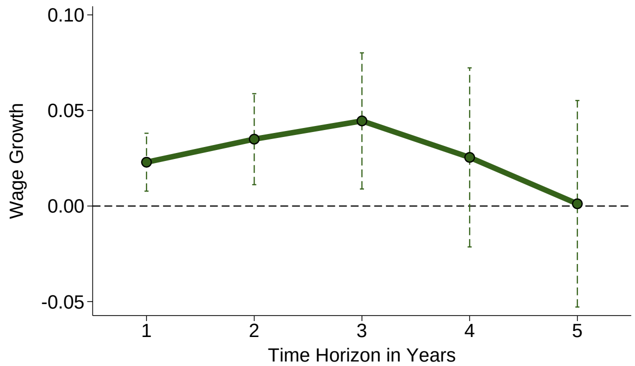

(a) Modern-sector status

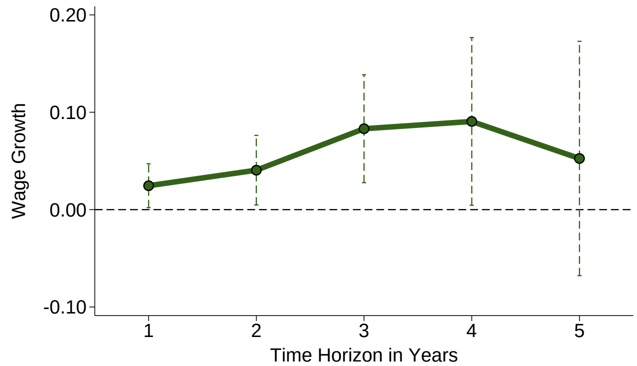

(b) Wage-bill growth

Notes: Figure D10 replicates Figure 5 omitting the firm-size bracket from the definition of peer groups. In Panel D10(a) we control for an indicator for modern-sector employment, Modern_{it}. In Panel D10(b) we control for the growth of the labor market's total wage bill between $t-2$ and $t-1$, $t-1$ and t, and t and $t+1$. The remaining controls are the same as in Figure D9. Vertical dotted lines denote 95 percent confidence intervals.

D.4 Life-Cycle Wages in Levels: Model vs Data

Figure D11: Life-Cycle Wages in Levels: Model vs Data

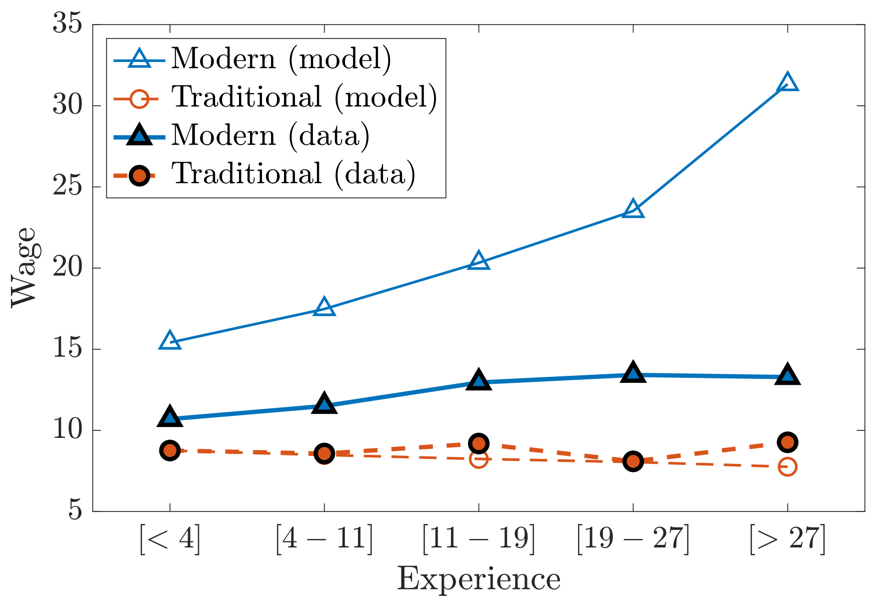

Notes: Figure D11 displays average wages by experience bin for modern and traditional workers in the model and in the data. Model averages are computed over the same experience-quintile bins as in Figure 1(a), weighting ages by surviving sector mass, and model wages are normalized so that the model matches the traditional average wage in the first experience bin. The data series coincide with those reported in Figure 1(a).

Figure D12: Skill Distributions Across Labor Markets

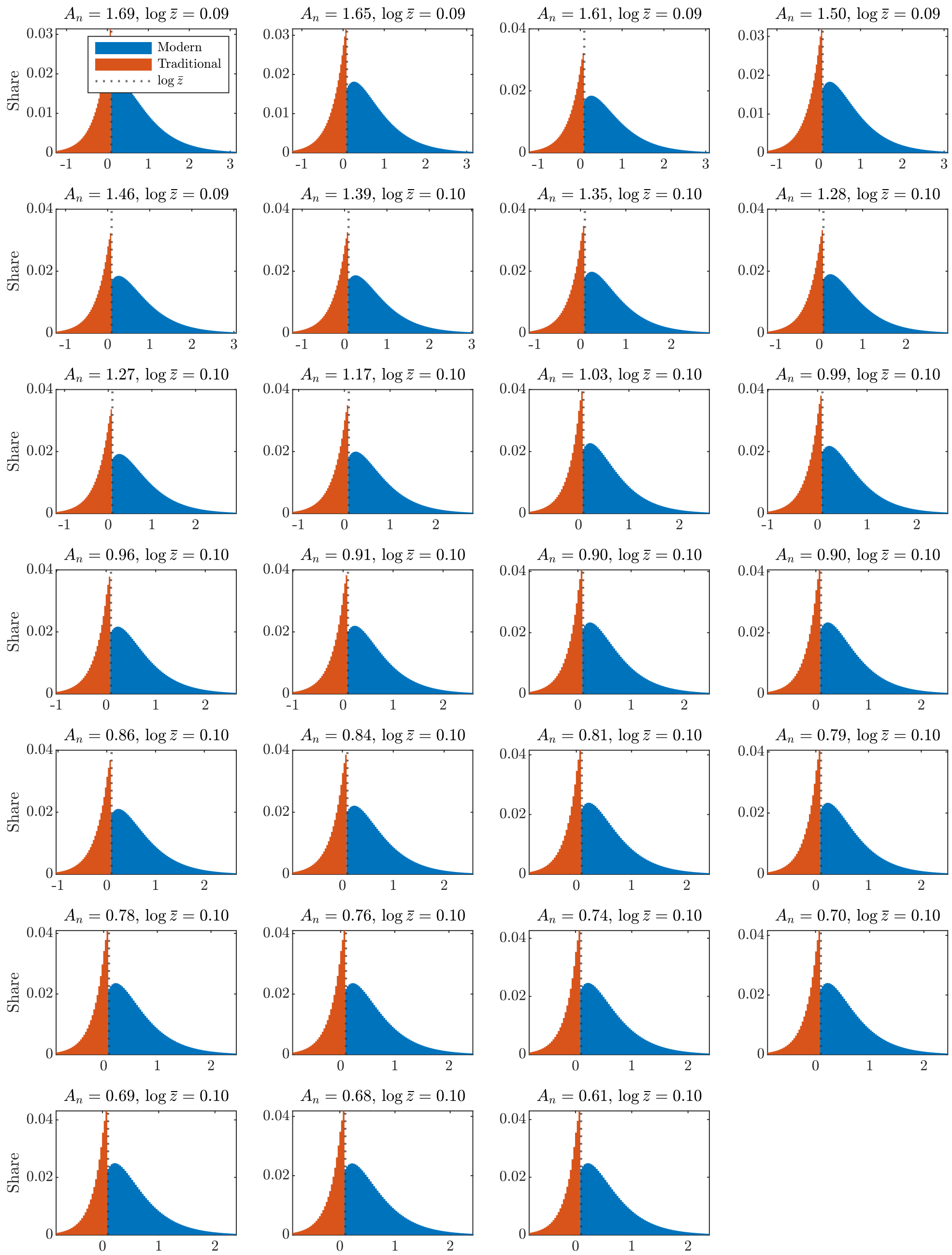

Notes: Figure D12 displays the stationary distribution of workers over log skill by sector in each of the 27 labor markets, expressed as a share of each market's workers. Markets are sorted by productivity A_n, with the most productive market first; each panel's title reports the market's productivity and modern-sector cutoff, and the dotted vertical line denotes the cutoff $\log \bar{z}$.

D.5 Learning-Channel Welfare Effects of Raising Payroll Taxes

Figure D13 replicates the left panel of Figure 9 for the counterfactual economy with a higher payroll tax, $\tau = 0.20$. The welfare effects are roughly the mirror image of those from eliminating payroll taxes, with losses concentrated among movers, who now switch from the modern to the traditional sector.

Figure D13: Welfare Losses from Peer Learning: Higher Payroll Taxes

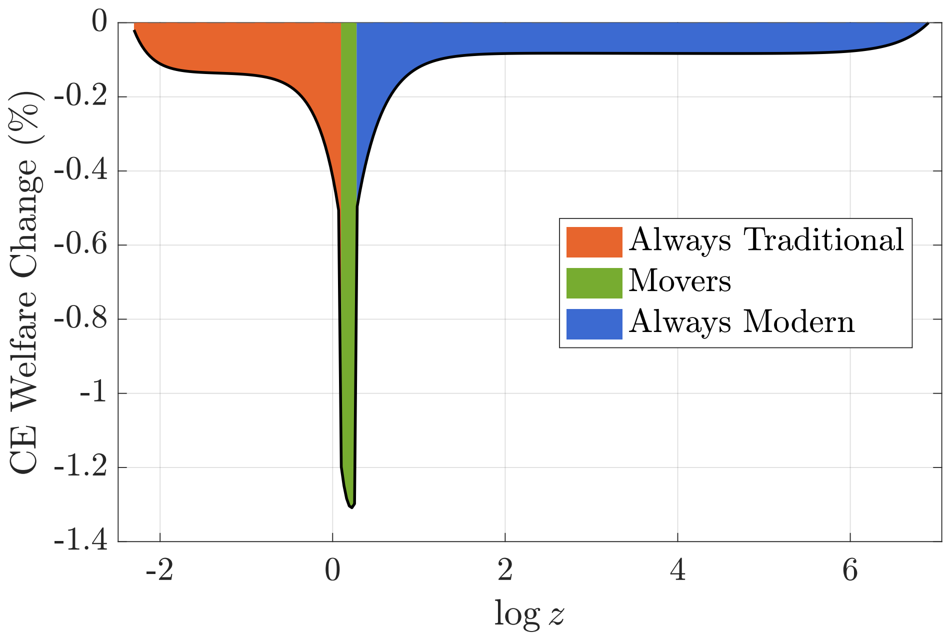

Notes: Figure D13 decomposes learning welfare losses in the counterfactual economy with a payroll tax of $\tau = 0.20$. The x-axis denotes log skill, while the y-axis denotes consumption-equivalent welfare changes from the learning channel. The shaded areas split workers into always-traditional (orange), movers (green), and always-modern (blue) groups, where movers now switch from the modern to the traditional sector after the tax increase.

E Additional Tables

Table E1 reports estimates of the modern-traditional wage gap from equation (14), discussed in Section 3.

Table E1: Modern-Traditional Wage Gap

	Dependent variable: $\log w_{i,t}$		
	(1)	(2)	(3)
Modern	0.395***	0.093***	0.082***
	(0.015)	(0.014)	(0.018)
Corr(Modern$_{it}$, α_i)			0.095
			(0.011)
Observations	58,714	58,714	58,714
Adj R-squared	0.074	0.459	0.841
Controls		✓	✓
Worker Fixed Effects			✓

Notes: Table E1 reports estimates for β in equation (14). Column (1) displays the raw gap without any controls. Column (2) controls for worker characteristics, including experience in the modern and traditional sectors and firm size fixed effects. Column (3) adds worker fixed effects. Controls include age, education, gender, occupation, industry, region, firm size, experience in each sector, and time fixed effects. Corr(Modern$_{it}$, α_i) reports the correlation between the modern-sector indicator and the estimated worker fixed effects across worker-year observations, weighted by survey expansion factors, with standard errors clustered at the worker level. Standard errors in parentheses are clustered at the worker level. *** $p < 0.01$, ** $p < 0.05$, * $p < 0.1$.

Table E2 reports estimates from a pooled specification that allows the peer effect in equation (17) to differ for workers above and below the mean wage of their labor market.

Table E2: Peer Effects on Wage Growth: Workers Above and Below Average Wage

	Dependent variable: $\Delta \log w_{i,t+h}$ Time horizon h in years				
	1	2	3	4	5
Peer wages × Above	0.029***	0.081***	0.116***	0.144***	0.109***
	(0.010)	(0.014)	(0.019)	(0.026)	(0.036)
Peer wages × Below	0.014*	0.036***	0.040***	0.069***	0.074***
	(0.009)	(0.013)	(0.015)	(0.019)	(0.024)
Observations	39,338	29,997	21,577	15,124	9,704
Adj R-squared	0.086	0.163	0.224	0.267	0.266

Notes: Table E2 reports estimates of a pooled version of equation (16) in which log peer wages are interacted with indicators for the worker's wage being above or below the leave-one-out mean wage of her labor market, and the above-mean indicator enters directly (coefficient not reported). Controls are the same as in Figure 4, with coefficients common to the two groups. Standard errors in parentheses are clustered at the labor-market level. *** $p < 0.01$, ** $p < 0.05$, * $p < 0.1$.

Table E3 describes the composition of the region, industry, and occupation groups that define the labor markets used in the model quantification of Section 4.

Table E3: Labor-Market Groups

(1) Group	(2) Components
Panel A: Regions	
1	Tarapacá, Antofagasta, Atacama, Coquimbo
2	Metropolitana (Santiago)
3	Valparaíso, O'Higgins, Maule, Biobío, La Araucanía, Los Lagos, Aysén, Magallanes, Los Ríos
Panel B: Industries	
1	Mining, Utilities, Finance/Real Estate
2	Manufacturing, Construction, Transportation/Communication, Other
3	Agriculture/Fishing, Retail/Hospitality, Community Services
Panel C: Occupations	
1	Management, Science/Intellectuals, Technical
2	Clerical, Operators/Craftsmen, Operations Personnel, Other
3	Service/Sales, Agricultural/Fishery, Laborers

Notes: Table E3 lists the composition of the region, industry, and occupation groups that define the $N = 27$ labor markets used in Section 4. Each labor market is a Region group × Industry group × Occupation group cell. Industry and occupation groups are ordered by mean hourly wage in the baseline sample (group 1 highest, group 3 lowest). Industry and occupation categories follow the EPS classification.

Table E4 reports the full welfare decomposition behind the payroll-tax counterfactuals of Section 5.

Table E4: Payroll-Tax Counterfactuals: Welfare Decomposition

	Consumption-equivalent welfare change (%)							
	Total		Flow utility			Continuation value		
τ	Full	Fixed b	Full	Fixed b	Transfer	Learning	Volatility	Migration
0.20	-0.30	-5.98	1.29	-4.48	6.04	-0.36	-0.14	0.00
0.15	-0.01	-3.19	0.76	-2.44	3.28	-0.18	-0.05	0.00
0.10	$\cdots$	$\cdots$	$\cdots$	$\cdots$	$\cdots$	$\cdots$	$\cdots$	$\cdots$
0.05	-0.27	3.61	-1.07	2.77	-3.74	0.20	0.14	0.00
0.00	-0.78	7.66	-1.99	6.35	-7.84	0.37	0.03	0.00

Notes: Table E4 decomposes the consumption-equivalent welfare change in counterfactual economies with different payroll tax rates, τ, relative to the baseline stationary equilibrium ($\tau = 0.10$, shown with $\cdots$ where changes are zero by construction). All entries are utilitarian aggregates weighted by the baseline distribution of workers, in percentage terms. The first "Total" column reports the full welfare change; the second holds the wage subsidy b fixed at its baseline level. The "Flow utility" columns decompose the flow-utility component into its full change, the change at the fixed baseline transfer (the wage-wedge component), and the transfer component; because b is allocation-neutral and uniform across workers, the split is exact and multiplicative: $(1 + \mathrm{CE}_u) = (1 + \mathrm{CE}_u^{\text{fixed-}b})(1 + \mathrm{CE}_{\text{transfer}})$. The "Continuation value" columns report the components of the change in workers' continuation value in (7): skill accumulation through learning (drift), skill volatility, and migration opportunities.